SEMMELWEIS EGYETEM

DOKTORI ISKOLA

Ph.D. értekezések

3136.

FEKETE ZSUZSANNA

Funkcionális idegtudományok

című program

Programvezető: Dr. Sperlágh Beáta, egyetemi tanár, az MTA doktora

Témavezető: Dr. Hájos Norbert, egyetemi tanár, az MTA doktora

SYNAPTIC PROPERTIES OF PERISOMATIC INHIBITORY CELLS IN CORTICAL STRUCTURES

PhD thesis

Zsuzsanna Fekete

János Szentágothai Doctoral School

Semmelweis University

Supervisor: Norbert Hájos, DSc

Official reviewers: Zita Puskár, PhD

Attila Szűcs, PhD

Head of the Complex Examination Committee:

Alán Alpár, DSc

Members of the Complex Examination Committee:

Lucia Wittner, DSc

Tibor Zelles, PhD

Budapest

2024

TABLE OF CONTENTS

LIST OF ABBREVATIONS

ACSF	artificial cerebrospinal fluid
AHP	afterhyperpolarization
AIS	axon initial segment
AMPAR	α-amino-3-hydroxy-5-methyl-4-isoxazolepropionicacid receptor
AnkG	Ankyrin G
AP	action potential
BA	basal amygdala
BC	basket cell
BLA	basolateral amygdala
Calb	calbindin
CB1	type 1 cannabinoid receptor
CCK	cholecystokinin
CCKBC	cholecystokinin positive basket cell
ChC	chandelier cell
CeA	central amygdala
CS	conditioned stimulus
DSI	depolarization induced suppression of inhibition
FS	fast-spiking
GABA	gamma-aminobutyric acid
HC	hippocampus
IEI	inter-event interval
IN	interneuron
ITC	intercalated cell
LA	lateral amygdala
LTP	long-term plasticity
MD	mediodorsal thalamus
mEPSC	miniature excitatory postsynaptic current
PFA	paraformaldehyde
PN	principal neuron
PrL	prelimbic cortex
PTI	perisomatic region-targeting interneuron
PV	parvalbumin

PVBC	parvalbumin positive basket cell
Sst	somatostatin
STP	short-term plasticity
TTX	tetrodotoxin
uEPSC	unitary excitatory postsynaptic current
uIPSC	unitary inhibitory postsynaptic current
US	unconditioned stimulus
VIP	vasointestinal polypeptide
VGlut3	type 3 vesicular glutamate transporter
VGSC	voltage gated sodium channel
ZT	Zeitgeber time

1. INTRODUCTION

To efficiently cope with challenges, the animal brain evolved to complete tasks like aversive or reward memory formation, planning and decision making. Revealing how neuronal networks that carry out these tasks operate is a fundamental goal for scientific research. Two brain regions that are indispensable in executing these functions in mammals are the prefrontal cortex and the amygdala, areas where we performed our investigations. In the next chapters I will briefly introduce these brain regions, their role in behaviour and our current knowledge regarding their neuronal networks, with the focus on a specialized group of inhibitory neurons and their synaptic connections.

1.1. Medial prefrontal cortex and its role in cognitive processes

The prefrontal cortex (PFC) is located in the frontal part of the neocortex across mammalian species including humans, positioned high in the functional hierarchy of brain regions. In terms of its role in behavior, it is one of the most studied brain regions. High-level cognitive functions such as decision making, reward processing, working memory or attention are attributed to the healthy operation of this region (Goldman-Rakic, 1988; Mesulam, 1998; Fuster, 2006). Alterations in PFC function on the other hand have been implicated in disorders like schizophrenia, addiction and depression (Price & Drevets, 2010; Goldstein & Volkow, 2011; Dienel et al., 2022; Howes et al., 2024). Despite the importance of PFC in executive functions, precisely defining the PFC has been challenging due to the difficulty of finding appropriate criteria that can be applied across species. Historically, PFC was defined by the dense projection arriving from the mediodorsal nucleus of the thalamus (MD)(Rose & Woolsey, 1948). Since then, the specificity of MD projections to the PFC were disproven in several mammalian species and the use of connectivity alone as defining criterion was expanded by the following aspects: the embryological development, functional properties and the presence and distribution of neuroactive substances and receptors are now also considered when homology between species is examined (Uylings et al., 2003). These aspects and the fact that model animals can also execute behaviors similar to those that are attributed to the PFC in humans (like delayed-response tasks or rule switching) validate research directions in rodents (Seamans et al., 2008; Le Merre et al., 2021). These features enable studying the PFC in model organisms in the quest of finding general principles which

might take us closer to a deeper understanding of how neuronal circuits operate in mammals as well as humans.

The rodent PFC is a layered, agranular structure (i.e. it lacks layer IV) that can be further divided into the following subregions (Figure 1): secondary motor cortex (M2); anterior cingulate cortex (ACC); prelimbic cortex (PrL); infralimbic cortex (IL), orbitofrontal cortex (OFC) and insular cortex (IC) (Carlén, 2017). Efforts have been made to assign specific functions to these subregions as well. For example, ACC participates in action selection, reward-guided learning and subjective feeling of pain (Fuchs et al., 2014; Rolls, 2023). Our study focused on the prelimbic cortex located in the medial part of the PFC (mPFC) especially because of the involvement of the PrL in fear-related behavior (Burgos-Robles et al., 2009; Sierra-Mercado et al., 2011; Chen et al., 2017).

The mPFC is highly interconnected with various parts of the brain. It sends projections to the periaqueductal gray that participates in defensive responses and aggression, and to the striatum, a region involved in reward-seeking behavior (Carrive, 1993; Nelson & Trainor, 2007; Cox & Witten, 2019; Anastasiades & Carter, 2021). The mPFC also has reciprocal connections with several brain region including the thalamus and the basal amygdala (Anastasiades & Carter, 2021). The bidirectional connection between the PFC and the amygdala plays a crucial role in emotional regulation and social interaction (Banks et al., 2007; Salzman & Fusi, 2010; Gangopadhyay et al., 2021; Tan et al., 2021; Wang et al., 2022). This extensive connectivity arising from and arriving to the mPFC ensures its role as an integrative region that exerts top-down control over behavior in a multitude of contexts.

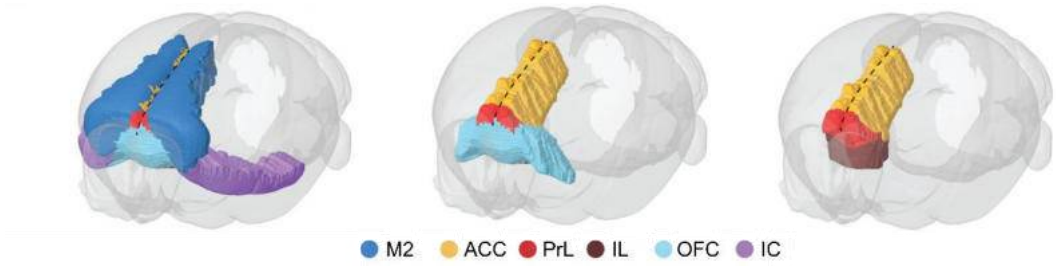

Figure 1. Regions of the mouse prefrontal cortex. ACC: anterior cingulate cortex; IC: insular cortex; IL: infralimbic cortex; M2: secondary motor cortex; OFC: orbitofrontal cortex; PrL: prelimbic cortex. (Adapted from Carlén, 2017).

1. 2. The basolateral amygdala and its functions in neuronal operation

The amygdaloid complex includes 13 different nuclei divided into 3 major groups with different developmental origin and elements in their neuronal circuits. It is an evolutionary conserved structure with homologous areas present in reptiles and the avian brain as well (Lanuza et al., 1998, Martinez-Garcia et al., 2008). One of the major groups of the amygdala nuclei is the basolateral complex which includes the lateral nucleus (LA), the basal nucleus (BA), together often referred to as the basolateral amygdala (BLA), and the basomedial nucleus (BM) (Figure 2). Common features of these nuclei include their cortical origin and their similar cytoarchitecture. Although neurons in these nuclei are not arranged into layers, lacking an apparent common dendritic orientation, some gradients can be observed within the nuclei, for example in the size of somata along the anteroposterior axis (Sah et al., 2003).

In terms of its function, the BLA has been the target of numerous studies that aimed to investigate reward processing, valence coding, decision making or aversive memory formation (Goosens & Maren, 2001; Murray, 2007; Tye et al., 2008; Gore et al., 2015), functions highly relevant to survival. BLA activity has been shown to play a crucial role in the fear conditioning learning paradigm, with numerous studies showing that local inhibitory cells in this region are indispensable in the acquisition, expression and extinction of fear memories (Herry et al., 2010; Tye et al., 2011; Wolff et al., 2014; Krabbe et al., 2019; Ito et al., 2020; Stujenske et al., 2022; Baldi et al., 2024).

Given its cortical origin, circuits in the BA share many features with the PFC regarding their cell types and the ratio of these cell types, as well as the circuit patterns established by them (McDonald, 1992; Spampanato et al., 2011, Capogna, 2014; Anastasiades & Carter, 2021). Inhibitory cells in the BA are similarly diverse as in the neocortex in terms of their molecular and physiological features, implying that they fulfill similar roles within local circuits (Hajos, 2021). Therefore, in the following section I will introduce these cell types generally.

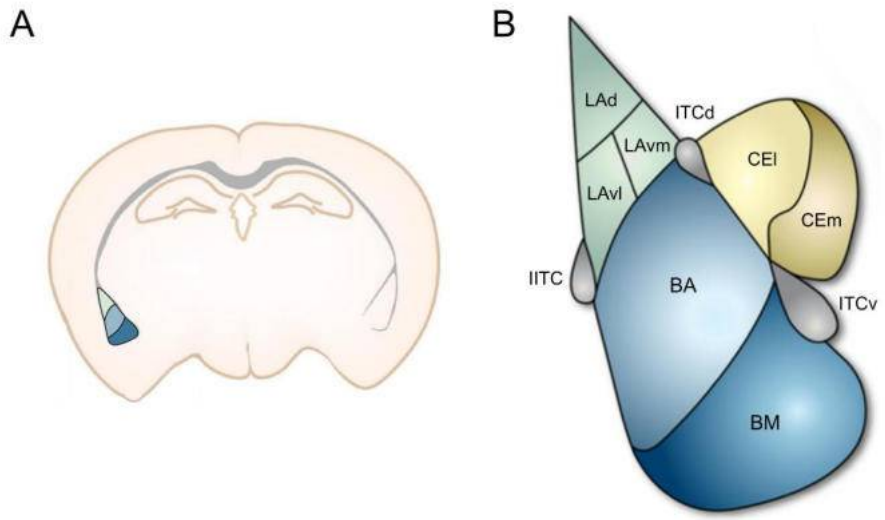

Figure 2. Location of the mouse amygdala and its nuclei involved in emotional learning. (A) Coronal section of the mouse brain at the plane containing amygdala nuclei important in emotional learning. Green and blue regions correspond to the area enlarged in panel B (modified from Aerts & Seuntjens, 2021). (B) Amygdala nuclei involved in the acquisition, expression and extinction of fear. BA: basal nucleus; BM, basomedial nucleus; CEl, CEm: lateral and medial part of central amygdala; ITCd, ITCv and lITC: dorsal, ventral and lateral paracapsular part of intercalated cell mass; LAd, LAvl and LAvm: dorsal, ventrolateral and ventromedial part of the lateral nucleus (Adapted from Lee et al., 2013).

1.3. Neuronal diversity in cortical structures

1.3.1. Features used for characterization of excitatory and inhibitory cells

Cortical neuronal networks are built up from excitatory glutamatergic cells and inhibitory GABAergic cells. The ratio of these broad categories are around 4 to 1 with glutamatergic neurons making up approximately 80-85% of the neuronal population across different brain regions including the PFC and the BA (DeFelipe & Farinas, 1992). Cortical excitatory neurons include pyramidal neurons and stellate cells, two groups that strikingly differ in their morphology that also bears functional consequences. Pyramidal neurons constitute the most numerous neuronal cell type therefore they are regarded as principal neurons (PNs). PNs also represent the major output source to remote brain

regions. PN somata resemble a rounded pyramid, from which a spiny apical dendrite and many basal dendrites emerge. In layered structures, the apical dendrites of PNs reach towards layer 1 (L1) as in the PFC, but without layers, they do not show apparent orientation, for example as in the BA. The dendritic spines are the main postsynaptic targets for excitatory synapses but can be innervated by inhibitory terminals as well (Gray, 1959; Shepherd, 1996; Nimchinsky et al., 2002; Kubota et al., 2007), although GABAergic signals on dendrites mostly arrive to the segments without spines (Megias et al., 2001). Inhibitory inputs also target the soma and the axon initial segment (AIS) of PNs with some inhibitory cell types specializing in innervating these regions (Freund & Buzsaki, 1996; Megias et al., 2001). In contrast to the morphology of pyramidal neurons, stellate cells extend their dendrites radially and have multipolar morphology. Stellate cells that are abundant in layer 4 of somatosensory cortices are involved in relaying information locally, receive monosynaptic connections mostly from neurons within the same cortical column but are also targeted by strong thalamic inputs (Stratford et al., 1996; Schubert et al., 2003). In contrast, stellate cells of the entorhinal cortex for example project to the hippocampus and form a continuum of morphological phenotypes between stellate cells and pyramidal cells (Tamamaki & Nojyo, 1993; Witter et al., 2017).

Due to the fact that PNs provide the majority of output from a given region, efforts for defining heterogeneity within such a large pyramidal neuronal population has focused on differences in PN projection areas. For example, pyramidal tract (PT) neurons in cortical layer 5 project to the brainstem and spinal cord and often to the thalamus, while projections of intratelencephalic (IT) cells avoid the thalamus but innervate the contralateral cortex, which is not targeted by PT cells in addition to the striatum. These principal cells differ in their electrophysiological properties (Hattox & Nelson, 2007) and are preferentially active in different states of the network *in vivo* (Kawaguchi, 2017), underlining the concept that PN projection sites have functional implications. Classification of PNs can also be based on their involvement in given tasks. For example, PNs in the BA that become sensitive for a neutral stimulus if that is repeatedly associated with a noxious stimulus can be referred to as fear neurons due to the causal relationship between their activity and fear behavior (Herry et al., 2008). Similarly, PNs in the hippocampus can become place cells by showing heightened activity at a given area, contributing to the neuronal representation of space (O'Keefe & Speakman, 1987; Moser et al., 2008).). In addition, firing of PNs in the PFC correlates with the animal behavior during working memory and decision-making (Passecker et al., 2019; Ozdemir et al.,

2020). Yet, these might be plastic roles on shorter timescales and not definitive categories, as there might be other tasks a given PN engages in. In terms of the electrophysiological properties of PNs, two broad categories were described based on their activity pattern in response to depolarizing current pulses: the regular spiking and the bursting type was recorded both *in vitro* and *in vivo* (McCormick et al., 1985; Chagnac-Amitai et al., 1990; Nunez et al., 1993). These types can also exhibit morphological differences for example in their somatic size and the thickness and arborization of dendrites (Degenetais et al., 2003).

Excitatory neurons, however, need inhibitory cells to guarantee balanced, controlled functioning of the network and fine-tune information flow on the spatial and temporal scale. The axons of these inhibitory neurons arborize locally and provide inhibitory input to thousands of neighboring neurons - hence the name interneuron (IN), although a small portion can project to remote cortical areas forming a group of GABAergic projection cells. Inhibitory interneurons show large heterogeneity in a number of aspects that are important for their description and classification: they can display distinct morphology, express specific neurochemical markers, exhibit certain electrophysiological properties or preferentially target cell types or subcellular domains. The canonical cortical IN types and their characteristic features are summarized in Figure 3.

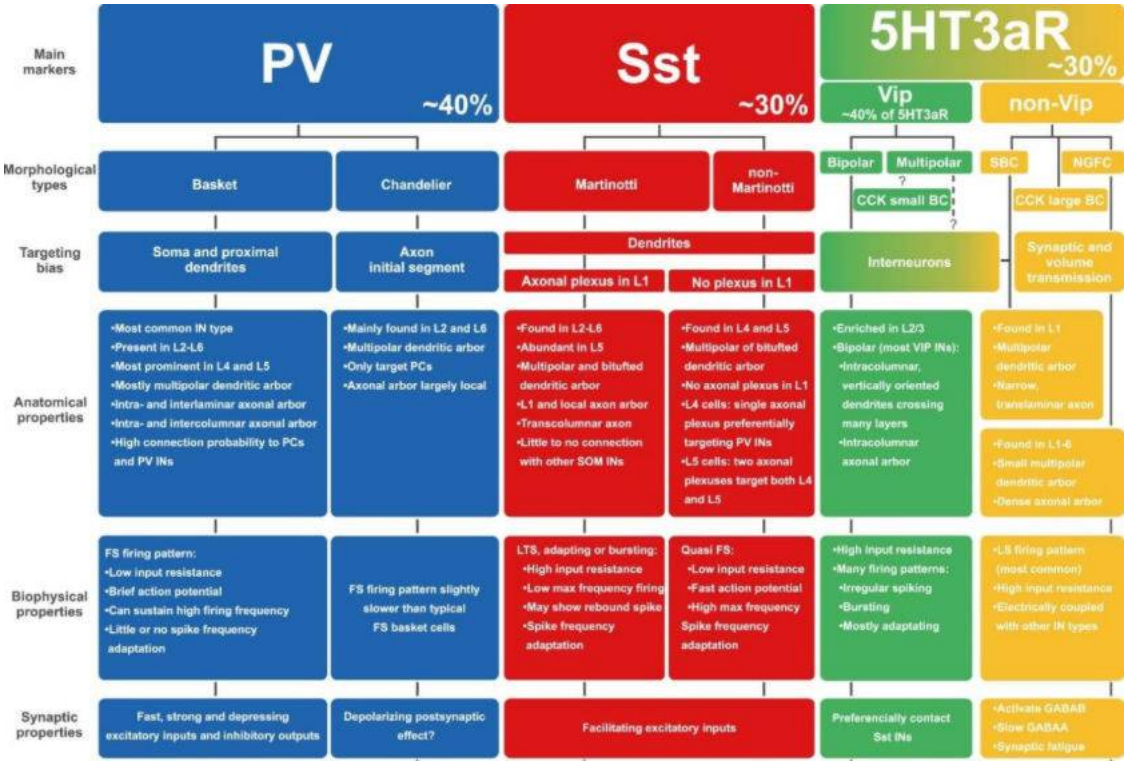

Figure 3. Major cortical interneuron classes. Neurochemical markers, targeting bias, anatomical and biophysical properties are traditionally used to describe and group INs. 5HT3aR: 5-hydroxytryptamine (serotonin) receptor; CCK: cholecystokinin; NGFC, neurogliaform cell; PV: parvalbumin; SBC, single bouquet cell; Sst: somatostatin; Vip: vasointestinal polypeptide. (Modified from Tremblay et al., 2016).

The definition of IN types was driven by the underlying motive that cell types would represent functional units within the network and that their features were relevant to the role they fulfill. Such a relationship between function and cellular properties is readily recognizable in terms of the biophysical properties that shape neuronal excitability and activity patterns enabling a specialized relationship between the input and output of a cell type. The magnitude of the effect a given input will have on the membrane potential of a neuron for example will be determined by its input resistance, with higher input resistance leading to larger deflections and more potent excitation or inhibition. The time course of these deflections is largely influenced by the membrane time constant of the cell, which determines how long these deflections in the membrane potential last, meaning that cell types with longer membrane time constant integrate inputs on a wider timescale. At the output side, cell types can differ in the width and the rate of their action potentials with some cells being able to maintain a firing rate while others show large accommodation (i.e. their spiking slows down considerably). Differences in these properties shape the dynamics of calcium influx into presynaptic terminals, kinetics of the release and how fast and how faithfully a cell type can translate its excitatory input into action potentials. These intrinsic membrane properties can show large variability between cell types (Figure 3) and therefore represent an important factor that contributes to the divergent functions performed by different cell types.

Another feature that has been proven to be of major significance in terms of the functional role certain INs play is whether they show targeting bias and in what way. This is a consequence of the morphology and the biophysical properties of neurons. Dendrites represent a large surface for receiving input and performing local computations. The somatic region is where inputs converge and the signal reaches the axon initial segment, which has the highest density of voltage-gated sodium channels necessary for action potential (AP) generation. The consequence of the specialized domains is that inhibitory inputs arriving to different sub-compartments of a neuron will serve distinct roles in shaping postsynaptic activity. Utilizing this, different IN types specialize in innervating

distinct parts of their postsynaptic partners, and these patterns appear throughout cortical regions, including the amygdala (Figure 4, Hajos, 2021). For instance, somatostatin (Sst) expressing Martinotti cells tend to innervate the dendritic region of PNs (Kawaguchi & Kubota, 1996; Wang et al., 2004). Neurogliaform cells that reside in layer 1 mostly exert their effect via volume transmission also on dendritic branches entering this layer, therefore, these cell types are more suited to influence the input of PNs (Tamas et al., 2003; Olah et al., 2009). VIP cells are less selective for the subcellular region, but they mostly target other INs, therefore their activity reduces the inhibition that targets PNs (Acsady et al., 1996, Hajos et al., 1996, Pi et al., 2013). On the other hand, a group of INs focuses on innervating the soma, the proximal dendrites and the axon initial segment of their postsynaptic partner, collectively called the perisomatic region (Freund & Katona, 2007). As these cell types are in the focus of our research, I will introduce them in the following chapters in more detail.

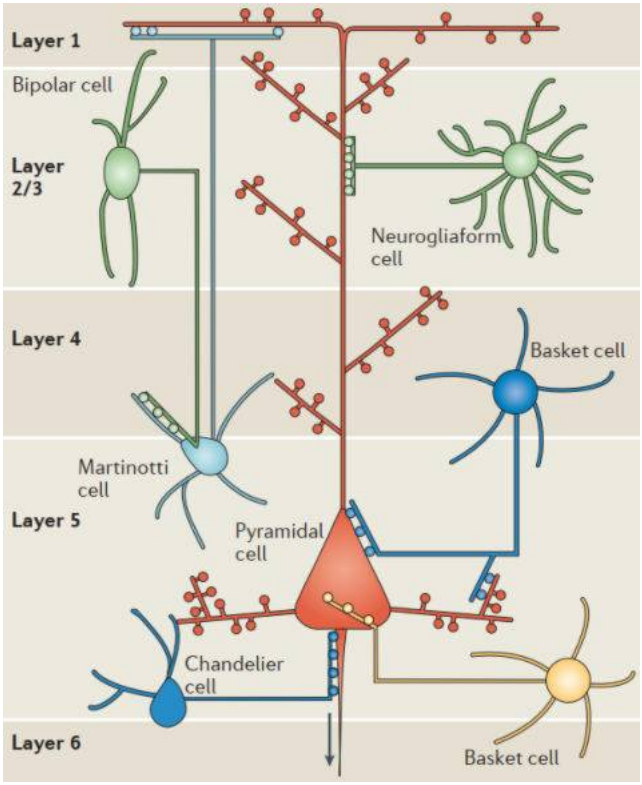

Figure 4. Different subcellular domains of PNs are preferentially innervated by different types of INs. Certain cell types, like Martinotti cells or neurogliaform cells target the distal dendritic region of PNs, while others synapse on the proximal dendrites,

the soma, or the axon initial segment. This latter group that includes basket cells and chandelier cells constitutes the perisomatic region-targeting interneurons. These differences in the position of synapses dictate the role of IN types within neuronal circuits. (Adapted from Marin, 2012.)

1.3.2. Perisomatic region-targeting interneurons (PTIs) and their significance

An attribute that PTIs have in common is their preference for innervating the perisomatic region of their postsynaptic partners. This region includes the soma, the proximal dendrites and the axon initial segment (AIS), the regions where arriving inputs converge and the output of neurons is generated. The group of PTIs is comprised of 3 cell types: the parvalbumin expressing basket cell (PVBC), the chandelier cell (ChC) that includes parvalbumin positive and negative subpopulations, and the cholecystokinin and CB1 expressing basket cell (CCKBC).

The importance of PTIs in local circuit operation has been demonstrated by anatomical and functional investigations (Buhl, Halasy, & Somogyi, 1994; Cobb et al., 1995; Miles et al., 1996). Previous studies showed that the ratio of GABAergic synapses on the dendrites of PNs increase towards the soma in the hippocampus and the primary somatosensory cortex as well, which can increase up to 90 % (Megias et al., 2001; Bloss et al., 2016; Iascone et al., 2020). In a previous study, we identified that approximately 90% of GABAergic inputs on PN somata express either PV or CB1 in the prelimbic cortex (Nagy-Pal et al., 2023) and 70% in BLA (Vereczki et al., 2016), the two markers for basket cells, results which are in good correspondence with those obtained in the hippocampus (Takacs et al., 2015). Furthermore, by quantifying the ratio of postsynaptic targets of CCKBC or PVBC terminals using biocytin-filled cells, we determined that a quarter of the synapses of both BC types contact PN somata and another quarter innervates proximal dendrites in the PrL (Nagy-Pal et al., 2023). These findings demonstrate that the contribution of BCs to inhibitory innervation of PNs is significant. The third PTI type, ChCs on the other hand specialize in innervating the AIS and they almost exclusively target PNs (Somogyi, 1977; Fairen & Valverde, 1980; DeFelipe et al., 1985). ChC synapses are concentrated at the region where action potentials are initiated in the AIS (Veres et al., 2014). The number of contacts an individual PN receives from ChCs can vary with multiple ChCs potentially converging on one postsynaptic cell. In the

visual cortex for example where almost all PNs are targeted by at least one ChC, most of the individual AISs receive about 10 synaptic contacts but can be targeted by up to 30 boutons (Schneider-Mizell et al., 2021).

Besides the spatial organization of GABAergic synapses established by PTIs, functional studies also demonstrate the important role of these cells in regulating PN activity. Since the activity of neurons manifests in the binary code of action potentials, inputs physically close to the site of action potential generation are well positioned to strongly influence neuronal activity. Indeed, previous studies have shown that both BC types are able to efficiently control the spiking of their targets (Cobb et al., 1995; Miles et al., 1996; Stark et al., 2014; Woodruff & Sah, 2007; Veres et al., 2017). Similarly, activation of a few ChC synapses can inhibit PN spiking (Veres et al., 2014). In the following sections, I will introduce the different PTI types in more detail.

1.3.2.1. Parvalbumin-expressing basket cell (PVBC)

The name of basket cell reflects the structure created by the axonal boutons, namely, the way they surround postsynaptic somata with multiple boutons, but basket cell axons also frequently contact dendrites (Tamas et al., 2000; Kisvarday et al., 2002; Kubota et al., 2015). Basket cells are further categorized into parvalbumin-containing basket cells (PVBCs) and cholecystokinin-containing basket cells (CCKBCs) that also express type 1 cannabinoid receptor (CB1) on their somatic and presynaptic membrane. Despite targeting the same subcellular domain of PNs both in the PrL and the BA (Veres et al., 2017; Nagy-Pal et al., 2023), the two BC types differ in many molecular, electrophysiological and functional aspects.

The calcium binding protein PV is expressed in the soma as well as the synaptic terminals of PVBCs where it acts as a slow Ca^{2+} buffer and prevents synaptic facilitation (Caillard et al., 2000; Eggermann & Jonas, 2011). PVBCs fire narrow spikes due to the rapid inactivation of Na^{+} channels and the expression of fast-activating Kv3 channels that repolarize the membrane (Martina et al., 1998; Rudy & McBain, 2001; Lien & Jonas, 2003; Hu et al., 2018). Together with the rapid recovery of Na^{+} channels, these features enable high-frequency firing in PVBCs that can reach up to 150 Hz (Rudy & McBain, 2001; Hu et al., 2018), PVBCs are therefore also referred to as fast spiker cells. The energy required for such high intensity activation is provided by large density of mitochondria in the somata and presynaptic terminals (Takacs et al., 2015) and the high

expression of cytochrome c oxidase (Gulyas et al., 2006) which plays a critical role in ATP synthesis. As an action potential invades the presynaptic boutons of PVBCs, a series of factors contribute to the quick release of GABA from their terminal (Huang 2014). Ca^{2+} entry is mediated by the fast-conducting P/Q-type Ca^{2+} channels that are located at the active zones of PVBC synapses (Hefft & Jonas, 2005), leading to the fast exocytosis of synaptic vesicles (Zaitsev et al., 2007; Bucurenciu et al., 2008). Postsynaptic currents evoked by PVBCs therefore arise with small latency and high precision (Hefft & Jonas, 2005). Their short membrane time constant allows PVBCs to follow their input faithfully (Glickfeld & Scanziani, 2006), although their transmitter release is modulated by neuromodulatory signals via their μ-opioid receptor and their type 2 muscarinic acetylcholine receptors, that are absent from CCKBC terminals (Hajos et al., 1998; Drake & Milner, 2002; Yi et al., 2014).

PV cell somata are surrounded by a complex structure called perineuronal net (PNN), made up by components of the extracellular matrix. PNNs have been implicated in the regulation of synaptic plasticity in multiple brain regions including the visual cortex, PFC and the hippocampus (Carulli et al., 2010; Miyata et al., 2012; Carceller et al., 2020; Cope et al., 2022; Biro et al., 2023). Moreover, a study from the BLA suggested that PNN protects fear memories from erasure in adult mice even after fear extinction, which is not the case in juvenile animals prior to the maturation of PNNs (Gogolla et al., 2009).

PVBCs are mostly known for their ability to regulate and synchronize the activity of large neuronal populations (Buzsaki & Wang, 2012). They can establish synapses on more than a 1000 postsynaptic partners (Vereczki et al., 2016; Sik et al., 1995), and they often target other PVBCs by synaptic contacts (Sik et al., 1995; Bartos et al., 2002; Klausberger et al., 2002) or establish gap junctions, which increase synchrony (Galarreta & Hestrin, 1999; Galarreta & Hestrin, 2002; Fukuda & Kosaka, 2000; Tamas et al., 2000). These connectivity patterns combined with the temporal precision of their postsynaptic effect enables PVBCs to fulfill a key role in regulating synchronous network activity (Tamas et al., 2000; Bartos et al., 2002; Buzsaki & Wang, 2012). Sharp-wave ripples for example, these short episodes of high-frequency rhythmic activities in the hippocampus that support memory formation and consolidation can be induced by optogenetic activation of PV cells (Schlingloff et al., 2014). PVBC spiking is phase locked to theta and gamma oscillation both *in vitro* and *in vivo* (Hajos et al., 2004; Tukker et al., 2007; Klausberger & Somogyi, 2008; Hartwich et al., 2009; Massi et al., 2012), and their activity during theta rhythm was also shown to be required for phase-coupled PN spiking

(Struber et al., 2022). Numerous studies have shown that their firing is crucial in the induction and maintenance of rhythmic network activities (Sohal et al., 2009; Gulyas et al., 2010; Schlingloff et al., 2014; Stark et al., 2014; Gan et al., 2017). Their direct role was also demonstrated in processes such as working memory (Kim et al., 2016; Lagler et al., 2016) and sensory processing (Cardin et al., 2009; Atallah et al., 2012).

As a consequence of the multifaceted role PVBCs fulfill, alterations in PVBC function also have important health implications. Since oscillations underlie important cognitive processes (e.g. gamma oscillation in attention), disruptions in these abilities have been associated with disturbances in rhythmic activities and PVBC function (Benchenane et al., 2011; Hijazi et al., 2023). As key players in regulating excitatory/inhibitory balance, PVBCs are particularly implicated in conditions where pathological shifts arise in the excitability at the network level, accompanied by altered PV excitability as well, like in Alzheimer's disease (Olah et al., 2022; Hijazi et al., 2023; Shu et al., 2023). Although uncovering the precise relationships between cause and effect is still a goal for future investigations, this goal may be fostered by a better understanding of the synaptic interactions of BCs.

1.3.2.2. Cholecystokinin-expressing basket cell (CCKBC)

Due to challenges with labelling techniques that would provide sufficient specificity, CCKBCs are the least well characterized cell type within PTIs. Markers for CCKBCs traditionally included CCK and CB1 receptor that are both highly expressed in pyramidal cells. Nonetheless, due to their distinct features compared to fast-spiking PTIs, CCKBCs might take part in modulating circuit activity in a unique way.

CCKBCs express CB1 receptors in their presynaptic terminals and are therefore sensitive for retrograde cannabinoid signaling (Freund, 2003). Via these G-protein coupled receptors, endocannabinoids released from PNs upon depolarization suppress GABA release by blocking direct Ca^{2+} entry into the CCKBC axon terminals via the N-type of voltage gated Ca^{2+} channels, known as depolarization-induced suppression of inhibition (DSI) (Pitler & Alger, 1992; Katona et al., 1999; Szabo et al., 2014; Dudok et al., 2024). Further receptors expressed by the somatic membrane of CCKBCs include muscarinic and nicotinic acetylcholine receptors and serotonin receptors, while their axonal boutons can also express estrogen receptor alpha (Cea-del Rio et al., 2010; Freund, 2003; Freund & Katona, 2007; Hart et al., 2007; Keimpema et al., 2012; Morales et al.,

2008). The sensitivity for neuromodulators endow CCKBCs a role of conveying the information of ascending subcortical pathways and thus fine-tuning local network operations (Freund & Katona, 2007).

CCKBCs have larger input resistance and slower membrane time constant than PVBCs, therefore they are more suited for the integration of incoming signals in a wider time window (Glickfeld & Scanziani, 2006; Hefft & Jonas, 2005; Bartos & Elgueta, 2012). Their firing pattern typically displays a regular spiking phenotype with accommodation (Cea-del Rio et al., 2010; Cope et al., 2002; Szabo et al., 2010). GABA release from CCKBC terminals was found to be less precisely timed compared to the presynaptic action potential than in fast-spiking PTIs (Hefft & Jonas, 2005). Ca^{2+} influx in these terminals is regulated by N-type Ca^{2+} channels that may be positioned further away from the Ca^{2+} sensors compared to that observed in PVBC terminals (Bucurenciu et al., 2008), contributing to the slower exocytosis of vesicles (Hefft & Jonas, 2005). CCKBCs are also capable of asynchronous transmitter release upon discharging several action potentials, meaning that the release of synaptic vesicles decouples from action potentials and continues without the spiking of CCKBC (Hefft & Jonas, 2005).

CCK is a neuropeptide highly abundant in certain cell types and acts as a neuromodulator (Crawley, 1985; Kow & Pfaff, 1988; Crawley & Corwin, 1994). Although the mechanism by which it is released from CCK+ cells or the conditions required are still unknown, previous studies showed that CCK has diverse, synapse type-dependent effects (S. Y. Lee & I. Soltesz, 2011). Its receptors, CCK_1 and CCK_2 are G-protein coupled receptors involved in different signaling pathways which also depend on the cell type affected by CCK. In PNs, downstream effects of CCK includes the enhancement of endocannabinoid synthesis, which retrogradely suppresses the inhibitory effect of presynaptic CCKBC activity (Foldy et al., 2007). PVBCs on the other hand are depolarized by CCK and their transmission is enhanced, similarly to the excitatory synaptic transmission (Deng et al., 2010; S. H. Lee & I. Soltesz, 2011). On the network level, CCK was implicated in the regulation of fear and anxiety (Bowers et al., 2012).

Additionally, subpopulations of CCKBCs express calbindin or VGluT3 in a mutually exclusive manner in the hippocampus, neocortex and the BA, where the two populations show no difference in terms of their morphology or electrophysiological properties (Somogyi et al., 2004; Rovira-Esteban et al., 2017). However, VGluT3+ CCKBCs have been shown to co-release GABA and glutamate (Pelkey et al., 2020), but whether and

how this influences network functions under physiological conditions needs to be further elucidated.

The contribution of CCKBCs to network operations appears to be more subtle or dispersed compared to the fast-spiking PTIs, and they might exert their effect on a larger timescale. So far, only a few studies investigated the role of CCKBCs *in vivo*. During rhythmic activity like theta oscillations, CCKBCs fire at earlier phase compared to PVBCs (Klausberger & Somogyi, 2008). In contrast to the PVBC population, CCKBC activity is heightened in rest (Dudok, Klein, et al., 2021). Based on *in vitro* studies it has been hypothesized that CCKBCs might have a role in place cell formation in the hippocampus via DSI, ensuring that only the most active PNs can escape from the inhibition of CCKBC and participate in coding (Freund, 2003; Freund & Katona, 2007; Losonczy et al., 2010). A recent elegant study has shown that indeed DSI in CCKBCs occurs *in vivo* and it plays an important role in place cell formation (Dudok et al., 2024), a phenomenon that endows CCKBCs a key role in spatial navigation and memory formation. Whether DSI in CCKBCs in other brain areas has important function in controlling region-specific behavior – i.e. fear memory formation in the BA or decision making in PFC- is yet to be determined. Furthermore, inhibition provided by hippocampal CCKBCs was shown to be sensitive for enriched environment (Feng et al., 2021; Hartzell et al., 2018).

1.3.2.3. Chandelier cells (ChCs)

Chandelier cells, named after their boutons lining up on axon initial segments are a distinctive group of cortical interneurons in terms of their morphology and target-specificity. ChCs selectively innervate the AIS of nearby PNs which results in a pattern of vertically aligned cartridges in layered structures due to the strict orientation of PN AISs (Somogyi, 1977). In the lack of parallelly aligned AISs in the BA, the morphological features of ChCs provide less obvious guidance for their identification compared to that observed in the mPFC.

ChCs often express parvalbumin and display a fast-spiking phenotype, similarly to PVBCs (DeFelipe et al., 1989; Buhl, Han, et al. (1994)). However, depending on the exact brain region, PV content in a subset of ChCs cannot be revealed by immunostaining (Taniguchi et al., 2013). For example, the ratio of PV-lacking ChCs can be as high as

30% in the BA (Vereczki et al., 2021). Indeed, reporter mouse lines that utilize PV as a genetic marker seem to only label ChCs in the L2/3 but not in deeper layers (Jiang et al., 2015), although depending on the cortical region, the ratio of ChCs localized in deeper layers can exceed the number of ChCs situated in L2/3 (Taniguchi et al., 2013). Therefore, mouse lines generated to fluorescently label ChCs irrespective of their PV content are becoming more popular as they provide better specificity for ChC labelling than PV-based methods. More importantly, investigating the features of potentially non-overlapping populations of ChCs helps to gain a wider understanding of ChC function. Example mouse lines for targeting ChCs include the Nkx2.1-CreER (Taniguchi et al., 2013; Lu et al., 2017), the Vipr2-cre (Nakashima et al., 2022; Seignette et al., 2024) and the Unc5b-CreER (Dudok, Klein, et al., 2021: Paul et al., 2017) lines. In the BLA, the expression of calbindin (CB) distinguishes PVBCs from ChCs, and can be used as a tool to identify them (Vereczki et al., 2016), but this is not the case in the mPFC or the hippocampus (unpublished observations and Freund & Buzsaki, 1996).

Due to the technical challenges of targeting ChCs, current knowledge is limited regarding their precise postsynaptic effect. Although ChCs were considered to be inhibitory GABAergic interneurons since their discovery (Somogyi et al., 1985; Buhl, Han, et al., 1994), this view was challenged when ChCs were reported to exert depolarizing effect postsynaptically (Szabadics et al., 2006). Also, the reliable disynaptic effect following ChC spiking that is sensitive for glutamatergic and GABAergic receptor blockers raised the possibility that ChCs might cause excitation (Szabadics et al., 2006; Woodruff et al., 2006; Perumal et al., 2021). Moreover, activation of ChCs in the BLA were shown to be instrumental in generating high-frequency bursts of activation called sharp-waves (Perumal et al., 2021). Subsequent studies aimed to elucidate this question by trying not to affect intracellular Cl^- concentration, a factor that determines the direction of Cl^- movement upon $GABA_A$ receptor channel opening, or by manipulating the resting membrane potential of PNs (Glickfeld et al., 2009; Woodruff et al., 2011; Veres et al., 2014). The conclusion that ChCs mostly hyperpolarize their targets was also supported by in vivo data (Lu et al., 2017; Dudok, Klein, et al., 2021), but under the appropriate conditions, ChCs are capable of facilitating spike generation (Woodruff et al., 2011). Given that the resting membrane potential of PNs fluctuates greatly *in vivo* (Poulet & Petersen, 2008; Crochet et al., 2011), the effect of ChCs might change dynamically, depending on the state of their postsynaptic partners (Woodruff et al., 2011). Adding a further layer to this discussion, it has also been proposed that the relationship between the

resting membrane potential and the reversal potential for Cl^- is not the only factor that determines how GABAergic synapses at the AIS influence the spiking probability of PNs. Instead, the opening of $GABA_A$ receptors at the AIS when the driving force on Cl^- is depolarizing can still lead to hyperpolarization by an indirect mechanism that leads to the opening of the KCNQ potassium channel (Jones et al., 2014).

As ChCs target the AIS of their postsynaptic partners, where the action potentials are generated, they are in the best position to control the output of their postsynaptic partner (Kole & Stuart, 2012). Indeed, in the amygdala, it has been shown that the input of as few as 2-3 ChCs is enough to effectively veto PN firing (Veres et al., 2014), implying that the simultaneous recruitment of ChCs endows this interneuron type a powerful control on the output of PNs during network activities. *In vivo* and *in vitro* studies have proven that in the hippocampus, ChCs show phase-coupled rhythmic firing during theta oscillation and moderate coupling to gamma oscillations, although their activity is not coupled to sharp-wave ripples (Hajos et al., 2013; Klausberger et al., 2003; Tukker et al., 2007; Klausberger & Somogyi, 2008; Viney et al., 2013; Topolnik & Tamboli, 2022). In addition, more and more studies imply that ChCs are crucial for processing information of salient stimuli, or pain, as ChCs both in the mPFC and in the BA are highly responsive to noxious stimuli (Massi et al., 2012; Bienvenu et al., 2012). In the visual cortex, ChCs show highly correlated, synchronous activity to events eliciting arousal, e.g. locomotion and visuomotor mismatch (Seignette et al., 2024). A recent study from the hippocampus also showed a tight link between locomotion and ChC activity (Dudok, Szoboszlay, et al., 2021). Despite the large connectivity rate between ChCs and neighbouring PNs, decreasing ChC activity artificially was shown to evoke a rather local or mild effect on network activity (Jung et al., 2023; Seignette et al., 2024), in line with the interpretation of ChC function that argues for a targeted inhibitory effect as opposed to a network-level effect (Woodruff et al., 2011, Jung et al., 2023).

Nevertheless, impairment in ChC function was implicated in severe neurological diseases such as autism spectrum disorder, epilepsy and schizophrenia (Gallo et al., 2020) showing their crucial role in physiological network functions. A specific alteration affecting the AIS of PNs in the PFC is the significant change in $GABA_A$ receptor subunit expression in subjects with ASD or subunit compositions in subjects with schizophrenia compared to healthy controls (Hong et al., 2020; Volk et al., 2002). Moreover, in the PFC of schizophrenic patients, PV cell densities are not affected but the expression levels of PV mRNA and the protein itself in single PV cells is decreased (Hashimoto et al., 2003;

Enwright et al., 2016) although these results might include data from the ChC and BC population as well.

1.3.3. Synaptic connections and mapping connectivity

Although action potentials in a simplified view render the activity of a neuron into two states (silent or active), the postsynaptic effect of a single spike is largely variable. Chemical synapses represent a site in the flow of information where the possibility of fine-tuning takes many forms and synaptic features greatly depend on the synaptic partners. Therefore, the role of PTIs in any microcircuit cannot be separated from the features of the synapses they establish and receive.

A technique that provides insight into the postsynaptic effect of a neuron on the single-cell level is dual whole-cell recording, which enables us to activate a presynaptic cell and record the unitary postsynaptic currents or potentials in the monosynaptically coupled partner cell that arise in response to the presynaptic action potential (Figure 5). Such direct measurement of the effect of PTI activity on individual PNs have described that PVBCs in the BA and the hippocampus evoke unitary inhibitory postsynaptic currents (uIPSCs) in local PNs with shorter latency than CCKBCs (Hefft & Jonas, 2005; Veres et al., 2017), while the amplitudes of these currents were described as comparable to (Glickfeld & Scanziani, 2006; Daw et al., 2009; Veres et al., 2017) or larger (Szabo et al., 2010) than those evoked by CCKBC firing. ChCs were also shown to provide larger uIPSCs than CCKBCs (Szabo et al., 2010; Kohus et al., 2016). Generally, CCKBC synapses exhibit higher failure rate when contacting PNs compared to PVBC or ChC output synapses, meaning that postsynaptic currents are evoked following CCKBC spikes with the lowest likelihood among the 3 PTI types. However, despite the high release probability from PVBC and ChC synapses in response to an action potential, subsequent spikes evoke smaller uIPSCs in the postsynaptic PNs, while uIPSCs evoked by CCKBCs show smaller short-term depression (the decrease in current amplitude), if any (Veres et al., 2014; Kohus et al., 2016; Barsy et al., 2017). These results show that PTIs provide inhibition to local PNs with markedly different features, but despite their position to efficiently regulate PN output, the features of these connection types have not been compared in association cortices like the mPFC.

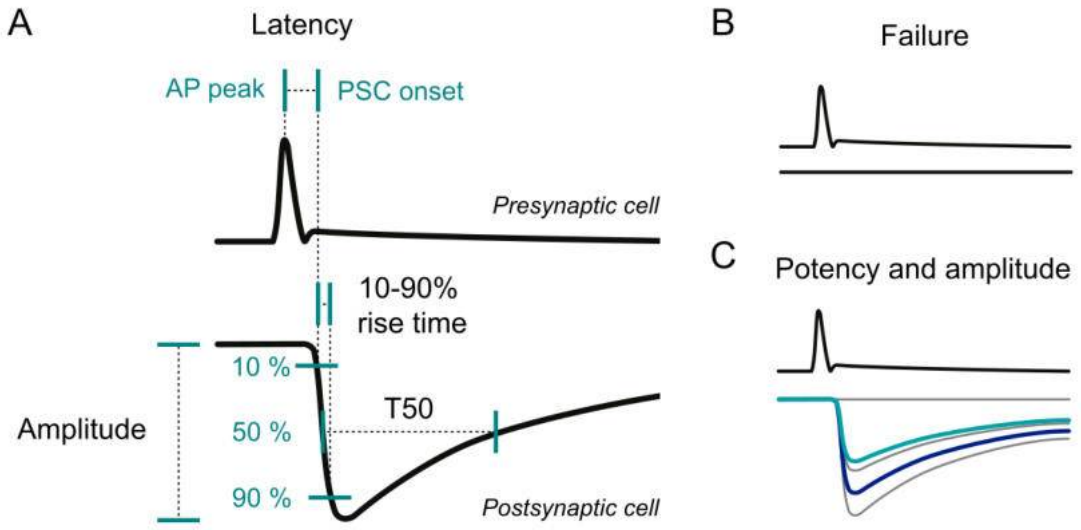

Figure 5. Properties of synaptic currents. (A) In response to a presynaptic action potential (top), several features of postsynaptic currents (bottom) can be quantified. Synaptic properties are denoted with black letters, points used for measuring them are marked with blue. (B) In the case of transmission failure, presynaptic action potential does not evoke a postsynaptic current. (C) Action potentials can be followed by transmission failures and postsynaptic currents with different properties. Synaptic potency (dark blue) is calculated by averaging individual postsynaptic currents without transmission failures, while synaptic amplitude (light blue) is an average that includes transmission failures as well. AP: action potential; PSC: postsynaptic current.

Excitatory connections from local PNs represent a major excitatory input to BCs (Ahrlund-Richter et al., 2019; Hafner et al., 2019), however, these connections received even less attention. An early influential study that investigated the excitation received by the two BC types in the hippocampus focused on the innervation provided by a population of PNs and not individual cells (Glickfeld & Scanziani, 2006). This work described that PVBCs received stronger excitation by the stimulated afferent pathways but did not explore the potential variances in single connections between PNs and BCs. In our previous paper, we showed with paired recordings that CCKBCs in the BA receive smaller unitary excitatory postsynaptic currents (uEPSCs) from local PNs than PVBCs and these currents have longer latency and longer decay (Andrasi et al., 2017). Another work in the mPFC found that the amplitude of uEPSCs evoked in PVBCs and ChCs are similar but did not include data from CCKBCs (Lu et al., 2017).

Since individual cells receive innervation from both BC types, BCs might enhance their role in regulating PN activity by inhibiting the other BC type. Shifts in the balance of innervation received by individual cells from the two BC types were reported on local excitatory cells in the hippocampus in response to spatial exploration or environmental enrichment (Hartzell et al., 2018; Feng et al., 2021; Yap et al., 2021), although these data do not confirm connectivity between the two BC types. However, more recent results suggest that the inverse relationship between hippocampal PV and CCKBC activity during locomotion is explained by the control of PV cells over CCKBC activity (Dudok, Klein, et al., 2021). On the other hand, no connectivity was found between the two BC types in the BA (Andrasi et al., 2017). As the role of a cell type can be tightly linked to their postsynaptic target (see ChCs or VIP cells that specialize in inhibiting other interneurons), investigating the connectivity between BCs in the PFC could contribute to our understanding of the microcircuit operations.

However, beyond the primary circuit motifs and synaptic features, connections are continuously shaped by experience. To understand how the intricate balance in the wiring of PTIs and PN networks plays a crucial role in a higher level cortical operations, such as memory formation, we investigated the changes in the excitation of PTIs in a classical learning paradigm, the Pavlovian fear conditioning, introduced in the next chapter.

1.4. The amygdala and fear learning

1.4.1. Pavlovian fear conditioning

Pavlovian fear conditioning is a paradigm to study the mechanisms underlying associative learning by utilizing the evolutionary conserved motivation to avoid danger. As animals learn that a previously neutral stimulus like a tone predicts a noxious stimulus like a footshock, they begin to express fear behavior in response to the tone as well, which is now the conditioned stimulus (CS). The CS can be associated with the footshock, the unconditioned stimulus (US) in just a few repetitions, if the CS co-terminates with the unavoidable US and rodents will display freezing behavior as a sign of fear, which is used as a measure of learning efficacy. These memories can last days or even weeks and trigger freezing when the animal is exposed to the CS, but can also be overwritten if the CS is no longer followed by the US, which is called extinction. From the initial theory of

forgetting, general consensus now views extinction as the formation of new memory (Myers & Davis, 2007). Investigation of the alterations associated with fear learning have provided useful insights into the correlates of learning from the synaptic to the circuit level.

Early studies established that the center for fear learning is the amygdala (LeDoux, 2003), but since then, multiple brain regions have been put on the map due to the extensive input and output connectivity of the amygdala nuclei (Sah et al., 2003; Janak & Tye, 2015). In general, the route of information during fear conditioning is as follows: higher order thalamic nuclei project to the LA, the nucleus regarded as the location where the association between CS and US happens (Rogan et al., 1997; Quirk et al., 1997). Then, information from the LA is transmitted to the BA and the central amygdala (CeA), the latter being responsible for evoking freezing behavior via its projections (Ciocchi et al., 2010; Amano et al., 2011; Janak & Tye, 2015; Yu et al., 2016). However, the BA has reciprocal connections with the PFC, which contributes to both fear memory expression and extinction via its projections from the PrL and the IL, respectively, and provides a top-down control over emotional behavior (Quirk et al., 2000; Runyan et al., 2004; Senn et al., 2014). The thalamus takes part in fear learning by relaying sensory information, although recent results suggested the thalamus as the location of association between CS and US, too (Barsy et al., 2020). Subcortical regions that provide neuromodulatory input to the amygdala like the ventral tegmental area or locus coeruleus are also involved in fear learning since release of dopamine and norepinephrine in the BLA also has a major impact on fear learning (Singewald et al., 2003; Fadok et al., 2009; de Oliveira et al., 2011; Giustino & Maren, 2018).

Taking a closer look at the local processes, it has been shown that fear learning involves the synaptic potentiation of projections arriving to the LA (McKernan & Shinnick-Gallagher, 1997; Rogan et al., 1997; LeDoux, 2000; Rumpel et al., 2005). These projections carry information about the CS and possibly the US from the posterior intralaminar (PIL) and suprageniculate (SG) thalamic nuclei, and can also converge on the same LA cell (Romanski et al., 1993; Bordi & LeDoux, 1994; Lanuza et al., 2008). As a result of fear conditioning, a subset of neurons in the LA (but also in input regions) become more responsive to the conditioned stimulus and these cells with increased responsiveness to the CS may drive changes in behavior (Collins & Pare, 2000; Sigurdsson et al., 2007; Herry et al., 2008). Fear neurons, cells that increase their activity in response to the CS were shown to emerge within the BA as well (Herry et al., 2008).

The emergence of fear neurons is dependent on many factors including the activity of local INs, the excitability of a given cell and the neuromodulators released by subcortical fibers (Han et al., 2007; Han et al., 2009; Yiu et al., 2014; Ryan et al., 2015; Bocchio et al., 2017). Dopamine for example was shown to promote synaptic plasticity and cue-dependent fear learning (Bissiere et al., 2003; Fadok et al., 2009), while norepinephrine also influences the effect of thalamic input that targets LA projection neurons by permitting long-term plasticity (LTP) at these synapses (Tully et al., 2007).

1.4.2. The importance of inhibitory circuits in fear conditioning

In addition to the excitatory and neuromodulatory inputs that enter the amygdala, the inhibitory circuitry also has a major role in fear learning (Figure 6, Tovote et al., 2015, Krabbe et al., 2018, Perumal et al., 2021). Clusters of intercalated cells (ITC) that can be found medially and laterally to the BLA are comprised of GABAergic cells. Via its monosynaptic connections on BLA output cells, ITC was shown to potently regulate fear extinction (Hagihara et al., 2021). Another amygdalar region that mainly consists of GABAergic cells is the CeA, a nucleus also tightly involved in fear acquisition and extinction due to the interactions within its inhibitory microcircuits (Ciocchi et al., 2010). Here, disinhibition was proposed as the circuit mechanism that determines the activity of projection neurons which will ultimately lead to freezing (Whittle et al., 2021).

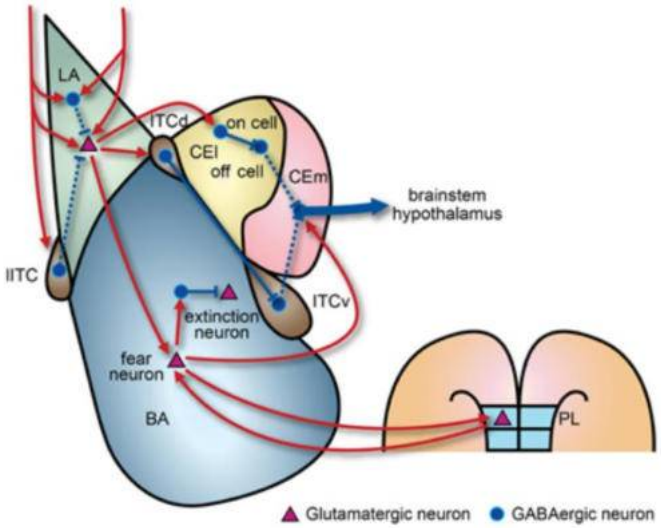

Figure 6. Successful fear conditioning involves the interplay of glutamatergic and GABAergic neurons in the BLA. During fear conditioning, incoming information

targets both PNs and INs in the LA. The information is transmitted to the BA, where local processes are also affected by the bidirectional connection with the PrL. BA: basal amygdala; ITC: intercalated cells; CEm: medial part of central amygdala; CEl: lateral part of central amygdala; LA: lateral amygdala; PL: prelimbic cortex (Adapted from Lee et al., 2013).

Within the BLA, inhibition was also recognized as a crucial factor in promoting or regulating fear learning (Bissiere et al., 2003; Shaban et al., 2006; Ehrlich et al., 2009). Interfering with the tonic level of inhibition in the BLA by $GABA_A$ receptor antagonists has anxiogenic effects (Sanders & Shekhar, 1995). Local GABAergic cells, promoted by cortical projections, provide an inhibitory tone that needs to be reduced so that LTP and fear learning can take place. Specifically, disinhibition in the BLA is a prerequisite for the acquisition of emotional memories (Bissiere et al., 2003; Tully et al., 2007). Among the numerous interneuron types, PV interneurons have been particularly implicated in disinhibiting the dendrites of local PNs and thereby promoting fear learning, but in parallel, they may control the precise spiking of PNs via their direct perisomatic inhibitory synapses. During the cue presentation, PV cells were shown to display higher activity and to inhibit somatostatin (Sst)-expressing inhibitory cells that preferentially target PN dendrites (Figure 7) (Wolff et al., 2014; Vereczki et al., 2016). This way PN dendrites are released from the inhibitory control of Sst cells which contributes to the association of the cue and the shock (Wolff et al., 2014). On the other hand, US presentation activates VIP cells in the BLA, the IN type that preferentially inhibits Sst and PV cells, and thereby promotes PN activation (Figure 6) (Krabbe et al., 2019).

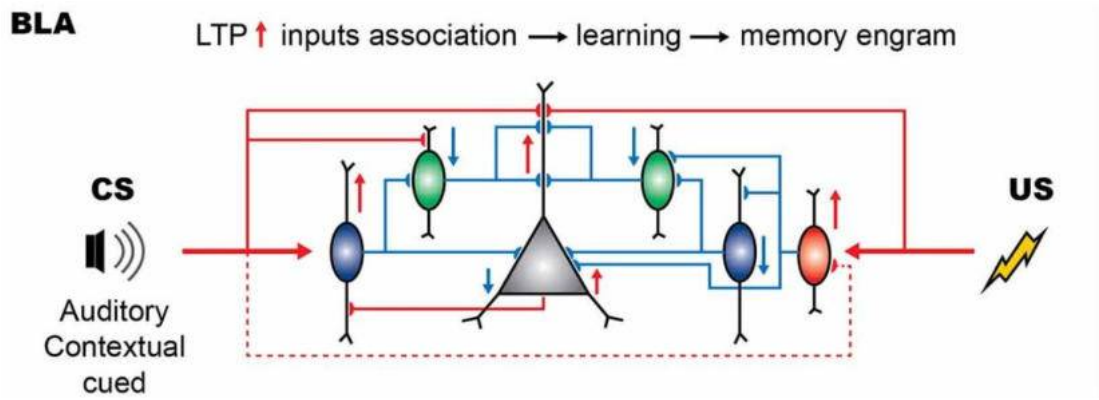

Figure 7. **Inhibitory cells in the BLA have different roles in fear conditioning.** Presentation of the CS excites PV neurons (blue) that inhibit dendrite-targeting Sst cells (green), leading to the disinhibition of PN dendrites that enables the association between the tone and the shock. In response to US presentation, VIP cells (red) that target both Sst and PV cells increase their activity and cause disinhibition at the somatic region of PNs. (Adapted from Singh & Topolnik, 2023)

Despite compelling evidence showing how IN activity is necessary for fear memory formation, fear expression and extinction, synaptic plasticity at the input site of INs that could drive changes in their activity has received less attention. A study from the BLA compared the changes of synaptic inputs on PV interneurons in the LA and BA after fear learning and found that the rate of mEPSCs in PV interneurons is changed only in the LA but not in the BA (Lucas et al., 2016). However, in that study PVBCs and ChCs were not distinguished, and given the fact that they respond to the CS markedly differently (Bienvenu et al., 2012), pooling data from these cells might mask changes in the input of the specific PTI types. Moreover, despite having the same potency to influence PN activity as PVBCs (Veres et al., 2017), there is no data yet regarding the changes in the excitatory input of CCKBCs following the fear conditioning paradigm. In our work we aimed to address the question whether the associative learning induces changes in the excitatory input of the 3 PTI types. Recording miniature events allowed us to study network changes not during fear conditioning but on a longer timescale.

2. OBJECTIVES

In order to uncover how the perisomatic region-targeting interneurons are embedded into the microcircuits of the PrL, and to investigate in the BA how excitatory inputs of PTIs are affected in a higher order cortical operation like memory formation, our aims were to:

1) Investigate how prelimbic PTIs integrate their input and translate it to output activity;
    - What are the active and resting membrane properties of PTIs?

2) Reveal the electrophysiological properties of excitatory and inhibitory connections between PNs and PTIs in the PrL;
    - What are the synaptic features of the uEPSCs evoked by PNs on PTIs?
    - How do uIPSCs evoked by PTIs on PNs differ?

3) Identify the connectivity of BCs in in the PrL;
    - Are the two BC types synaptically connected in the mPFC or do they form separate circuits?

4) Determine the changes in the excitatory inputs of PTIs in the BA following fear memory formation;
    - What are the effects of a tone, a footshock and complete fear conditioning on the features of mEPSCs recorded from the three PTIs?

3. METHODS

3.1. Animals

All procedures involving animals were performed according to methods approved by the Hungarian legislation (1998. XXVIII. section 243/1998, renewed in 40/2013) and institutional guidelines. All procedures were in compliance with the European convention for the protection of vertebrate animals used for experimental and other scientific purposes (Directive 2010/63/EU). Every effort was taken to minimize animal suffering and the number of animals used.

For the PFC study, both male and female adult mice (median age = 79 days, 1st and 3rd quartile: 72 and 98 days) were used in the electrophysiological experiments from the following transgenic mouse strains: BAC-CCK-DsRed (n=35) (Mate et al., 2013), BAC-PV-eGFP (n=48) (Meyer et al., 2002) and Pvalb-IRES-Cre crossed with BAC-CCK-DsRed (n=3). For anatomical quantification, C57Bl6 (n=3) and VGAT-IRES-Cre::BAC-CCK-GFP-coIN (n=4) (Vereczki et al., 2021) adult (P49-150) mice were used. Pvalb-IRES-Cre and VGAT-IRES-Cre were obtained from Jax.org (JAX stock: #008069 and #028862, respectively).

For the BA study, adult male mice (P40-100) were used from the following strains: BAC-CCK-DsRed, n =16; BAC-PV-eGFP, n =19; or their offspring expressing both eGFP and DsRed controlled by Pvalb and Cck promoters, respectively, were used (*n* =4).

3.2. Behavioral tests

Mice were housed in groups of 4–6 in the animal facility on a 12h light/dark cycle under controlled temperature (26.5℃). Four days before the experiments, mice were kept individually to avoid cross-influence of stress levels in behavioral experiments. Cue-dependent fear conditioning took place in a chamber with black dotted white background, slightly curved walls, metal rod floor, white illumination and was cleaned with 70% ethanol (context A). First, mice were allowed to habituate to this context for 5 min at Zeitgeber time (ZT) 2–3 h, then returned to their home cage. After 1 h, mice were transferred back to context A, where, after a 120 s long acclimation period, either of the following three protocols were used: (1) only CS group (n = 14): CS (7.5 kHz sound for 20 s) was presented 7 times without US (with 110 ± 23 s intervals; mean ± SD); (2) unsigned US group (n = 12): 7 CS and 7 US (mild electrical shocks, 2 mA for 1 s) were

presented randomly [with 111 ± 21 s intervals for CS and 110 ± 33 s intervals for US (mean ± SD)]; (3) signed US group (n = 13): 20 s-long CS presentations were co-terminated with the 1s-long US, pairs repeated 7 times at random intervals (110 ± 23 s; mean ± SD). On the next day at ZT 1–2 h, for testing cued fear expression, after a 120 s-long acclimation period, mice were subjected to a 20 s-long CS in a novel context (context B: square chamber with white background, paper floor, red illumination, cleaned with 1% acetic acid). Freezing (as an index of fear) was *post hoc* measured manually on video recordings with an in-house software (H 77, courtesy of Prof. József Haller, Institute of Experimental Medicine, Budapest, Hungary) by trained observers blind to the animal treatment. Freezing was defined as no visible movement of the body except that required for respiration. Freezing levels are expressed as a percentage (duration of freezing within the CS/total time of the CS or duration of freezing during baseline/total time of the baseline, respectively).

3.3. Electrophysiological recordings

3.3.1. Slice preparation

Animals that underwent the fear expression test were immediately transferred to the anesthetizing chamber and sacrificed for slice preparation. The brain was quickly removed from the skull following deep anesthesia induced by isoflurane and was placed into an ice-cold solution containing (in mM) 252 sucrose, 2.5 KCl, 26 $NaHCO_3$, 0.5 $CaCl_2$, 5 $MgCl_2$, 1.25 NaH_2PO_4 and 10 glucose, bubbled with 95% O_2/5% CO_2 (carbogen gas). Coronal slices of 200 µm thickness containing the PrL or horizontal slices of 200 µm thickness containing the BA were prepared with a vibratome (VT1200S, Leica Microsystems) and were incubated in an interface-type holding chamber for at least 1 hour in artificial cerebrospinal fluid (ACSF) that contained (in mM): 126 NaCl, 2.5 KCl, 1.25 NaH_2PO_4, 2 $MgCl_2$, 2 $CaCl_2$, 26 $NaHCO_3$, 10 glucose, bubbled with carbogen gas, and was let to gradually cool down from 36 °C to room temperature.

3.3.2. Electrophysiological recordings

During recordings, slices were placed into a submerged-type of chamber and were perfused with ACSF kept at 32 °C with a flow rate of 1.5-2 ml/min. Patch-clamp recordings were performed under visual guidance of a differential interference contrast

microscope (Nikon FN-1 model or BX61W Olympus upright microscope) using a 40x water dipping objective. Neurons were visualized with an sCMOS camera (Zyla 5.5, Andor Technology, Belfast, UK) and fluorescent protein expression was tested with the aid of a mercury arc lamp. Patch pipettes (4-7 MΩ) were pulled with a PC-10 puller (Narishige) from borosilicate capillaries with an inner filament (thin-walled, OD 1.5).

Pipettes used for patching interneurons for paired recordings with PNs were filled with an intracellular solution containing (in mM): 110 K-gluconate, 4 NaCl, 2 Mg-ATP, 20 HEPES, 0.1 EGTA, 0.3 GTP (sodium salt) and 10 phosphocreatine, adjusted to pH 7.3 using KOH with an osmolarity of 290 mOsm/L, while 10 mM GABA and 0.2% biocytin were added on the day of the experiments. This solution was used to record mEPSCs without adding GABA but with an additional 0.1 mM spermine. The intracellular solution used for recording PNs contained (in mM): 54 K-gluconate, 4 NaCl, 56 KCl, 2 Mg-ATP, 20 HEPES, 0.1 EGTA, 0.3 GTP (sodium salt) and 10 phosphocreatine adjusted to pH 7.3 using KOH, with an osmolarity of 290 mOsm/L. This solution was used with an additional 0.2% biocytin and 10 mM GABA when paired recordings were performed between two interneurons. For optogenetic and pharmacological experiments the following intracellular solution was used (in mM): 60 Cs-gluconate, 80 CsCl, 1 $MgCl_2$, 2 Mg-ATP, 10 HEPES, 3 NaCl, 5 QX-314-Cl adjusted to pH 7.4 using HCl with an osmolarity of 280 mOsm/L and 0.2% biocytin was added on the day of the experiments.

Whole-cell patch clamp recordings were performed with a Multiclamp 700B amplifier (Molecular Devices, San Jose, CA, USA), low-pass filtered at 3 kHz, digitized at 10-50 kHz and not corrected for junction potential. Data were recorded with Clampex 10.4 (Molecular Devices) or an in-house acquisition and stimulus software (Stimulog, courtesy of Prof. Zoltán Nusser, Institute of Experimental Medicine, Budapest, Hungary), and were analyzed with Clampfit 10.4 (Molecular Devices), EVAN 1.3 (courtesy of Prof. Istvan Mody, Department of Neurology and Physiology, University of California, Los Angeles, CA) and OriginPro 2018 (OriginLab Corp, Northampton, MA, USA).

3.3.2.1. Single-cell properties

The protocol used for recording firing patterns in current-clamp mode consisted of alternating 800-ms-long depolarizing and hyperpolarizing current steps with an amplitude increasing to +100 and -100 pA in 10 pA increments, then to +300 pA in 50 pA

increments, and finally to 600 pA in 100 pA increments. A holding potential of -65 mV was applied during the recordings.

3.3.2.2. Paired recordings.

Analyzed synaptic connections between interneurons and PNs were recorded with 5 action potentials elicited at 33 Hz with an inter-stimulus interval of 20 seconds. Series resistance (Rs) of the postsynaptic cell was continuously monitored and recordings in which the Rs exceeded 20 MΩ or changed more than 20%, or in which the analyzed features of the postsynaptic response showed changes were not included in the analysis of postsynaptic currents. Postsynaptic cells were clamped at -65 mV. Reported features of the postsynaptic currents are based on the analysis of the postsynaptic response evoked by the 1st action potential in each train of stimuli. The potency of synaptic connections were calculated by averaging the amplitudes of individual uPSCs excluding transmission failures, while the amplitude of synaptic connections was calculated by dividing the sum of the amplitudes of individual uPSCs by the number of stimulus trains i.e. this measure includes transmission failures. Latency was measured from the peak of presynaptic action potential to the onset of the postsynaptic current, defined by 10% of the peak amplitude. The presence of gap junctions between interneurons was tested by injecting 800-ms-long current steps into one of the recorded cells that induced hyperpolarization of at least 10 mV of amplitude while simultaneous voltage deflections were monitored in the other cell in current-clamp mode (I=0). Chemical connections between homotypic BCs were recorded by eliciting 10 action potentials at 40 Hz with an inter-stimulus interval of 20 seconds in the presence of AM251 (1 μM).

3.3.2.3. Miniature excitatory postsynaptic currents (mEPSCs)

Neurons were held at a holding potential of -65 mV in voltage clamp mode to record mEPSCs in the presence of tetrodotoxin (TTX, 1 μM) and gabazine (5 μM) in the PFC or TTX (0.5 μM) and picrotoxin (100 μM) in the BA. TTX blocks voltage-gated Na^+ channels, whereas gabazine and picrotoxin antagonize $GABA_A$ receptors. Recordings were obtained within the series resistance (Rs) range of 9–15 MΩ but analysis was carried out on segments of recordings during which the series resistance did not change by more than 10%. The average Rs values for BA recordings in each group were (mean ± SD in MΩ): PVBC only CS: 11.29 ± 1.30, unsigned US: 11.23 ± 1.76, signed US: 10.49 ± 0.81;

CCKBC only CS: 10.85 ± 1.71, unsigned US: 10.24 ± 1.23, signed US: 10.28 ± 1.53; AAC only CS: 11.63 ± 1.80, unsigned US: 11.30 ± 1.58, signed US: 11.29 ± 1.08).

Analysis was performed on the recordings obtained between 5 and 10 min after establishing whole cell configuration. The analyzed time period (30–120 s) contained 110-130 events from 5 CCKBCs and 5 PVBCs recorded in the mPFC or approximately 200 consecutive events/neuron from the BA. The instantaneous rate, amplitude and rise time kinetics were measured on mEPSCs recorded in the mPFC on individual events and decay time constants were quantified on averages from each cell. Kinetics of mEPSCs recorded from the BA were analyzed on the average trace of approximately 150 selected events. 10–90% of rise time was measured with Clampfit 10.4, the decay time constant (tau) was calculated by fitting an exponential curve on the average trace in Origin 2021. Statistical analysis was performed on the pooled datasets in each group.

3.3.2.4. Pharmacological experiments

The presence of inhibitory inputs on PVBCs originating from CCKBCs was tested by evoking postsynaptic currents in PVBCs by using extracellular stimulation with theta electrodes in brain slices prepared from BAC-PV-eGFP mice. Blockade of ionotropic glutamate receptor-mediated postsynaptic currents was achieved by adding 2 mM kynurenic acid in the recording solution. The electrode was placed into the slice approximately 200-250 µm away from the recorded PVBC, minimizing the chance of direct stimulation. The intensity of the 1-ms-long stimuli was set to evoke responses with the amplitude of at least 300 pA while neurons were held at -65 mV in voltage-clamp mode. QX-314 was intracellularly applied to eliminate action potential generation due to the outward flow of Cl^- ions upon the opening of $GABA_A$ receptors.

3.3.2.5. Optogenetic experiments

For testing PVBC input on CCKBCs, we performed simultaneous whole-cell recordings from CCKBCs and PNs in brain slices prepared from mice obtained by crossing the Pvalb-IRES-Cre with the BAC-CCK-DsRed mice. Offspring were injected with AAV5-EF1a-DIO-hChR2-eYFP (200 nl, $3.2x10^{12}$ vg/ml, University of North Carolina Vector Core, catalog# 35509-AAV5) in the mPFC at P120 to enable optogenetic control of local PVBC activity. ChR2 expression was allowed for 4-6 weeks before animals were sacrificed for *in vitro* experiments. Optogenetic stimulation was achieved

by 3 pulses of 5-ms-long blue laser illumination (447 nm, Thorlabs) at 20 Hz at 2.5 mW/mm^2 intensity applied through a 40x objective. Recording postsynaptic currents at the same time from PNs and CCKBCs held at -65 mV proved the optical stimulation of PV+ cells to be successful in all slices.

3.3.3. *Post-hoc* identification of cell types

After the recordings, slices were placed into a fixative solution containing 4% paraformaldehyde in 0.1 M phosphate buffer (pH=7.4) to enable *posthoc* visualization of biocytin filled interneurons by applying fluorophore conjugated streptavidin (Cy3-SA or Alexa488-SA (1:10,000, Sigma-Aldrich and Molecular Probes, respectively)).

Biocytin-filled PVBCs in the PFC were distinguished from fast-spiking ChCs based on the morphology of their axons (Nagy-Pal et al., 2023), while CCKBCs showed strong DsRed expression and accommodating firing pattern. To distinguish between PVBCs and ChCs in the BA, immunostaining against calbindin was performed (rabbit anti-calbindin 1:3000 (Swant, CB-38a) or chicken anti-calbindin, 1:1000 (SYSY #214006)), revealed with Cy3-coupled donkey anti-rabbit or anti-chicken secondary antibodies, respectively, (1:500, Jackson)). Interneurons with calbindin expression in their somata and/or axon terminals were considered BCs (Vereczki et al., 2016), while ChCs were defined by no immunoreactivity for calbindin and displayed characteristic cartridges of terminals surrounding putative axon initial segments (AISs), that were visualized with Ankyrin G staining in case of 7 ChCs (rabbit anti-Ankyrin G, 1:100, Santa Cruz sc-28,561, visualized with Cy3-coupled donkey anti-rabbit antibody, Jackson) (Gulyas et al., 2010; Veres et al., 2014). CB1 content of CCKBCs in the PFC was tested with immunolabeling using rabbit anti-CB1 primary antibody (1:1000, Cayman, # 10006590)) and revealed with Alexa405-coupled donkey anti-rabbit secondary antibody (1:500, Jackson). In the BA, immunostaining using rabbit anti-CB1 (1:1000, Cayman, # 10006590) or guinea pig anti-CB1 (1:1000, Frontier Institute, CB1-GP-Af530) were visualized either with Alexa647-coupled donkey anti-rabbit secondary antibody (1:500, Jackson) or Alexa405-coupled donkey anti-guinea pig secondary antibody (1:500, Jackson). Only those cells with CB1 receptor expression on their axonal boutons were included in the study. PNs in the mPFC were identified based on their slower membrane kinetics and their distinctive firing pattern characterized by regular spiking and characteristic afterhyperpolarization.

Slices were mounted in Vectashield (Vector Laboratories) and confocal images were taken using a Nikon C2 microscope using CFI Super Plan Fluor 20X objective (N.A. 0.45; z step size: 1 µm, xy: 0.31 µm/pixel) and CFI Plan Apo VC60X Oil objective for higher magnification (N.A. 1.40; z step size: 0.25 µm, xy: 0.08 µm/pixel).

3.4. Immunohistochemistry to label heterotypic basket cell contacts in the mPFC

For labeling putative contacts in the mPFC to visualize CCKBC input on PVBCs, C57Bl6 (wild type) mice (n=3) were deeply anaesthetized and transcardially perfused with 4% paraformaldehyde in 0.1 M phosphate buffer (pH7.4). Coronal sections of 80-µm thickness containing the mPFC were prepared with a vibratome (VT1000S, Leica Microsystems). The mixture of goat anti-CB1 (1:1000, Frontier Institute; catalog no. CB1-Go-Af450), mouse anti-Gephyrin (1:1000, SYSY, #147 021) and guinea pig anti-PV primary antibodies (1:5000, SYSY; catalog no. 195 004) was used for 3 days: first night at room temperature, then at 4 ^{o}C. Then the following mixture of secondary antibodies was used for 4 hours at room temperature: donkey anti-goat coupled with Alexa405, donkey anti-mouse coupled with Alexa488 and donkey anti-guinea pig coupled with Alexa647.

For labeling putative contacts on CCKBCs from PVBCs, mPFC slices were prepared from VGAT-IRES-Cre::BAC-CCK-GFP-coIN mice (n=4) as described above. The mixture of goat anti-CB1, chicken anti-GFP, mouse anti-Gephyrin and guinea pig anti-PV primary antibodies was used for 2 days: first night at room temperature, then at 4 ^{o}C. Then the following mixture of secondary antibodies was used for 4 hours at room temperature: donkey-anti goat coupled with Alexa405, donkey-anti chicken coupled with Alexa488, donkey-anti mouse coupled with Cy3, donkey-anti guinea pig coupled with Alexa647.

Slices were mounted in Vectashield, then confocal images were taken using a Nikon microscope with CFI Plan Apo VC60X Oil objective (N.A. 1.40; z step size: 0.125 µm, xy: 0.08 µm/pixel). Using 3D confocal images, interneurons within ~30 µm depth from the surface of the sections were selected for analysis irrespective of the number of synaptic contacts on them. The surface of the somata and the putative contacts on it (i.e., where a bouton closely opposed the cell surface and a gephyrin puncta was found between them) were manually labeled and quantified with Neurolucida 10.53 software (MBF Bioscience).

3.5. Statistical tests

In the mPFC study, Kruskal-Wallis ANOVA and *post hoc* Dunn's test was used to assess statistical significance in the case of single cell properties and uIPSC datasets. Data from only the two BC types were compared with Mann-Whitney U-test. Cumulative frequency distributions of mEPSC parameters in mPFC recordings were compared with Kolmogorov-Smirnov test. Recordings of the three PTI types in the BA were compared with Kruskal-Wallis ANOVA and *post hoc* Dunn's test. The level of significance was set to 0.05. Statistics were performed using Origin 2018 or Origin 2021.

3.6. Personal contribution to the results

In the PFC study, I performed most of the paired recordings and their analysis. Single cell properties were analysed by colleagues. I carried out all the remaining electrophysiological experiments (mEPSC recordings and investigating heterosynaptic BC connections with optogenetics and pharmacological tools) and their analysis. Virus injections, immunostainings and anatomical quantifications of heterotypic BC connections were performed by colleagues.

I participated in the BA study by performing about half of the mEPSC recordings. Behavioral tests and their analysis and the analysis of mEPSC properties were performed by colleagues.

4. RESULTS

4.1. Part I: The microcircuit of pyramidal neurons and perisomatic region-targeting inhibitory cells in the mouse prefrontal cortex

4.1.1. Contrasting active and resting membrane properties of basket cells in the PrL

One of the key factors that determine the function of a given cell type is how its inputs are integrated and converted into output activity. Therefore, we first studied the active and resting membrane properties of PTIs. Acute slices containing the PrL were prepared from BAC-CCK-DsRed or BAC-PV-eGFP mice, where CCKBCs or PVBCs and ChCs express fluorescent proteins, respectively (Nagy-Pal et al., 2023), allowing their identification prior to recordings. Following in vitro electrophysiological recordings, *post hoc* identification based on morphology (Nagy-Pal et al., 2023) and firing pattern ensured that only PTIs were included in the study (Figure 8A, 8B). Analysis of voltage responses upon the injection of hyperpolarizing and depolarizing current steps revealed that PVBCs had the smallest input resistance, the fastest membrane time constant and more hyperpolarized spike threshold than CCKBCs and ChCs (Figure 8C, Table 1). Among the three PTI types, ChCs had the smallest capacitance. CCKBCs fired with the lowest maximum rate, while PVBCs and ChCs exhibited a fast spiking phenotype and showed significantly less accommodation than CCKBCs (Figure 8B, 8C, Table 1), a notable difference between the PTI types also found previously in other cortical areas (Pawelzik et al., 2002; Glickfeld & Scanziani, 2006; Daw et al., 2009; Szabo et al., 2010; Barsy et al., 2017). The spikes of ChCs and PVBCs were similarly narrow, but were followed by significantly larger afterhyperpolarization (AHP) in PVBCs (Figure 8C, Table 1). These diverse membrane properties suggest that signals in the three PTI types are translated into distinct activity patterns and have different integration properties in the PrL as it has been first proposed about basket cells in the hippocampus (Glickfeld & Scanziani, 2006).

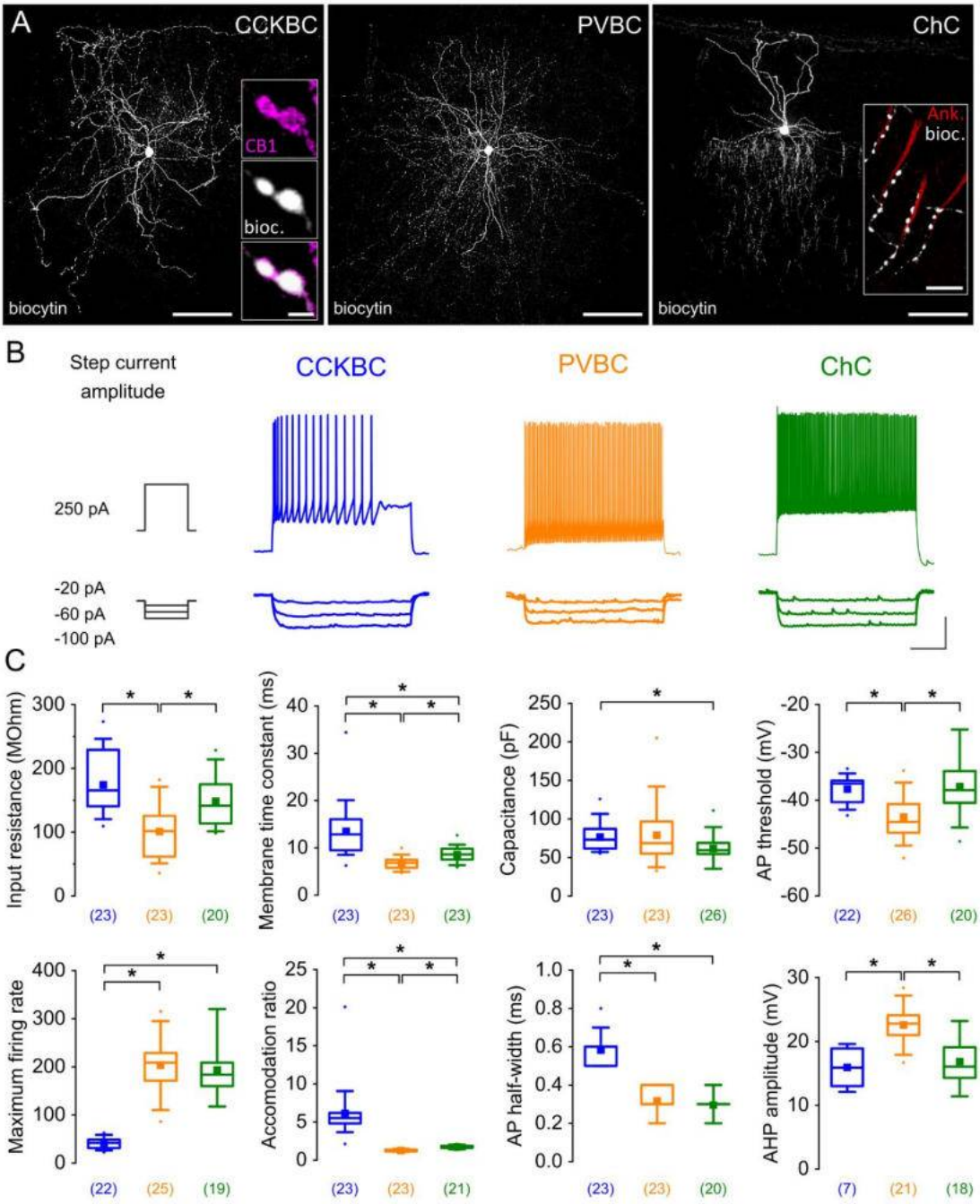

Figure 8. Analysis of in vitro recorded PTI firing patterns reveals significant differences regarding their intrinsic membrane properties. (A) Maximum intensity projections of a biocytin-filled CCKBC, PVBC and ChC in the PrL. Insets: Axon terminals of a CCKBC co-express CB1 and biocytin (left), axonal cartridges surround AISs visualized with Ankyrin G staining (right). Scale bars: 100 µm and 1 µm. (B) Representative traces of PTI responses following step current injections. Scale bar: x=200 ms, y=20 mV. (C) Comparison of intrinsic electrophysiological properties uncovers

substantial differences between the three PTI types. Boxes in this and the other figures represent the interquartile range; filled square: mean; whiskers: 5th and 95th percentile. Numbers in parentheses represent the number of analyzed recordings from n=13, n=12 and n=13 animals for CCKBC, PVBC and ChC recordings, respectively. For details see Table 1. AP: action potential; AHP: afterhyperpolarization. (Figure modified from Fekete et al., 2024).

Table 1. Summary of single-cell features, properties of uPSCs and mEPSCs.

P-values below the level of significance are in bold. AP, action potential; AHP, afterhyperpolarization; KS, Kolmogorov-Smirnov test; mEPSC, miniature excitatory postsynaptic current; MTC, membrane time constant; MW, Mann-Whitney test; RT, rise time, uEPSC, unitary excitatory postsynaptic current; uIPSC, unitary inhibitory postsynaptic current. (Modified from Fekete et al., 2024).

	Parameter	Cell type	median (1st and 3rd quartile)	N	Group comparison (KW-ANOVA)	Pairwise comparison	p-value of pairwise comparison
Single cell properties	Input resistance (MΩ)	CCKBC	165.5 (140.6, 229.1)	23	**< 0.001**	CCKBC vs. PVBC	**<0.001**
		PVBC	101.5 (61.55, 125.5)	23		CCKBC vs. ChC	0.436
		ChC	113.63 (141.5, 176.98)	20		PVBC vs. ChC	**0.004**
	MTC (ms)	CCKBC	12.85 (9.49, 16.04)	23	**< 0.001**	CCKBC vs. PVBC	**<0.001**
		PVBC	6.83 (5.78, 7.47)	23		CCKBC vs. ChC	**0.004**
		ChC	7.54 (8.6, 9.81)	23		PVBC vs. ChC	**0.007**
	Capacitance (pF)	CCKBC	73.11 (61.63, 87.13)	23	**0.014**	CCKBC vs. PVBC	0.588
		PVBC	68.58 (54.97, 96.53)	23		CCKBC vs. ChC	**0.011**
		ChC	53.78 (59.46, 69.55)	26		PVBC vs. ChC	0.342
	AP threshold (mV)	CCKBC	-36.5 (-40.4, -35.9)	22	**< 0.001**	CCKBC vs. PVBC	**<0.001**
		PVBC	-44.55 (-46.8, -40.8)	26		CCKBC vs. ChC	1
		ChC	-40.83 (-37.9, -33.85)	20		PVBC vs. ChC	**<0.001**
	AP half-width (ms)	CCKBC	0.6 (0.5, 0.6)	23	**< 0.001**	CCKBC vs. PVBC	**<0.001**
		PVBC	0.3 (0.3, 0.4)	23		CCKBC vs. ChC	**<0.001**
		ChC	0.3 (0.3, 0.3)	20		PVBC vs. ChC	1

	Parameter	Cell type	median (1st and 3rd quartile)	N	Group comparison (KW-ANOVA)	Pairwise comparison	p-value of pairwise comparison
Single cell properties	AHP amplitude	CCKBC	15.9 (13, 18.9)	7	**< 0.001**	CCKBC vs. PVBC	**0.001**
		PVBC	22.8 (21, 24.1)	21		CCKBC vs. ChC	1
		ChC	14.2 (16.05, 19.3)	18		PVBC vs. ChC	**<0.001**
	Accomodation ratio	CCKBC	5.51 (4.81, 6.2)	22	**< 0.001**	CCKBC vs. PVBC	**<0.001**
		PVBC	1.27 (1.15, 1.38)	25		CCKBC vs. ChC	**<0.001**
		ChC	1.58 (1.82, 1.87)	19		PVBC vs. ChC	**<0.001**
	Max. firing rate (Hz)	CCKBC	41.9 (31.3, 48.8)	22	**< 0.001**	CCKBC vs. PVBC	**<0.001**
		PVBC	208.8 (171.3, 228.8)	23		CCKBC vs. ChC	**<0.001**
		ChC	160 (183.8, 208.8)	19		PVBC vs. ChC	1.00
uEPSC	Potency (pA)	CCKBC	17.27 (16.06, 19.8)	13	-	MW	**< 0.001**
		PVBC	60.56 (35.04, 84.46)	20			
	Amplitude (pA)	CCKBC	15.09 (13.02, 17.4)	13	-	MW	**< 0.001**
		PVBC	50.89 (27.95, 84.46)	20			
	Failure rate	CCKBC	0.12 (0.03, 0.19)	13	-	MW	0.523
		PVBC	0.06 (0, 0.16)	20			
	Latency (ms)	CCKBC	1.23 (0.84, 1.8)	12	-	MW	**< 0.001**
		PVBC	0.64 (0.48, 0.82)	18			
	RT 10-90% (ms)	CCKBC	0.79 (0.38, 0.81)	13	-	MW	**< 0.001**
		PVBC	0.3 (0.21, 0.35)	20			
	T50 (ms)	CCKBC	2.86 (1.68, 3.5)	12	-	MW	**< 0.001**
		PVBC	1.29 (0.84, 1.71)	18			
mEPSC	Instantaneous rate (s^{-1})	CCKBC	10.91 (5.42, 25.46)	622	-	KS	**< 0.001**
		PVBC	20.42 9.18, 48.79)	626			
	Amplitude (pA)	CCKBC	15.83 (13.2, 20.52)	617	-	KS	**< 0.001**
		PVBC	28.48 (18.68, 44.89)	616			

	Parameter	Cell type	median (1st and 3rd quartile)	N	Group comparison (KW-ANOVA)	Pairwise comparison	p-value of pairwise comparison
mEPSC	RT 20-80% (ms)	CCKBC	0.44 (0.25, 0.66)	613	-	KS	**< 0.001**
		PVBC	0.21 (0.13, 0.34)	612			
	Decay time constant (ms)	CCKBC	1.99 (1.96, 2.5)	5	-	MW	**0.022**
		PVBC	1.33 (1.29, 1.41)	5			
uIPSC	Potency (pA)	CCKBC	29.83 (16.65, 60.18)	19	0.14	-	-
		PVBC	38.21 (29.96, 120.62)	21			
		ChC	28.54 (44.86, 56.06)	22			
	Amplitude (pA)	CCKBC	18.71 (9.39, 38.3)	19	**0.009**	CCKBC vs. PVBC	**0.009**
		PVBC	38.21 (29.8, 120.62)	21		CCKBC vs. ChC	0.065
		ChC	26.36 (41.6, 56.06)	22		PVBC vs. ChC	1.000
	Failure rate	CCKBC	0.35 (0.08, 0.5)	19	**< 0.001**	CCKBC vs. PVBC	**<0.001**
		PVBC	0 (0, 0.06)	21		CCKBC vs. ChC	**<0.001**
		ChC	0 (0, 0.1)	23		PVBC vs. ChC	1.000
	Latency (ms)	CCKBC	1.38 (0.98, 1.71)	19	**< 0.001**	CCKBC vs. PVBC	**<0.001**
		PVBC	0.71 (0.63, 0.83)	21		CCKBC vs. ChC	**0.002**
		ChC	0.6 (0.94, 1.08)	23		PVBC vs. ChC	0.319
	RT 10-90% (ms)	CCKBC	0.61 (0.53, 0.75)	17	0.117	-	-
		PVBC	0.58 (0.47, 0.66)	21			
		ChC	0.45 (0.52, 0.63)	22			
	T50 (ms)	CCKBC	4.55 (3.34, 5.55)	16	0.416	-	-
		PVBC	4.08 (3.31, 4.95)	21			
		ChC	3.37 (3.8, 4.55)	21			
Homotypic connections	Potency (pA)	CCKBC	26.7 (21.07, 37.53)	4	-	MW	0.241
		PVBC	33.28 (28, 116.85)	6			
	Failure rate	CCKBC	0.62 (0.5, 0.65)	5	-	MW	**0.013**
		PVBC	0.03 (0, 0.09)	6			

	Parameter	Cell type	median (1st and 3rd quartile)	N	Group comparison (KW-ANOVA)	Pairwise comparison	p-value of pairwise comparison
Homotypic connections	Latency (ms)	CCKBC PVBC	1.02 (0.9, 1.36) 0.64 (0.44, 1.06)	4 6	-	MW	0.166

4.1.2. Local PNs evoke larger uEPSCs on PVBCs with short latency and fast kinetic properties

To determine how PTIs are embedded into the local excitatory network, we investigated the excitatory connections between PNs and PTIs by performing paired recordings and analyzed the properties of the unitary excitatory postsynaptic currents (uEPSCs) evoked by the 1st action potential in each spike train (Figure 9A, 9B, Table 1). Our recordings revealed that uEPSCs evoked in PVBCs have significantly larger amplitude than those evoked in CCKBCs (Figure 9C, Table 1). Moreover, uEPSCs in PVBCs followed the presynaptic action potentials with significantly shorter latency than those in CCKBCs (Figure 9C, Table 1), suggesting that over the course of the first milliseconds after the activation of PNs, local excitatory signals reach different BC populations. Besides this temporal preference for exciting PVBCs, release from excitatory synapses to CCKBCs or PVBCs were found to be similarly successful. Kinetic properties of uEPSCs recorded from CCKBCs were significantly slower both in terms of their 10-90% rise time and half-width of events, the time span measured at the half amplitude (T50) (Figure 9C, Table 1). Due to the low connectivity rate between PNs and ChCs sampled in our experiments (12.2%, 6 pairs from 49 tests), data from these recordings are not included in the analysis, as only 3 pairs met the criteria of low series resistance and sufficient number of uIPSCs.

Synaptic connections are characterized by diverse dynamics at the short-term time scale that are dependent on the pre- and postsynaptic partners (Ali et al., 1998; Reyes et al., 1998). To unravel whether excitatory synapses on BCs become potentiated or depressed during sustained presynaptic activation we delivered trains of square pulses to evoke 5 action potentials at 33 Hz and compared the amplitude of the postsynaptic currents (Figure 9D, 9E). The amplitude of uEPSCs in PVBCs received from local PNs did not decrease considerably and remained in the 80-106% range of the first uEPSC on average (2nd uEPSC: 106.08±4.96% and 5th uEPSC: 79.64±5.86%). Conversely,

CCKBCs were found to be innervated by depressing excitatory synapses, as the amplitude of the 2nd and 5th uEPSCs decreased on average to 56.23±5.31% and 30.02±3.5% of the first uEPSC, respectively. The probability of finding a connection was dependent on the cell type ($p=0.023$, chi-square=7.508) and was highest with PVBCs (Figure 9F) in agreement with previous studies (Andrasi et al., 2017; Lu et al., 2017). Taken together, our data suggest that the excitation generated within the prelimbic networks distinguishes between the two types of BCs in a number of aspects: PVBCs receive larger and faster synaptic excitation that is maintained if repetitive firing in PNs is induced, whereas the local PN population gives rise to smaller and slower postsynaptic events in CCKBCs that show prominent depression when trains of action potentials are evoked in PNs.

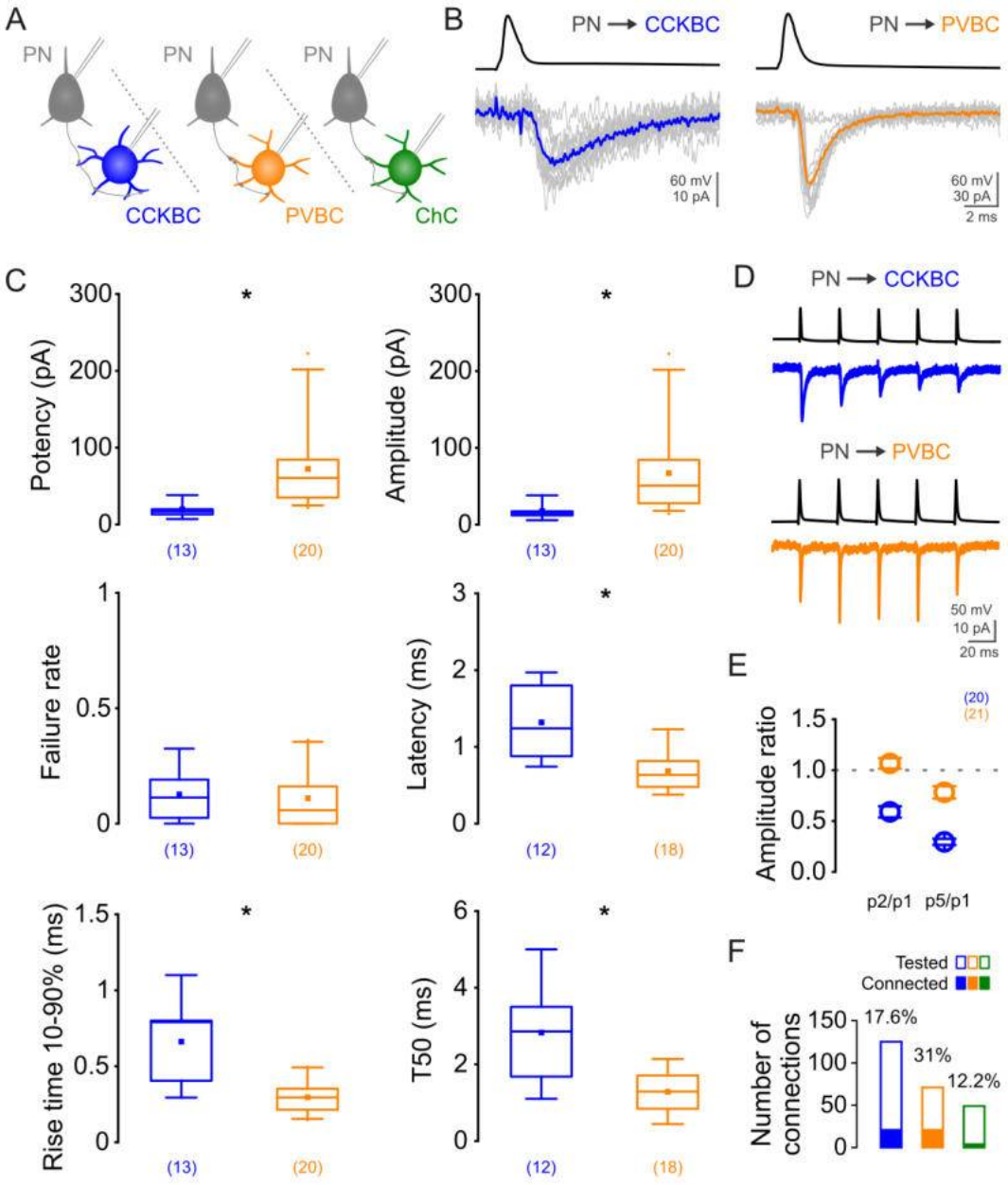

Figure 9. Paired recordings between PNs and PTIs unveil larger unitary excitatory postsynaptic currents (uEPSCs) in PVBCs exhibiting faster kinetics than uEPSCs in CCKBCs. (A) Schematic illustration of the experiment. (B) Representative traces of the first evoked AP in a train of 5 APs in PNs (top) and the postsynaptic uEPSCs recorded in PTIs (bottom). Fifteen consecutive traces in gray, average in color. (C) Comparison of the main properties of the first uEPSCs. For details see Table 1. (D) Representative traces of synapse type-dependent short-term plasticity revealed by 5 evoked APs in the presynaptic cell. (E) Ratio of the amplitude of the 2nd and 1st (2/1) or the 5th and 1st (5/1) uEPSCs summarizes the short-term dynamics of

the excitatory connections between PNs and PTIs. Data presented as mean ± SEM. Numbers in parentheses represent the number of analyzed recordings from n=17, n=16 and n=20 animals for CCKBC, PVBC and ChC recordings, respectively. (F) Connection probability was largest between PNs and PVBCs. (Adapted from Fekete et al., 2024)

4.1.3. Kinetic properties of mEPSCs

To address whether the different kinetic properties of uEPSCs from neighboring PNs were a general feature of excitation arriving onto BCs in the PrL, we recorded miniature excitatory postsynaptic currents (mEPSCs) in the two BC types in the presence of tetrodotoxin (TTX, 1 μM) and gabazine (5 μM) to block voltage-gated Na^+ channels and $GABA_A$ receptors, respectively (Figure 10A, 10B). Comparison of a similar number of recorded events (110-130 mEPSCs) from each cell revealed that PVBCs received mEPSCs at a higher rate and these events had larger peak amplitudes than those arriving on CCKBCs (Figure 10C, Table 1). The rise time 20-80% of miniature events on CCKBCs were slower, similarly to the unitary events evoked in paired recordings (Figure 10C, Table 1). Furthermore, peak scaled averages also demonstrate the slower decay of mEPSCs recorded in CCKBCs (Figure 10D), confirmed by the decay time constant assessed on the averaged events in case of each recorded cell (Figure 10E, Table 1). These results suggest that the differential kinetic properties of excitatory postsynaptic events obtained in paired recordings are not due to sampling biases in our data but reflect the distinct features of local excitatory inputs on the two BC types.

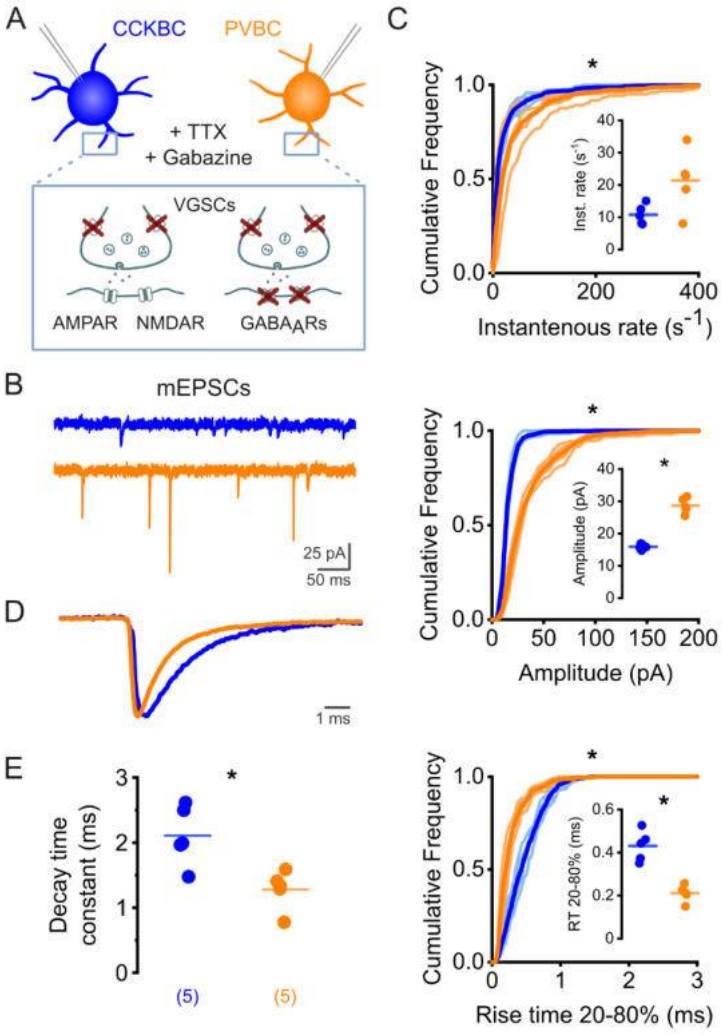

Figure 10. Differences in the kinetics of mEPSCs recorded in BCs resemble the uEPSCs evoked in paired recordings. (A) mEPSCs recorded in BCs in the presence of TTX (1 µM) and gabazine (5 µM) to block voltage-gated sodium channels (VGSCs) and $GABA_A$ receptors ($GABA_ARs$). (B) Representative traces of recordings obtained in the two BC types. (C) Cumulative frequency plots showing that PVBCs receive miniature events with higher instantaneous rate (top), amplitude (middle) and exhibit faster rise time kinetics (bottom). Thin lines represent data from individual cells, thick lines represent average. Insets: median values of mEPSC parameters obtained in each cell (n = 5 for both cell types). (D) Normalized averages of mEPSCs recorded in CCKBCs and PVBCs (n = 5 for both cell type) demonstrate the slower decay kinetics of mEPSCs recorded in CCKBCs. (E) mEPSCs in CCKBCs on average are characterized by longer decay time constants. Data points represent decay time constants measured on the averages of mEPSCs recorded in individual cells, lines

represent mean. Numbers in parentheses represent the number of analyzed recordings from n=2 animals for CCKBC and n=2 animals for PVBC recordings. (Adapted from Fekete et al., 2024)

4.1.4. Fast spiking INs innervate local PNs with reliable but depressing synapses

The influence of PTIs on prelimbic processes is largely determined by their impact on postsynaptic partners. To uncover the effect of single PTIs on neighboring PNs in the PrL we performed paired recordings between these cells (Figure 11A, 11B). Action potentials evoked in PVBCs elicited unitary inhibitory postsynaptic currents (uIPSCs) in PNs with significantly larger amplitude than those evoked by CCKBC spikes (Figure 11C, Table 1). While PVBC and ChC synapses were highly reliable, almost every third action potential in CCKBCs failed to evoke a uIPSC in PNs, leading to a significant difference between their failure rates. Notably, postsynaptic events upon PVBC and ChC discharges showed significantly shorter latency than those following CCKBC activation. Nonetheless, the three PTI types evoke postsynaptic events in PNs with similar kinetics both in terms of their 10-90% rise time and T50 (Table 1).

Investigation of the short-term dynamics in these inhibitory synapses with the same protocol described above revealed that uIPSCs evoked by CCKBCs became neither potentiated nor depressed (90.68±5.6% and 100.85±8.29% of the 1st response) (Figure 11D, 11E) (Hefft & Jonas, 2005; Galarreta et al., 2008). On the other hand, synapses arriving from PVBCs showed significant short-term depression (2nd and 5th uIPSC amplitude decreased to 71.4±3.4% and 46.27±2.62% of the 1st response), a phenomenon previously observed in other cortical regions as well (Galarreta & Hestrin, 1998; Hefft & Jonas, 2005; Szabo et al., 2010; Barsy et al., 2017) (Figure 11D, 11E). ChC synapses also evoked depressing postsynaptic currents very similarly to PVBCs (72.07±3.5% and 56.02±4.8%). Neighboring PNs were innervated by PTIs with a probability that was dependent on the cell type ($p<0.001$, chi-square=39.011), with highest probability by ChCs (Figure 11F). Taken together, our results indicate that FS INs generate fast and reliable inhibition with PVBC spikes evoking significantly larger uIPSCs than CCKBCs, but in case of prolonged PTI activation, PNs can receive a steadier level of inhibition from CCKBCs.

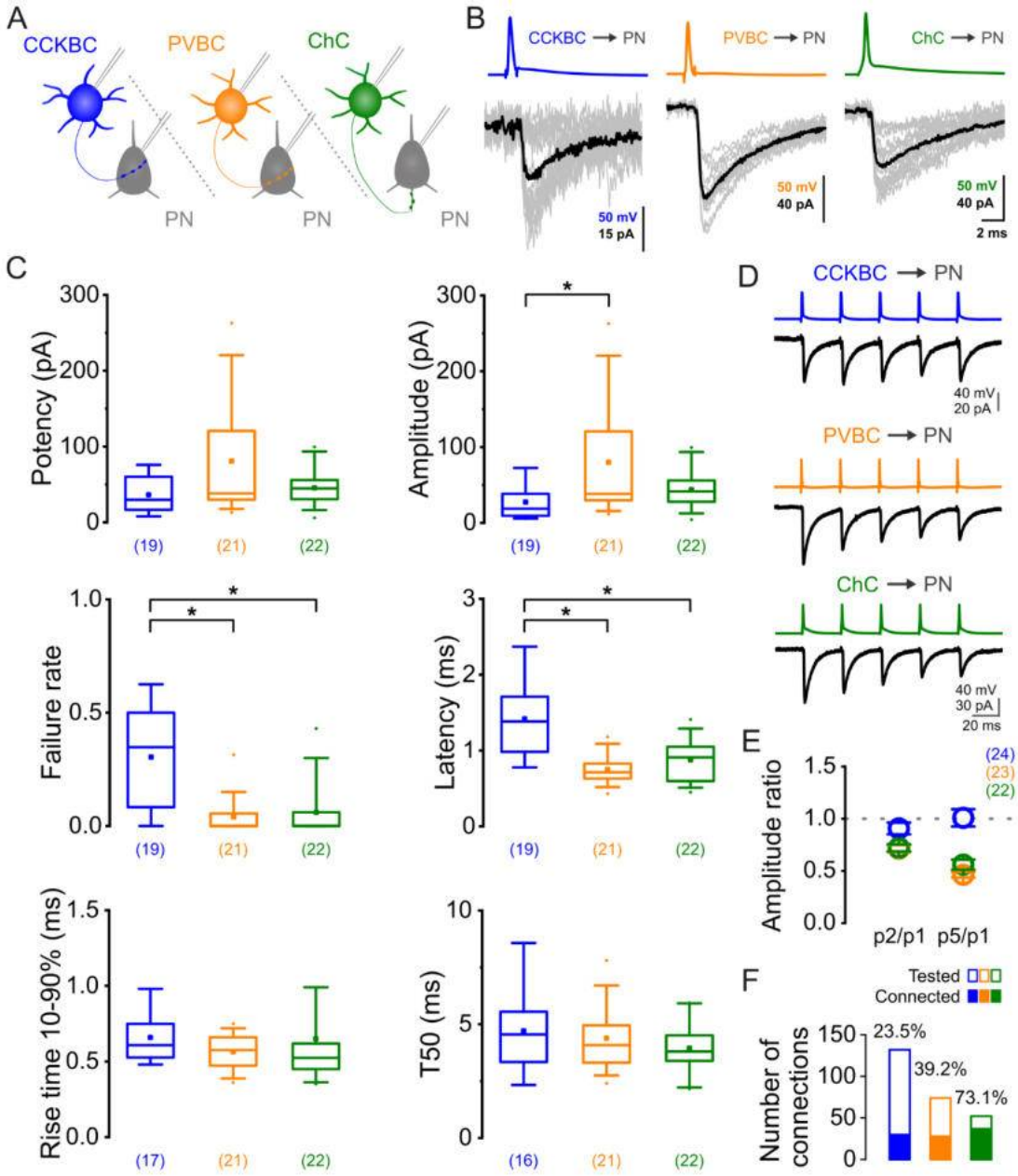

Figure 11. Paired recordings between PTIs and PNs reveal that FS cells provide reliable inhibition with short latency followed by strong synaptic depression. (A) Schematic illustration of the experiment. (B) Representative traces of the first presynaptic AP in a train of 5 APs evoked in PTIs (top) and the postsynaptic uIPSCs recorded in PNs (bottom). Fifteen consecutive traces in gray, average in black. (C) Comparison of the main properties of the first uIPSCs. Boxes represent the interquartile range; filled square: mean; whiskers: 5th and 95th percentile. Numbers in parentheses represent the number of analyzed recordings. For details see Table 1. (D) Representative traces of synapse type-dependent short-term plasticity revealed by

eliciting 5 APs in the presynaptic cell. (E) Ratio of the amplitude of the 2nd and 1st (2/1) or the 5th and 1st (5/1) uIPSC summarizes the short-term dynamics of the inhibitory connections between BCs and PNs. Data presented as mean ± SEM. Numbers in parentheses represent the number of analyzed recordings from n=17, n=16 and n=20 animals for CCKBC, PVBC and ChC recordings, respectively. (F) Probability of finding inhibitory connections between PTIs and PNs was highest with ChCs. (Figure modified from Fekete et al., 2024)

4.1.5. Basket cells form chemical synapses and gap junctions with their own cell type

Electrical synapses between neurons of the same inhibitory cell type are generally common in cortical circuits (Galarreta & Hestrin, 1999; Gibson et al., 1999; Tamas et al., 2000; Andrasi et al., 2017), while the preference of inhibitory neurons for establishing homotypic chemical synapses is cell type-dependent (Pfeffer et al., 2013; Tremblay et al., 2016). To reveal the extent to which BCs are synaptically interconnected and the electrophysiological properties of their contacts in the PrL, we performed paired recordings between the same type of BCs (Figure 12A). Testing electrical coupling was conducted by injecting hyperpolarizing current steps in one of the cells while recording membrane potential changes in the other cell (Figure 12B, top). Chemical synapses were tested by eliciting 10 action potentials at 40 Hz (Figure 12B, bottom). CCKBCs were frequently coupled electrically (16/23 tests, 69.6%) but chemical connections seemed less numerous between them (9/31 tests, 29%), despite the elimination of any tonic activation of CB1 by AM251 application (1 μM). In contrast, every second recorded PVBC evoked uIPSCs in other PVBCs in paired recordings (13/25 tests, 52%) but only 25% of the tested cells were connected via gap junctions (2/8 tests). ChCs were not recorded simultaneously and therefore were not tested for connectivity.

In terms of the main properties of the chemical connections, uIPSCs evoked by the first action potential tended to have larger potency in synapses between PVBCs (Figure 12D, Table 1). Although there was a tendency for uIPSCs evoked by CCKBC spikes to start off with larger latency than uIPSCs in homotypic PVBC synapses, the difference did not reach the level of significance ($p=0.17$, Figure 12D, Table 1). On the other hand, the rate of failure for the first action potential was significantly higher for CCKBC than for PVBC synapses (Figure 12D, Table 1) suggesting a more reliable neurotransmission between the latter BCs. Sustained presynaptic activity, however, revealed that homotypic

CCKBC synapses display strong facilitation, while PVBCs receive uIPSCs of decreasing amplitude (Figure 12E). Taken together, homotypic BC pairs display different synaptic characteristics and connectivity patterns in the PrL.

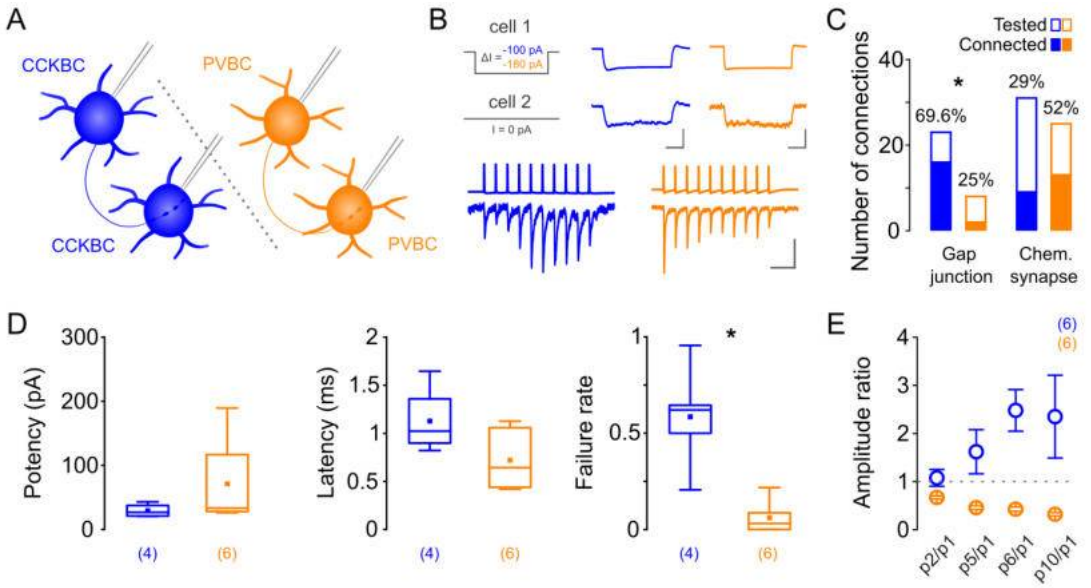

Figure 12. Paired recordings from homotypic BCs demonstrate that BCs innervate their own kind with chemical synapses and gap junctions as well. (A) Schematic illustration of the experiment. (B) Example traces of gap junctions revealed by injecting hyperpolarizing current steps into one of the recorded cells, averages of 50 consecutive traces (top). Example traces of recorded chemical synapses between the same type of BCs, averages of 10 consecutive traces (bottom). Scale bars: gap junctions: CCKBC x: 20 mV, 1 mV; y: 200ms; PVBC: x: 15 mV, 0.5 mV; y: 200 ms; chemical synapses: x: CCKBC: 70 mV, 20 pA; PVBC: 70 mV, 50 pA; y: 50 ms. (C) Comparison of connection probabilities. Filled bars represent the number of connections, empty bars represent the number of tests (p=0.043 and p=0.103 for gap junctions and chemical synapses, respectively, Fisher's exact test). (D) Features of the first postsynaptic responses in homotypic connections between CCKBCs and PVBCs. Numbers in parentheses represent the number of analyzed recordings from n=7 animals for both CCKBC and PVBC recordings. For details see Table 1. (E) Ratio of the amplitude of the 2nd, 5th, 6th and 10th uIPSC to the 1st response summarizes the short-term dynamics of the inhibitory connections between homotypic BCs. (Adapted from Fekete et al., 2024)

4.1.6. CCKBCs innervate PVBCs

Previous studies have shown that the two BC types are interconnected in the hippocampus (Dudok, Klein, et al., 2021) but not in the amygdala (Andrasi et al., 2017). To determine the presence or absence of functional synaptic connections on PVBCs established by CCKBCs in the PrL, we used a pharmacological approach and took advantage of CB1 expression on CCKBC axon terminals (Nagy-Pal et al., 2023, Figure 8A) that is selective for this cell type among cortical inhibitory neurons (Wilson et al., 2001). Extracellular stimulation was used to evoke IPSCs in PVBCs (Figure 13A), while glutamatergic synaptic transmission was blocked by 2 mM kynurenic acid applied in the external solution. Bath application of the CB1 agonist WIN55,212-2 (1 μM) reduced the amplitude of evoked postsynaptic currents in the recorded cells below 50% of the initial amplitude values (Figure 13B) demonstrating the presence of CB1-sensitve inputs to PVBCs. These electrophysiological data were further supported by our anatomical results showing CB1+ axonal boutons opposed to the majority of sampled PV+ somata (29 out of 33 cells, 87.9%) (Figure 13C, 13D). Immunostaining against gephyrin (the anchoring protein of $GABA_A$ receptors (Sassoe-Pognetto & Fritschy, 2000)) was used to ensure that only inhibitory synapses are included in the quantification. Taken together, our two independent approaches provide evidence that CB1-sensitive inputs from CCKBCs are present on PVBCs.

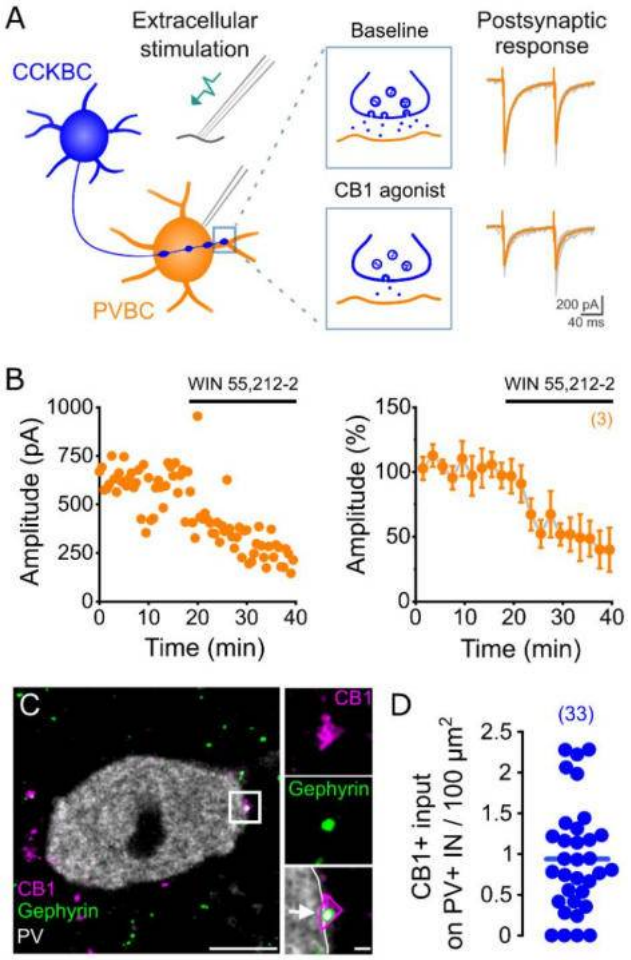

Figure 13. **Pharmacological experiments and immunolabeling demonstrate the presence of functional CB1-positive inhibitory inputs received by PVBCs.** (A) Schematic illustration of the experiment (left). Excitatory currents were blocked by 2 mM kynurenic acid in the recording solution. Representative traces of evoked IPSCs before (right, top) and after the application of CB1 agonist (right, bottom). (B) Inhibitory postsynaptic currents in a PVBC evoked by focal electrical stimulation are reduced by bath application of CB1 agonist WIN 55,212-2 (1 µM). Data from a representative experiment (left) and normalized data from n = 3 cells (right) from n=3 animals. Data points represent the mean ± SEM of 4 consecutive responses with an inter-stimulus interval of 30 seconds. (C) Confocal image of the soma of a PV+ interneuron labeled with immunostaining against PV. Inset: a terminal apposed to gephyrin labeling on the soma is immunopositive for CB1. Scale bars: 5 and 0.5 µm. (D) Quantification of the density of CB1+ terminals on PV-immunopositive somata (n=33) from n=3 C57Bl6 mice. (Adapted from Fekete et al., 2024)

4.1.7. PVBCs innervate CCKBCs

To study the potential synaptic connections established by PVBCs on CCKBCs, we crossed BAC-CCK-DsRed mice with PV-Cre mice. Therefore, in offspring, we could target fluorescently labeled CCKBCs (Nagy-Pal et al., 2023) and activate PVBCs via Cre-dependently expressed channelrhodopsin (ChR2) in the same preparations. After 4-6 weeks following the injection of AAV5-EF1-DIO-hChR2-eYFP into the PrL, we prepared acute slices and recorded from CCKBCs and PNs simultaneously in whole-cell configuration (Figure 14A). The cell types of the recorded neurons were verified by *post hoc* immunostaining against biocytin and CB1. Successful optogenetic activation of the PV+ population upon light stimulation was evident from the large IPSCs evoked in PNs (Figure 14B), while CCKBCs also received prominent inhibition without exception. The amplitude of these inhibitory currents varied between cells but the mean amplitude of IPSCs recorded from CCKBCs reached 11.1% of the IPSCs evoked simultaneously in PNs (Figure 14B). Latency of the responses measured from the beginning of light illumination was significantly larger for CCKBCs than for PNs (Figure 14B). In addition to these experiments, we also identified PV+ inhibitory synaptic contacts on the somata of CCKBCs in slices containing the PrL prepared from the offspring generated by crossing VGAT-IRES-Cre and BAC-CCK-GFP-coIN mice (Figure 14C). Immunostaining against PV and gephyrin revealed that the majority of the CCK/GFP+ somata received PV+ input (27 out of 32 cells, 84.4%) (Figure 14D). In summary, these results demonstrate the reciprocal innervation between the two BC types in the PrL.

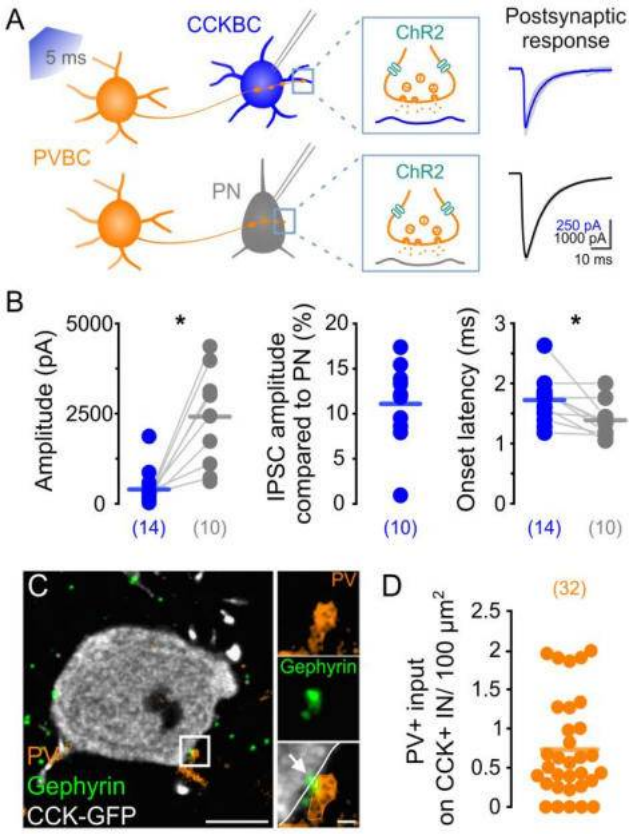

Figure 14. Postsynaptic responses upon light activation of PV+ cells via ChR2 together with anatomical data demonstrate that PVBCs innervate CCKBCs. (A) Schematic illustration of the experiment. Representative traces of light-evoked responses recorded simultaneously in a CCKBC (right, top) and a PN (right, bottom). Ten consecutive traces in gray, average in color. (B) Features of the light-evoked postsynaptic responses. Data points representing simultaneously obtained recordings are connected on the graph. Left: mean amplitude of IPSCs recorded in CCKBCs and PNs (CCKBC: 235.25 (87, 523) pA; PN: 2721.5 (1103, 3126) pA, $p<0.001$, MW). Middle: mean IPSC amplitude recorded in CCKBCs compared to the amplitude of IPSCs simultaneously recorded in PNs. Right: onset latency of IPSCs (CCKBC: 1.78 (1.51, 1.84); PN: 1.35 (1.15, 1.44), $p = 0.02$, MW). Numbers in parentheses represent the number of analyzed recordings from n=3 animals. (C) Confocal image of the soma of a GFP-labelled CCK+ IN in the PrL of a VGAT-IRES-Cre::BAC-CCK-GFPcoIN mouse. Inset: a terminal immunopositive for PV apposed to gephyrin labeling, indicating the presence of an inhibitory synapse. Scale bars: 5 and 0.5 µm. (D) Quantification of the density of PV+ terminals on CCK+ interneurons (n=32) in n=4 VGAT-IRES-Cre::BAC-CCK-GFPcoIN mice. (Adapted from Fekete et al., 2024)

4.2. Part II: Fear learning and unsigned noxious stimuli change excitatory inputs on perisomatic region-targeting inhibitory cells in the basal amygdala

4.2.1. Separation of the effects of fear memory formation and sensory inputs

To distinguish between the effects of fear memory formation and the CS/US presentations on the excitatory synaptic inputs of BA PTIs, either of the following three behavioral paradigms were used (Figure 15A1). In the first paradigm, to test the behavioral consequences of the CS presentation, mice were repeatedly subjected to the CS (tone) without the US (shock, Figure 15A2, only CS group, black). As expected, these mice showed no elevated freezing levels upon the CS demonstration the next day in a different context (Figure 15B, black). In the second group, to test the effects of CS and US without association, tones and shocks were presented randomly during conditioning (Figure 15A2, unsigned US group, red). In this group, the delivery of the US was not signed by the CS, therefore, the association between CS and US did not form, as demonstrated by the lack of freezing upon the cue presentation the next day (Figure 15B, red). In contrast, when tones co-terminated with mild electrical shocks in case of the third group, i.e., the oncoming US was signed by a CS (Figure 15A2, signed US group, blue), the fear memory was formed. The result of the CS-US association was clear the next day when the CS presentation induced significant freezing in a different context (Figure 15B cue, K-W ANOVA $p = 3 \times 10\text{-}6$), while there was no elevated freezing during the baseline period (Figure 15B baseline, K-W ANOVA $p = 0.29$). Thus, in line with previous findings, pairing a CS with a US resulted in lasting changes in neuronal networks, assessed at the behavioral level (LeDoux, 2003). Importantly, there was no difference in the cue evoked freezing levels of BAC-PV-eGFP and BAC-CCK-DsRed mice in the unsigned US and signed US group (Mann–Whitney test, $p = 0.78$ and $p = 0.69$, respectively), indicating that distinct BAC insertion in the two mouse lines does not compromise the fear memory processes. Our experimental design, therefore, allows the separation of the consequences of fear memory formation from those caused by the sensory signals using the three mouse groups.

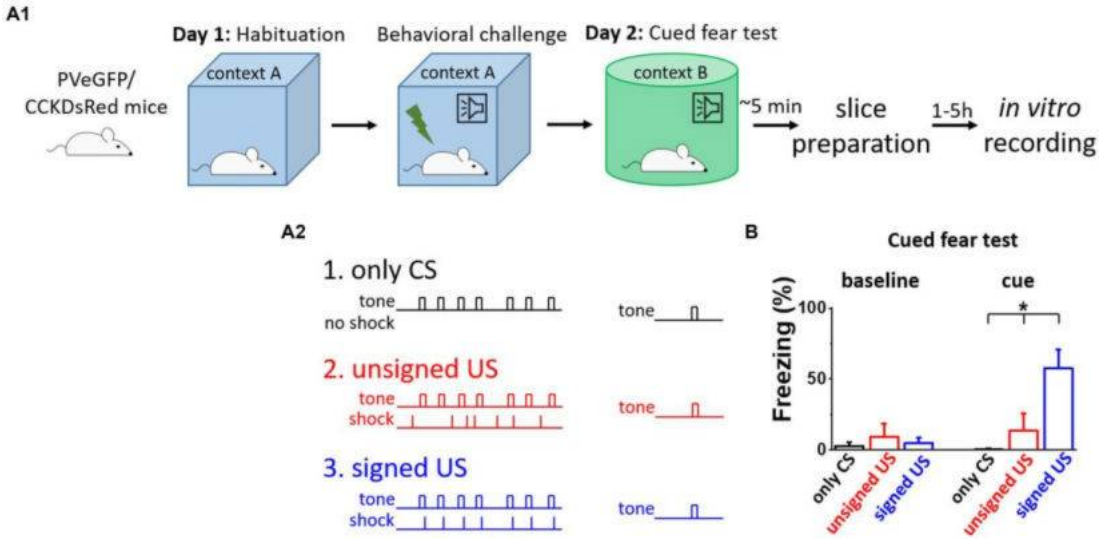

Figure 15. Fear memory effectively formed upon signed US presentation, but not in other conditions. (A1) Experimental design. (A2) The three mouse groups with different combinations of CS (tone) and US (shock) presentation. (B) Freezing tested on the consecutive day was elevated only in the signed US group, therefore the other two conditioning paradigms can serve as assessments of the effects of the sensory inputs on the network. Asterisk indicates significant difference (K-W ANOVA $p = 3\times10\text{-}6$, only CS vs. unsigned US $p = 0.39$, only CS vs. signed US $p = 2\times10\text{-}6$, unsigned US vs. signed US $p = 0.003$). Box represents mean, whiskers SEM. Only CS group n = 14, unsigned US group n = 12, signed US group n = 13. (Adapted from Veres et al., 2023)

4.2.2. Excitatory synaptic inputs in PVBCs are reduced upon the US presentation

To test whether excitatory synaptic inputs in different PTI types are capable of plastic changes, acute brain slices containing the amygdala were prepared immediately after cued fear testing. PV neurons in the BA were visually targeted based on their eGFP expression and their calbindin content was confirmed *post hoc* (Figures 16A, 16B). Calbindin is a neurochemical marker for PVBCs in the rodent amygdala that separates these interneurons from PV ChCs (Bienvenu et al., 2012; Vereczki et al., 2016). mEPSCs were recorded in whole-cell patch-clamp mode in the presence of 0.5 µM tetrodotoxin (TTX, voltage-gated Na^+ channel blocker) and 100 µM picrotoxin ($GABA_A$ receptor antagonist) in slices from the three behavioral groups (Figure 16C; Tables 2, 3). The distribution of mEPSC amplitudes in PVBCs sampled in the three groups showed significant differences

(Figure 16D, K-W ANOVA p =1×10-16); we found a 11% decrease in mEPSC amplitudes in the unsigned group when compared to the only CS group (Dunn's test p =6×10-17) and a 5% decrease when we compared the signed US to the only CS group (Dunn's test p=0.025). Interestingly, there was a significant increase (7%) in this mEPSC feature in PVBCs if we compared those that were recorded in the unsigned and signed US groups (Dunn's test p=1×10-6). This observation implies that the US itself can elicit changes in mEPSC peak amplitudes in PVBCs, but the associated learning decreases those changes. When we compared the inter-event intervals (IEI) of mEPSCs (Figure 16E) we found significant changes among groups (K-W ANOVA p=3×10-22). The unsigned US presentation led to a 26% increase in IEIs (i.e. reduced rate) compared to the only CS group (Dunn's test p =2×10-17), and the signed US group also showed a 23% increase (Dunn's test p=2×10-17). There was no difference in mEPSC rates in the unsigned and signed US group (Dunn's test p =0.3), implying that the effect of CS and US association on this mEPSC characteristic is indistinguishable from those that are caused by the independent presentation of CS and US. Rise time and decay kinetics of mEPSCs were not different in the three paradigms (Table 3, K-W ANOVA p=0.758 and p=0.598, respectively). Taken together, these results suggest that the US presentation decreases mEPSC amplitudes and their occurrence in PVBCs, but fear memory formation may cause a slighter reduction in the amplitude of their excitatory synaptic inputs in comparison to CS presentation only.

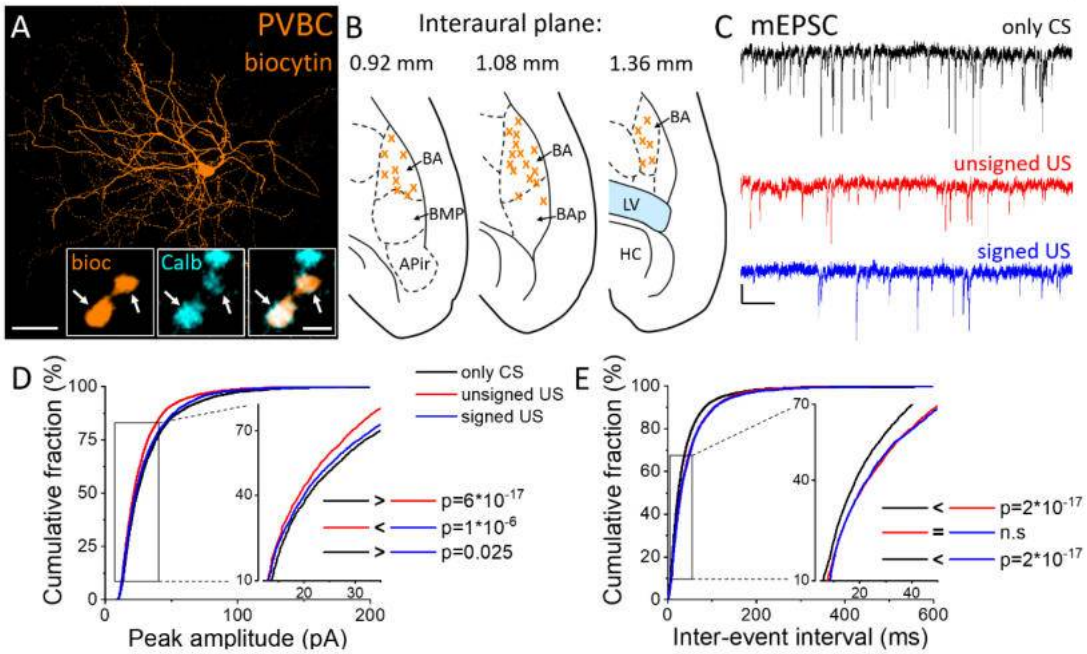

Figure 16. Differences in mEPSC properties in PVBCs recorded in slices prepared from the three groups of mice. (A) Maximum intensity projection of a biocytin-filled PVBC. Inset: Axon terminals of PVBCs (orange) are immunopositive for calbindin (Calb, cyan), a neurochemical marker that distinguishes PVBCs from ChCs in the BA. Arrows indicate colocalization. Scales: 50 µm and 1 µm (inset). (B) Position (orange x) of the recorded PVBC depicted on schematic drawings representing horizontal brain sections [based on Paxinos (2012)]. Out of the 50 recorded cells, only 30 randomly selected interneurons are shown for clarity. APir: piriform amygdalar area, BA: basal amygdala, BAp: posterior part of the basal amygdala, BMP: basomedial amygdala, posterior part, HC: hippocampus, LV: lateral ventricle. (C) Representative traces of miniature excitatory postsynaptic current (mEPSC) recordings in the presence of 0.5 µM tetrodotoxin (TTX) and 100 µM picrotoxin in the three groups. Scales: 20 pA (y) and 100 ms (x). (D,E) Cumulative distribution of mEPSC peak amplitudes (D) and inter-event intervals (E); data pooled from all cells in each group. Graphs in insets are plotted using a normal probability Y axis. P values show the result of K-W ANOVA *post hoc* Dunn's tests (see details in Table 1). n.s., non-significant difference. (Adapted from Veres et al., 2023)

Table 2. Data and statistical analysis of mEPSC amplitude and inter-event interval in the recorded PTIs. (Adapted from Veres et al., 2023)

Cell type	Variable	Group	Cell number (mouse number)	Value (median ± IQ range)	Group comparison p value (K-W ANOVA)	Paired comparison	P value (Dunn's Test)	Change
PVBC	Peak amplitude (pA)	only CS	17 (7)	24.35 ± 21.41	**<0.001**	only CS vs. unsigned US	**<0.001**	11% ↓
		unsigned US	17 (6)	21.66 ± 16.55		only CS vs. signed US	**0.0251**	5% ↓
		signed US	16 (7)	23.11 ± 20.85		unsigned US vs. signed US	**<0.001**	7% ↑
	IEI (ms)	only CS	17 (7)	23.70 ± 34.90	**<0.001**	only CS vs. unsigned US	**<0.001**	26% ↑
		unsigned US	17 (6)	30.00 ± 43.60		only CS vs. signed US	**<0.001**	23% ↑
		signed US	16 (7)	29.24 ± 44.55		unsigned US vs. signed US	1	-
CCKBC	Peak amplitude (pA)	only CS	23 (6)	17.13 ± 7.12	**0.001**	only CS vs. unsigned US	0.124	-
		unsigned US	24 (6)	17.32 ± 7.67		only CS vs. signed US	**<0.001**	3% ↑
		signed US	21 (6)	17.58 ± 7.96		unsigned US vs. signed US	0.303	–
	IEI (ms)	only CS	23 (6)	83.31 ± 137.0	0.175	-		
		unsigned US	24 (6)	85.35 ± 144.75				
		signed US	21 (6)	83.75 ± 131.30				
ChC	Peak amplitude (pA)	only CS	20 (7)	18.06 ± 10.51	0.406	-		
		unsigned US	14 (5)	17.76 ± 10.64				
		signed US	21 (7)	18.19 ± 11.17				
	IEI (ms)	only CS	20 (7)	58.75 ± 104.00	**0.031**	only CS vs. unsigned US	1	–
		unsigned US	14 (5)	56.45 ± 96.73		only CS vs. signed US	**0.026**	7% ↓
		signed US	21 (7)	54.45 ± 90.50		unsigned US vs. signed US	0.465	–

Table 3. Data and statistical analysis of mEPSC kinetic features recorded in PTIs. (Adapted from Veres et al., 2023)

Cell type	Variable	Group	Cell number (mouse number)	Value (median ± IQ range)	Group comparison p value (K-W ANOVA)	Paired comparison	P value (Dunn's Test)	Change
PVBC	Rise time 10-90% (ms)	only CS	17 (7)	0.28 ± 0.07	0.758	-		
		unsigned US	17 (6)	0.31 ± 0.06				
		signed US	16 (7)	0.34 ± 0.09				
	Decay time constant (ms)	only CS	17 (7)	0.94 ± 0.38	0.598	-		
		unsigned US	17 (6)	1.01 ± 0.40				
		signed US	16 (7)	1.06 ± 0.4				
CCKBC	Rise time 10-90% (ms)	only CS	23 (6)	0.60 ± 0.20	0.895	-		
		unsigned US	24 (6)	0.61 ± 0.09				
		signed US	21 (6)	0.60 ± 0.11				
	Decay time constant (ms)	only CS	23 (6)	1.91 ± 0.58	**0.006**	only CS vs. unsigned US	**0.004**	**17% ↓**
		unsigned US	24 (6)	1.57 ± 0.41		only CS vs. signed US	0.375	–
		signed US	21 (6)	1.80 ± 0.46		unsigned US vs. signed US	0.352	–
ChC	Rise time 10-90% (ms)	only CS	20 (7)	0.26 ± 0.09	0.230	-		
		unsigned US	14 (5)	0.33 ± 0.08				
		signed US	21 (7)	0.32 ± 0.09				
	Decay time constant (ms)	only CS	20 (7)	0.84 ± 0.20	0.289	-		
		unsigned US	14 (5)	0.93 ± 0.18				
		signed US	21 (7)	0.91 ± 0.24				

4.2.3. Increased amplitude and decreased decay time constant of mEPSCs in CCKBCs upon US presentation

Next, we assessed whether the excitatory synaptic inputs in the other main basket cell type, CCKBCs, are also capable of plastic changes in our paradigms. To selectively record from these cells, a CCK-DsRed mouse strain was used (Mate et al., 2013; Rovira-Esteban et al., 2017) to visually target CCKBCs based on their DsRed content (Figures 17A, 17B; Vereczki et al., 2016). After the recordings, CB1 content of axon terminals was confirmed with immunolabeling (Figure 17A insets). mEPSCs were recorded and analyzed by the same method as described above in PVBCs (Figure 17C; Tables 2, 3). The evaluation of changes in mEPSC characteristics recorded in CCKBCs showed a difference in their peak amplitudes (Figure 17D, K-W ANOVA p =0.001). There was a

slight (3%) but significant increase in mEPSC peak amplitudes in the signed US groups compared to the only CS controls (Dunn's test p =2×10-17). However, there was no significant difference between the only CS vs. unsigned US (Dunn's test p =0.12) and unsigned US vs. signed US comparisons (Dunn's test p =0.30). Interestingly, we could not find any difference in the IEI of mEPSCs (Figure 17E, K-W ANOVA p =0.175). Regarding the kinetic properties of mEPSCs (Table 3), the rise time was not different in the three paradigms (K-W ANOVA p =0.895), however, there was a significant 17% decrease in the decay time constant when we compared the only CS group to the unsigned US group (Dunn's test p =0.004). Taken together, these results show that the fear learning increases the amplitude of mEPSC and the unsigned US accelerates the mEPSC decaying phase in the CCKBC population.

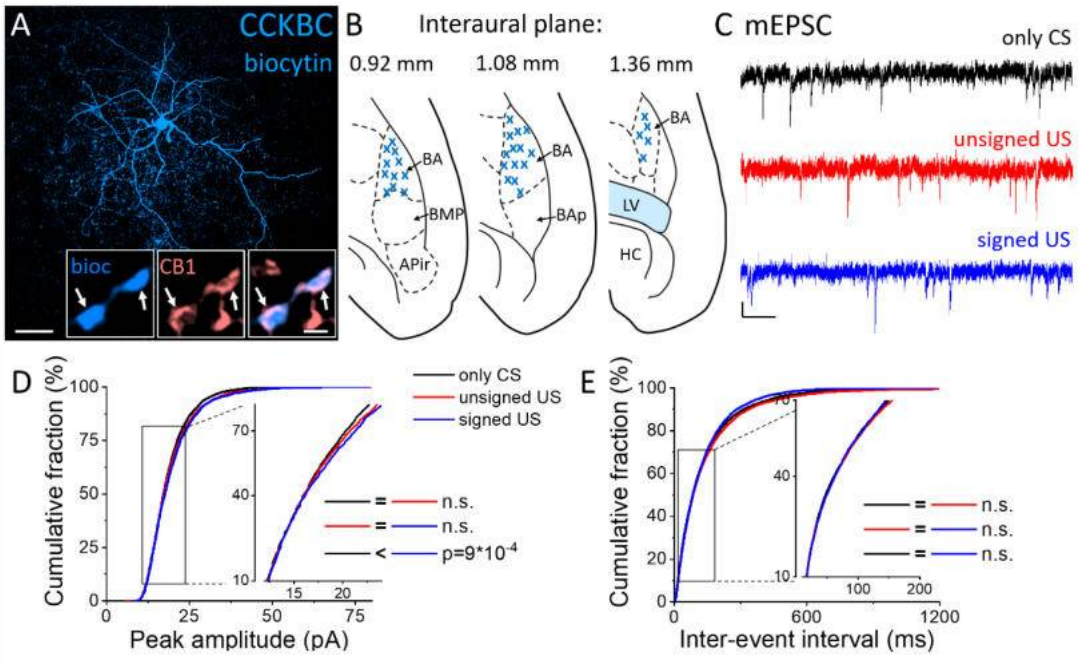

Figure 17. Increased amplitude of mEPSCs in CCKBCs upon US presentation. (A) Maximum intensity projection of a biocytin-filled CCKBC. Inset: Axon terminals of same CCKBC (blue) are immunopositive for type one cannabinoid receptors (CB1, pink). Arrows indicate colocalization. Scales: 50 µm and 1 µm (inset). (B) Position (blue x) of the recorded CCKBC depicted on schematic drawings representing horizontal brain sections [based on Paxinos (2012)]. Out of the 68 recorded cells, only 30 randomly selected interneurons are shown for clarity. APir: piriform amygdalar area, BA: basal amygdala, BAp: posterior part of the basal amygdala, BMP: basomedial

amygdala, posterior part, HC: hippocampus, LV: lateral ventricle. (C) Representative traces of miniature excitatory postsynaptic current (mEPSC) recordings in the presence of 0.5 μM TTX and 100 μM picrotoxin from the three groups. Scales: 10 pA (y) and 100 ms (x). (D,E) Cumulative distribution of mEPSC peak amplitudes (D) and inter-event intervals (E); data pooled from all cells in each group. Graphs in insets are plotted using a normal probability Y axis. p values show the result of K-W ANOVA *post hoc* Dunn's tests (see details in Table 2). n.s., non-significant difference. (Adapted from Veres et al., 2023)

4.2.4. Excitatory synaptic inputs in ChCs change only upon fear memory formation

Besides the two basket cell types, ChCs are the third PTI type that are capable to efficiently control the spiking activity of principal neurons (Veres et al., 2014). Therefore, any change in the excitatory synaptic inputs of ChCs as a consequence of fear conditioning could be pivotal in the accomplishment of their functions. ChCs were targeted in the BA based on their eGFP content in PV-eGFP animals and were separated *post hoc* from PVBCs based on their characteristic axonal cartridges formed around axon initial segments that can be visualized by Ankyrin G staining (Figures 18A, 18B) and the absence of calbindin immunolabeling in their somata and axon terminals. mEPSCs were recorded (Figure 18C; Tables 2, 3) and analysed as described above. Unlike in BCs, excitatory synaptic inputs in ChCs did not show change in terms of their amplitude (Figure 18D, K-W ANOVA $p = 0.406$), however, there was a slight but significant change in the rate of mEPSCs (Figure 18E, K-W ANOVA $p = 0.031$): in the signed US group the rate of mEPSCs were 7% higher than in the only CS group (Dunn's test $p = 0.026$). Rise time and decay kinetics of mEPSCs were not different in the three paradigms (Table 3, K-W ANOVA $p = 0.23$ and $p = 0.289$, respectively). Taken together, our data indicate that there is a unique increase in mEPSC rates in ChCs upon signed US presentation following fear memory formation that was not present in any other PTI type. The significant changes in mEPSC properties are summarized on Figure 19.

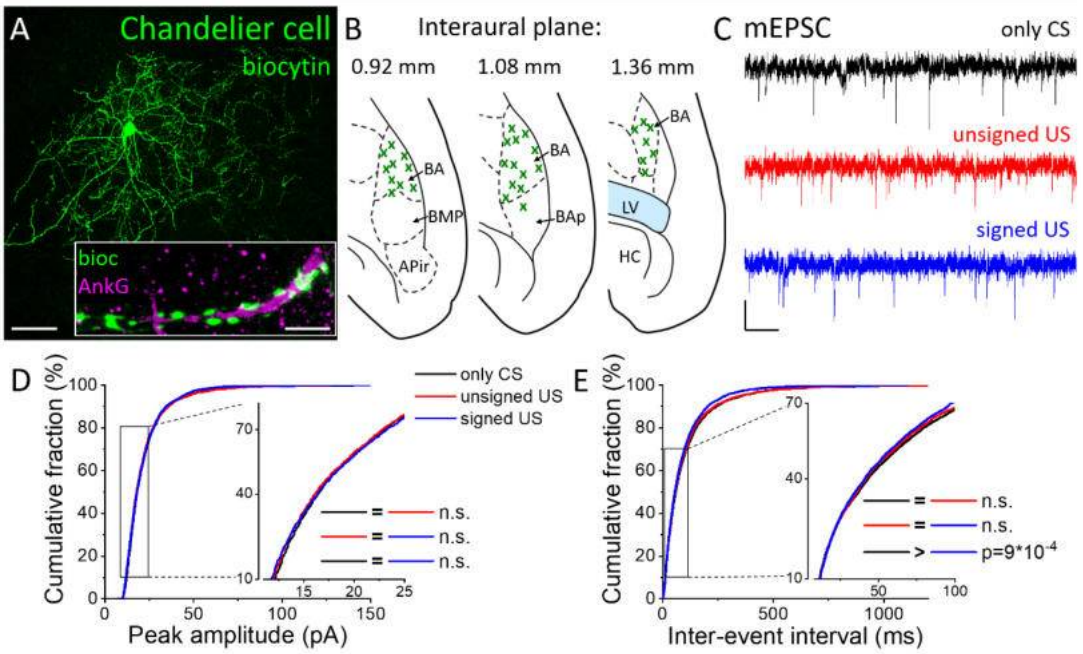

Figure 18. Excitatory synaptic inputs in ChCs change only upon the signed US presentation. (A) Maximum intensity projection of a biocytin-filled ChC. Inset: Axon terminals of the same ChC (green) form a characteristic cartridge along an Ankyrin G (magenta) labeled axon initial segment. Scales: 50 µm and 5 µm (inset). (B) Position (green x) of each recorded ChC depicted on schematic drawings representing horizontal brain sections [based on Paxinos (2012)]. Out of the 55 recorded cells, only 30 randomly selected interneurons are shown for clarity. APir: piriform amygdalar area, BA: basal amygdala, BAp: posterior part of the basal amygdala, BMP: basomedial amygdala, posterior part, HC: hippocampus, LV: lateral ventricle. (C) Representative traces of miniature excitatory postsynaptic current (mEPSC) recordings in the presence of 0.5 µM TTX and 100 µM picrotoxin obtained in ChCs sampled from the three groups. Scales: 10 pA (y) and 100 ms (x). (D,E) Cumulative distribution of mEPSC peak amplitudes (D) and inter-event intervals (E); data pooled from all cells in each group. Graphs in insets are plotted using a normal probability Y axis. *p* values show the result of K-W ANOVA *post hoc* Dunn's tests (see details in Table 2). n.s., non-significant difference. (Adapted from Veres et al., 2023)

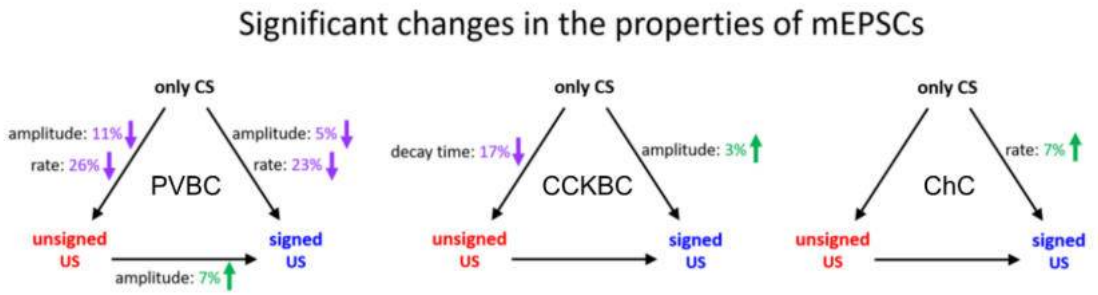

Figure 19. Summary of significant changes in the properties of excitatory synaptic inputs of PTIs in the BA in the three behavioral paradigm. Black arrows indicate the compared pairs, only the significant changes in mEPSC amplitude, rate and decay time are shown and are expressed in % values. Green numbers and upward arrows indicate increase, purple numbers and downward arrows indicate decrease. For the exact tests and significance values see Tables 2, 3. (Adapted from Veres et al., 2023)

5. DISCUSSION

In this study, we investigated the synaptic features of PTIs and PNs in the mPFC microcircuit as well as the connectivity motifs among PTIs. Furthermore, we studied the effect of fear memory formation and unsigned noxious stimulus on the excitatory input of PTIs in the BA to elucidate how the function of these cell types are impacted upon aversive signal presentation and associative learning. Our major findings are as follows: (1) The two BC types exhibited contrasting membrane properties, while the fast spikers also differed in terms of many features including their membrane time constant and AP threshold. (2) Our paired recordings revealed that PNs located in the PrL not only evoke larger unitary excitatory currents in PVBCs than in CCKBCs, but these currents have shorter latency and faster kinetic parameters. (3) Inhibition provided by PVBCs and ChCs is more reliable and follows presynaptic spiking with shorter latency compared to uIPSCs evoked by CCKBC firing. (4) We provided anatomical and electrophysiological evidence that the populations of the two BC type establish functional synapses on the other type as well as on their own. (5) Excitatory inputs on PVBCs in the BA are decreased in terms of their strength and rate when animals receive aversive stimuli either with or without the association with the CS. (6) mEPSC on CCKBCs show the fastest decay when the US is presented unsigned. (7) Fear learning enhances the rate of excitatory inputs selectively on ChCs.

5.1. Membrane properties of PTIs in the mouse mPFC

BCs have long been proposed to serve distinct circuit functions based on several differences in their single-cell features (Freund & Katona, 2007). Our results regarding the contrasting input resistance, membrane time constant and accommodation ratio are in line with previous findings obtained in the hippocampus (Pawelzik et al., 2002; Glickfeld & Scanziani, 2006; Cea-del Rio et al., 2010; Szabo et al., 2010; Lee et al., 2011), basal amygdala (Andrasi et al., 2017; Barsy et al., 2017) and neocortex (De-May & Ali, 2013; Miyamae et al., 2017; Koukouli et al., 2022). These data provide further support to the concept that BCs are built to perform different tasks within cortical networks, despite targeting the same cellular domain in the PrL (Nagy-Pal et al., 2023). ChCs and PVBCs, although both display a fast spiking phenotype, exhibited several differences in their membrane properties. For instance, ChCs had slower membrane time constant, more depolarized AP threshold and larger input resistance, this latter difference resembling that

described in the somatosensory cortex (Woodruff et al., 2009). PVBC firing was the least accommodating and its action potentials were followed by an afterhyperpolarization with the largest amplitude. The large AHPs following PVBC spikes compared to those after ChC spikes have been reported earlier from the rat and monkey mPFC as well (Povysheva et al., 2013). The differences and tendencies described in that paper in terms of additional membrane properties of PVBCs and ChCs do not match our observations, although this might be due to the different species used. However, all these results highlight the need for future studies to distinguish between these IN types.

5.2. Excitation on PTIs

Despite the fact that we tested the potential innervation of ChCs by PNs in 49 cases, we only found excitatory connections between these cells in 6 cases, 3 of which had to be excluded due to high series resistance or the low number of recorded postsynaptic events. A previous study from the PrL reported similarly low connection probabilities for excitatory synapses on ChCs by paired recordings (Lu et al., 2017), while PNs and ChCs in the BA were found to be reciprocally connected in about 50% of the cases (Veres et al., 2014). This difference might be explained by the fact that ChCs in the neocortex with their somata in L2/3 extend their dendrites into L1 where axons of L2/3 PNs, the PNs we targeted for paired recordings with ChCs do not arborize (Schuman et al., 2021; Huang et al., 2024), while ChCs in the BA do not show such polarity in the lack of layers in this nucleus (Vereczki et al., 2016; Miyamae et al., 2017).

By performing paired recordings, we showed that excitatory connections from local PNs give rise to significantly larger unitary currents in PVBCs compared to CCKBCs, in line with results obtained in the basal amygdala (Andrasi et al., 2017). Unitary EPSCs in PVBCs followed presynaptic spiking with shorter latency than in CCKBCs, which implies a general preference for the fast and precise activation of PVBCs over the recruitment of the CCKBC populations (Glickfeld & Scanziani, 2006). On the other hand, we found that transmitter release after PN activation was similarly reliable from synapses contacting either type of BCs, which is in contrast with results showing higher ratio of failure at synapses contacting CCKBCs in the basal amygdala (Andrasi et al., 2017). Given the larger input resistance of CCKBCs compared to PVBCs (Figure 8), increased transmission probability could be a way of recruiting CCKBCs more efficiently in the PrL compared to the basal amygdala. On the other hand, uEPSCs on CCKBCs showed

pronounced short-term depression compared to the steady uEPSCs recorded from PVBCs, a difference implying that sustained PN firing prefers to recruit PVBCs rather than CCKBCs. Although previous studies suggested that the synaptic transmission between PNs and PVBCs is strongly depressing (paired pulse ratio, PPR, ~0.6 in the hippocampus, Ali et al., 1998; Pouille & Scanziani, 2004; 0.7 in the neocortex, Reyes et al., 1998), recent investigations reported less pronounced depression at these synapses (PPR, 0.85 and 0.92 in the hippocampus, Karlocai et al., 2021; Aldahabi et al., 2022; 0.89 in the basal amygdala, T. Andrasi & N. Hajos, unpublished observations). Thus, PPR of 1.06 observed in PN-PVBC pairs in the PrL are in line with the latest results.

To address the reason behind the differential kinetics of uEPSCs on BCs we recorded mEPSCs and the differences in uEPSCs were recapitulated in both the rise time and decay kinetics of mEPSCs. Slower rise time of miniature events in CCKBCs may suggest that excitatory synapses on this cell type are electrotonically more distant from the soma than those on PVBCs. Indeed, PVBCs receive many excitatory synaptic contacts on their somata (Gulyas et al., 1999; Hioki et al., 2013; Rovira-Esteban et al., 2020), in contrast with CCKBCs (Mátyás et al., 2004). It should be noted however, that in the basal amygdala uEPSCs in PVBCs and CCKBCs have been shown to exhibit different rise time kinetics in spite of the fact that the distance between the soma and the actual synaptic contacts were found to be similar (Andrasi et al., 2017). The contrasting decay kinetics on the other hand might be explained, at least partially, by the AMPA receptor subunit composition on PVBCs, as these cells were shown to express glutamate receptor subunit 4 (GluR4) which dictates rapid decay kinetics for EPSCs (Geiger et al., 1997; Fuchs et al., 2007).

5.3. uIPSCs evoked by PTIs

PVBC output synapses have long been regarded as reliable, fast transmitting sites of communication (Buhl et al., 1995; Tamas et al., 1997; Maccaferri et al., 2000; Bartos et al., 2002; Gonzalez-Burgos et al., 2005; Hefft & Jonas, 2005; Glickfeld & Scanziani, 2006; Galarreta et al., 2008), features that we observed in the mouse PrL as well. ChC and PVBC output synapses gave rise to uIPSCs with similarly low failure rate and short latency, possibly due to the fast and reliable release machinery. The first uIPSCs evoked by these INs were followed by the strong depression in amplitude, as it is typical for synapses with high release probabilities (Zucker & Regehr, 2002). In contrast, CCKBCs

were able to maintain a steady level of inhibition during the time window of our action potential trains, although the amplitude of these uIPSCs remained small. Our observation that the two BC types evoked unitary currents in PNs with similar decay kinetics is in line with previous reports (Hefft & Jonas, 2005; Galarreta et al., 2008; Szabo et al., 2010; Kohus et al., 2016; Andrasi et al., 2017; Barsy et al., 2017; Veres et al., 2017) and the finding that hippocampal $GABA_A$ receptor subunit compositions are similar in synapses on PNs facing CCKBC or PVBC axon terminals (Kerti-Szigeti & Nusser, 2016). The smaller variance in decay kinetics of PVBC synapses could be, however, a necessary feature during rhythm generation (Buzsaki & Wang, 2012), as changes in IPSC decay kinetics were shown to also impact the frequency of neuronal oscillations (Fisahn et al., 1998; Pietersen et al., 2014; Heistek et al., 2010). Apart from the similarities in uIPSC kinetics, BC output synapses are characterized by contrasting strength, precision, and reliability in the mPFC as well. In terms of the latter two parameters, ChC synapses are comparable to PVBCs. However, the synaptic strength of ChC output synapses was less powerful compared to PVBC output synapses, although previous works reported from the hippocampus and BA that the potency of uIPSCs evoked by ChCs can match or even exceed PVBC-driven synaptic inhibition (Szabo et al., 2010; Kohus et al., 2016; Barsy et al., 2017). A factor that could contribute to this difference is the targeted ChC population, since the mouse strain we used only visualizes a portion of L2/3 ChCs but not those in deeper layers (Taniguchi et al., 2013; Raudales et al., 2024). The advent of further mouse strains for ChC labeling that are independent of PV content will facilitate the thorough description of how different subpopulations of ChCs affect their postsynaptic partners.

5.4. Homotypic and heterotypic basket cell connections

Electrical coupling and chemical synapses between inhibitory cells can serve as means of enhancing synchronous activity (Gibson et al., 1999; Tamas et al., 2000; Bennett & Zukin, 2004), a circuit motif also utilized by PVBCs to aid rhythm generation in local circuits (Beierlein et al., 2000; Bartos et al., 2002). Studies show that inhibitory cells of the same class are frequently coupled (Tamas et al., 2000; Szabadics et al., 2001; Meyer et al., 2002; Galarreta et al., 2008; Andrasi et al., 2017) and our recordings obtained from CCKBCs strengthen this general concept (Iball & Ali, 2011). However, PVBCs were connected to a lesser extent via gap junctions than expected based on prior studies, even though the recorded cells were located within 100 μm and innervated each other with

chemical synapses in 52% of the tests. A reason behind this contradiction could be that studies reporting high connectivity rates via electrical synapses were typically obtained in juvenile animals (Coulon & Landisman, 2017), while the number and strength of gap junctions between PVBCs were shown to decrease with age (Meyer et al., 2002). Our gap junction tests with PVBCs were recorded in animals older than P65 (mean age=76 days, n=4 animals), which might account for the decreased probability in electrical coupling between PVBCs. However, it cannot be ruled out that the low ratio of electrical connections between the sampled PVBCs was partly due to the considerable distance between the gap junctions and the location of the recording pipettes as these connections were shown to occur up to several hundred μm away from the somata (Fukuda et al., 2006). Chemical synapses on the other hand displayed similar tendencies in terms of their strength, reliability and latency as the synapses that contact PNs, and as in homotypic paired recordings obtained in the hippocampus, where CCKBCs establish facilitating synapses but PVBC connections show synaptic depression (Bartos et al., 2001; Daw et al., 2009; Kohus et al., 2016). This facilitation at 40 Hz in synapses between CCKBCs appears to be stronger than in CCKBC synapses contacting PNs both in the mPFC and the hippocampus (Kohus et al., 2016). However, the short-term dynamics of the homotypic basket cell connections in the PrL and the BA are also comparable (Andrasi et al., 2017).

Synaptic communication between the two BC types have only been investigated previously in a small number of studies (Karson et al., 2009; Andrasi et al., 2017; Dudok, Klein, et al., 2021), despite the fact that inhibitory regulation is a major factor in the activity of interneurons as well, and consequently, in the activity of neuronal circuits (Chamberland & Topolnik, 2012). According to the quantifications of immunolabeled terminals in the primary somatosensory cortex, CCKBCs indeed establish synaptic connections with PV+ cells by providing 12% of the inhibitory boutons contacting PV+ somata (Hioki et al., 2018). Moreover, paired recordings obtained in the hippocampus reported functional synapses between the two types of BCs originating from CCKBCs (Karson et al., 2009) or PVBCs (Kohus et al., 2016). On the other hand, the same method led to the conclusion that the two BC types avoid innervating each other in the basal amygdala (Andrasi et al., 2017). Our pharmacological and optogenetic approaches combined with immunocytochemical investigations provided higher throughput than dual whole-cell recordings and were able to reveal connections between BC types in the mPFC, providing a further step towards deciphering BC operation.

5.5. The effect of fear learning on PTI input

The BA is a center of emotional processing where correlates of aversive signal-driven associative learning can be assessed through a simple but powerful paradigm such as fear learning. Fear learning involves plasticity within the neuronal circuits of the BA, but our knowledge regarding the mechanisms that lead to changes in PTI activity is limited. To dissect how excitatory synaptic inputs on PTIs in the BA are shaped after fear memory formation versus processing aversive stimuli we used 3 groups of animals that underwent different paradigms. Since it has been shown that the activity of interneurons changes in response to both the CS and US (Krabbe et al., 2019), we assessed the effects of aversive stimuli by comparing the only CS group to the unsigned US. Then, to separate the effects of aversive stimuli and fear memory formation, we used the unsigned US group compared to the signed US group where the noxious stimulus was predicted by the presentation of the CS. With the use of these groups, we demonstrated that in response to the aversive stimulation and/or fear memory formation, excitatory synaptic inputs of all PTI types in the BA were modified.

Notably, CCKBCs were the only PTI type that showed a change in kinetic properties of their excitatory synaptic inputs. The faster decay of mEPSCs in the unsigned group may be related to changes in subunit composition of ionotropic glutamate receptors mediating the synaptic communication between the excitatory cells and CCKBCs. Such changes in kinetics upon environmental challenges have been described recently (Shultz et al., 2022). The increased mEPSC amplitude after fear conditioning may suggest that increasing excitation on CCKBCs can lead to a more potent recruitment of these interneurons upon learning. This elevated recruitment may cause an increased synaptic inhibition in the principal neuron populations that can be overcome only by those highly active, presumably coding, principal neurons that are able to trigger depolarization induced suppression of inhibition (DSI) at their GABAergic inputs from CCKBCs (Pitler & Alger, 1992; Wilson & Nicoll, 2001; Zhu & Lovinger, 2005; Losonczy et al., 2010), while the synaptic inhibition on the non-coding cells remains intact. This process, therefore, may be an efficient mechanism to improve the signal-to-noise ratio in BA networks during aversive stimulus processing (Grewe et al., 2017). Alternatively, the change in the excitatory synaptic transmission received by CCKBCs could reflect their

crucial role in stress responses evoked by the unpredictable noxious stimuli, a paradigm that also serves as a stress model (Matuszewich et al., 2007).

A previous study compared the changes of synaptic inputs on PV interneurons in the LA and BA after fear learning and found that the rate of mEPSCs in PV interneurons is altered only in the LA but not in the BA (Lucas et al., 2016). However, that study did not distinguish between PVBCs and ChCs. As the excitatory synaptic inputs of these GABAergic cell types in the BA underwent different alterations after learning, pooling their data may mask the changes in mEPSCs recorded from PVBCs and PV ChCs. Our previous study might also describe a mechanism that could explain the US-induced decrease in the amplitude of excitatory synaptic inputs observed in PVBCs, as we found that these inputs on PVBCs and ChCs can undergo LTD in a CB1 receptor dependent manner in the hippocampus (Peterfi et al., 2012). Although an earlier influential study that investigated PV cell function in fear learning reported heightened PV cell activity, our results do not necessarily contradict those findings (Wolff et al., 2014), since the increased PV activity in that paper was detected during tone presentation. Our results, however, provide insight into a general shift in the excitatory microcircuit targeting PTIs. Conceivably, this decrease in the rate and amplitude of excitatory events on PVBCs contributes to the decreased inhibitory tone in the BA, proposed by previous publications as a necessary alteration promoting learning (Bissiere et al., 2003; Tully et al., 2007; Lee et al., 2013). The increased mEPSC rate in ChCs after fear learning, however, indicates that synaptic mechanisms underlying the changes in mEPSC properties observed in PVBCs and ChCs during the different challenges are necessarily distinct.

Although the extent of the changes in mEPSC properties may seem rather small, it has to be kept in mind that both PV and CCK interneurons receive thousands of glutamatergic inputs (Gulyas et al., 1999; Mátyás et al., 2004) of which only a small portion is expected to be altered upon associative learning or noxious stimulus processing. This assumption is based on the observations that PTIs receive excitatory inputs from their neighboring principal neurons (Andrasi et al., 2017), of which only 10–15% is engaged in memory processes or pain processing (Trouche et al., 2013; Senn et al., 2014; Grewe et al., 2017; Corder et al., 2019). In addition, interneurons are innervated also by extraamygdalar excitatory afferents, e.g., from the thalamus (Krabbe et al., 2019). Although their ratio within the glutamatergic synapses received by distinct GABAergic cell types in the BA is unknown at present, these inputs may also undergo plastic modifications upon fear learning (Barsy et al., 2020), thus, they can also contribute to or

counteract the observed changes in this study. Moreover, not all GABAergic interneurons within a population have been found to participate in these neural processes (Bienvenu et al., 2012; Wolff et al., 2014; Krabbe et al., 2019). Thus, the excitatory inputs that underwent plastic changes on a randomly sampled interneuron pool in our circumstances may constitute only a small subset of the entire excitatory synapse population.

Taken together, our work highlights the differential contribution of the 3 PTIs to the microcircuits of the mPFC in its default state and the microcircuits of BA in mice subjected to a behavioral paradigm involving an evolutionary conserved function, namely, fear learning. PVBCs provide potent inhibition to the local network both in the mPFC and the BA (Veres et al., 2017) and were mostly targeted by changes in the excitatory network in the BA when behavioral challenges arose. Interestingly, CCKBCs, termed as the fine-tuners of perisomatic inhibition (Freund & Katona, 2007) are excited in the BA by faster decaying events in response to aversive stimuli implying changes in how they integrate incoming inputs. In the mPFC, CCKBCs evoke uIPSCs with modest but the steadiest amplitude during the STP protocol and possibly induce a longer lasting inhibitory effect. Interestingly, when comparing mEPSCs from CCKBCs and PVBCs across the PrL and the BA, the tendencies are similar in both brain regions. CCKBCs receive mEPSCs that show slower kinetic properties compared to PVBCs, while PVBCs receive mEPSCs with a higher rate and amplitude in line with previous results from the BA (Andrasi et al., 2017). ChCs, the cell type previously reported to be sensitive for noxious stimuli in the BA (Bienvenu et al., 2012) receive increased rate of mEPSCs following fear learning, therefore, the excitatory circuit might shift from activating PVBCs to recruiting ChCs. ChCs provide strong inhibition both in the BA (Veres et al., 2014; Barsy et al., 2017) and the PrL, but given the low connection probability from PNs in the PrL, the source of their excitation remains elusive.

6. CONCLUSIONS

By performing *in vitro* whole-cell recordings from PTIs of the PrL, we found that PVBCs significantly differ from the other two PTI types with their low input resistance, short membrane time constant or large AHP amplitude, while CCKBCs fired the widest action potentials with the lowest maximum firing rate. After obtaining paired recording, analysis of the uEPSCs recorded from PTIs showed that PVBCs receive synaptic excitation from local PNs with short latency and large amplitude from synapses that are less depressing than earlier works described. Unitary EPSCs from CCKBCs had the slowest kinetic properties, which seemed as a universal feature of the synaptic excitation targeting the two basket cells, as contrasting kinetics of mEPSCs resembled that of uEPSC. We found excitatory connections on ChCs in only a handful of cases, but ChCs innervated neighboring PNs with high probability and evoked uIPSCs very reliably that showed similar short-term depression as connections established by PVBCs. Activation of PVBCs and ChCs gave rise to uIPSCs with significantly shorter latency compared to events evoked by CCKBC spiking which could contribute to their role in selecting active members of the neuronal population.

Homotypic synaptic connections between basket cells are frequent and show cell type specific features in the PrL that resemble uIPSCs evoked in PNs. Our pharmacological and optogenetical tools supported by anatomical data allowed us to provide evidence for the functional connectivity between the two types of basket cell populations.

To study how the inputs of PTIs in the BA are affected by noxious stimulation and fear memory formation itself, we investigated how the mEPSCs recorded in PTIs are altered by the unsigned and signed footshock compared to when only the tone is presented. Using these 3 different behavioral conditions we found that ChCs were the only cells that received heightened rate of excitation following fear conditioning. Kinetics of the recorded events were affected only in CCKBCs after unsigned US presentation, while events recorded from PVBCs decreased both in their rate and amplitude. Therefore, these cell types might be differentially involved in processing aversive stimuli and fear memories.

7. SUMMARY

Cortical regions like the mPFC and the BA are responsible for diverse functions but consist of similar neuronal elements, including PTIs. PTIs are strategically positioned to regulate the activity of their targeted postsynaptic partners, therefore they are key components in balancing circuit activity. Still, knowledge regarding their connectivity and contribution to circuit functions at the synaptic level in these regions has been limited.

In this study, by using transgenic mouse lines and *in vitro* whole-cell recordings we targeted PTIs in the mouse mPFC to investigate how they are embedded in local circuits. Our paired recordings revealed that PNs located in the PrL not only evoke larger unitary excitatory postsynaptic currents in PVBCs than in CCKBCs, but these currents have shorter latency and faster kinetic parameters. We determined that although these cell types all provide inhibition preferentially to the perisomatic region, the connections these PTIs establish on the local excitatory cells differ in their speed, reliability, and their connectivity rates. Following prior publications that investigated the connectivity between BCs in the hippocampus and the BA, we provided anatomical and electrophysiological evidence that BCs innervate not only their own kind but also establish functional connections with the other BC type.

In the BA, a central component of emotional circuits controlling fear learning, we dissected how the excitatory postsynaptic inputs onto PTIs are affected by aversive stimulation, a neutral tone, and the association between the two that results in fear learning. As a measure of how excitatory networks targeting PTIs are reorganized in the BA in response to the 2 elements of fear conditioning (the CS and US) and the actual association between them, we recorded mEPSCs from PTIs. Our results show that fear learning induces distinct changes in these cell types, including the rate, the amplitude and the kinetics of these spontaneous events, implying that the recruitment of the three PTI types undergo long-term changes in response to fear memory formation.

8. REFERENCES

Acsady, L., Gorcs, T. J., & Freund, T. F. (1996). Different populations of vasoactive intestinal polypeptide-immunoreactive interneurons are specialized to control pyramidal cells or interneurons in the hippocampus. Neuroscience, 73(2), 317-334. https://doi.org/10.1016/0306-4522(95)00609-5

Aerts, T., & Seuntjens, E. (2021). Novel perspectives on the development of the amygdala in rodents. Front Neuroanat, 15, 786679. https://doi.org/10.3389/fnana.2021.786679

Ahrlund-Richter, S., Xuan, Y., van Lunteren, J. A., Kim, H., Ortiz, C., Pollak Dorocic, I., Meletis, K., & Carlen, M. (2019). A whole-brain atlas of monosynaptic input targeting four different cell types in the medial prefrontal cortex of the mouse. Nat Neurosci, 22(4), 657-668. https://doi.org/10.1038/s41593-019-0354-y

Aldahabi, M., Balint, F., Holderith, N., Lorincz, A., Reva, M., & Nusser, Z. (2022). Different priming states of synaptic vesicles underlie distinct release probabilities at hippocampal excitatory synapses. Neuron, 110(24), 4144-4161 e4147. https://doi.org/10.1016/j.neuron.2022.09.035

Ali, A. B., Deuchars, J., Pawelzik, H., & Thomson, A. M. (1998). Ca1 pyramidal to basket and bistratified cell epsps: Dual intracellular recordings in rat hippocampal slices. J Physiol, 507 (Pt 1)(Pt 1), 201-217. https://doi.org/10.1111/j.1469-7793.1998.201bu.x

Amano, T., Duvarci, S., Popa, D., & Pare, D. (2011). The fear circuit revisited: Contributions of the basal amygdala nuclei to conditioned fear. J Neurosci, 31(43), 15481-15489. https://doi.org/10.1523/JNEUROSCI.3410-11.2011

Anastasiades, P. G., & Carter, A. G. (2021). Circuit organization of the rodent medial prefrontal cortex. Trends Neurosci, 44(7), 550-563. https://doi.org/10.1016/j.tins.2021.03.006

Andrasi, T., Veres, J. M., Rovira-Esteban, L., Kozma, R., Vikor, A., Gregori, E., & Hajos, N. (2017). Differential excitatory control of 2 parallel basket cell networks in amygdala microcircuits. PLoS Biol, 15(5), e2001421. https://doi.org/10.1371/journal.pbio.2001421

Atallah, B. V., Bruns, W., Carandini, M., & Scanziani, M. (2012). Parvalbumin-expressing interneurons linearly transform cortical responses to visual stimuli. Neuron, 73(1), 159-170. https://doi.org/10.1016/j.neuron.2011.12.013

Baldi, R., Muthuswamy, S., Loomba, N., & Patel, S. (2024). Synaptic organization-function relationships of amygdala interneurons supporting associative learning. bioRxiv. https://doi.org/10.1101/2024.06.18.599631

Banks, S. J., Eddy, K. T., Angstadt, M., Nathan, P. J., & Phan, K. L. (2007). Amygdala-frontal connectivity during emotion regulation. Soc Cogn Affect Neurosci, 2(4), 303-312. https://doi.org/10.1093/scan/nsm029

Barsy, B., Szabo, G. G., Andrasi, T., Vikor, A., & Hajos, N. (2017). Different output properties of perisomatic region-targeting interneurons in the basal amygdala. Eur J Neurosci, 45(4), 548-558. https://doi.org/10.1111/ejn.13498

Barsy, B., Kocsis, K., Magyar, A., Babiczky, A., Szabo, M., Veres, J. M., Hillier, D., Ulbert, I., Yizhar, O., & Matyas, F. (2020). Associative and plastic thalamic signaling to the lateral amygdala controls fear behavior. Nat Neurosci, 23(5), 625-637. https://doi.org/10.1038/s41593-020-0620-z

Bartos, M., Vida, I., Frotscher, M., Geiger, J. R., & Jonas, P. (2001). Rapid signaling at inhibitory synapses in a dentate gyrus interneuron network. J Neurosci, 21(8), 2687-2698. https://doi.org/10.1523/JNEUROSCI.21-08-02687.2001

Bartos, M., Vida, I., Frotscher, M., Meyer, A., Monyer, H., Geiger, J. R., & Jonas, P. (2002). Fast synaptic inhibition promotes synchronized gamma oscillations in hippocampal interneuron networks. Proc Natl Acad Sci U S A, 99(20), 13222-13227. https://doi.org/10.1073/pnas.192233099

Bartos, M., & Elgueta, C. (2012). Functional characteristics of parvalbumin- and cholecystokinin-expressing basket cells. J Physiol, 590(4), 669-681. https://doi.org/10.1113/jphysiol.2011.226175

Beierlein, M., Gibson, J. R., & Connors, B. W. (2000). A network of electrically coupled interneurons drives synchronized inhibition in neocortex. Nat Neurosci, 3(9), 904-910. https://doi.org/10.1038/78809

Benchenane, K., Tiesinga, P. H., & Battaglia, F. P. (2011). Oscillations in the prefrontal cortex: A gateway to memory and attention. Curr Opin Neurobiol, 21(3), 475-485. https://doi.org/10.1016/j.conb.2011.01.004

Bennett, M. V., & Zukin, R. S. (2004). Electrical coupling and neuronal synchronization in the mammalian brain. Neuron, 41(4), 495-511. https://doi.org/10.1016/s0896-6273(04)00043-1

Bienvenu, T. C., Busti, D., Magill, P. J., Ferraguti, F., & Capogna, M. (2012). Cell-type-specific recruitment of amygdala interneurons to hippocampal theta rhythm and noxious stimuli in vivo. Neuron, 74(6), 1059-1074. https://doi.org/10.1016/j.neuron.2012.04.022

Biro, L., Miskolczi, C., Szebik, H., Bruzsik, B., Varga, Z. K., Szente, L., Toth, M., Halasz, J., & Mikics, E. (2023). Post-weaning social isolation in male mice leads to abnormal aggression and disrupted network organization in the prefrontal cortex: Contribution of parvalbumin interneurons with or without perineuronal nets. Neurobiol Stress, 25, 100546. https://doi.org/10.1016/j.ynstr.2023.100546

Bissiere, S., Humeau, Y., & Luthi, A. (2003). Dopamine gates ltp induction in lateral amygdala by suppressing feedforward inhibition. Nat Neurosci, 6(6), 587-592. https://doi.org/10.1038/nn1058

Bloss, E. B., Cembrowski, M. S., Karsh, B., Colonell, J., Fetter, R. D., & Spruston, N. (2016). Structured dendritic inhibition supports branch-selective integration in ca1 pyramidal cells. Neuron, 89(5), 1016-1030. https://doi.org/10.1016/j.neuron.2016.01.029

Bocchio, M., Nabavi, S., & Capogna, M. (2017). Synaptic plasticity, engrams, and network oscillations in amygdala circuits for storage and retrieval of emotional memories. Neuron, 94(4), 731-743. https://doi.org/10.1016/j.neuron.2017.03.022

Bordi, F., & LeDoux, J. E. (1994). Response properties of single units in areas of rat auditory thalamus that project to the amygdala. Ii. Cells receiving convergent auditory and somatosensory inputs and cells antidromically activated by amygdala stimulation. Exp Brain Res, 98(2), 275-286. https://doi.org/10.1007/BF00228415

Bowers, M. E., Choi, D. C., & Ressler, K. J. (2012). Neuropeptide regulation of fear and anxiety: Implications of cholecystokinin, endogenous opioids, and neuropeptide y. Physiol Behav, 107(5), 699-710. https://doi.org/10.1016/j.physbeh.2012.03.004

Bucurenciu, I., Kulik, A., Schwaller, B., Frotscher, M., & Jonas, P. (2008). Nanodomain coupling between ca2+ channels and ca2+ sensors promotes fast and efficient

transmitter release at a cortical gabaergic synapse. Neuron, 57(4), 536-545. https://doi.org/10.1016/j.neuron.2007.12.026
Buhl, E. H., Halasy, K., & Somogyi, P. (1994). Diverse sources of hippocampal unitary inhibitory postsynaptic potentials and the number of synaptic release sites. Nature, 368(6474), 823-828. https://doi.org/10.1038/368823a0
Buhl, E. H., Han, Z. S., Lorinczi, Z., Stezhka, V. V., Karnup, S. V., & Somogyi, P. (1994). Physiological properties of anatomically identified axo-axonic cells in the rat hippocampus. J Neurophysiol, 71(4), 1289-1307. https://doi.org/10.1152/jn.1994.71.4.1289
Buhl, E. H., Cobb, S. R., Halasy, K., & Somogyi, P. (1995). Properties of unitary ipsps evoked by anatomically identified basket cells in the rat hippocampus. Eur J Neurosci, 7(9), 1989-2004. https://doi.org/10.1111/j.1460-9568.1995.tb00721.x
Burgos-Robles, A., Vidal-Gonzalez, I., & Quirk, G. J. (2009). Sustained conditioned responses in prelimbic prefrontal neurons are correlated with fear expression and extinction failure. J Neurosci, 29(26), 8474-8482. https://doi.org/10.1523/JNEUROSCI.0378-09.2009
Buzsaki, G., & Wang, X. J. (2012). Mechanisms of gamma oscillations. Annu Rev Neurosci, 35, 203-225. https://doi.org/10.1146/annurev-neuro-062111-150444
Caillard, O., Moreno, H., Schwaller, B., Llano, I., Celio, M. R., & Marty, A. (2000). Role of the calcium-binding protein parvalbumin in short-term synaptic plasticity. Proc Natl Acad Sci U S A, 97(24), 13372-13377. https://doi.org/10.1073/pnas.230362997
Capogna, M. (2014). Gabaergic cell type diversity in the basolateral amygdala. Curr Opin Neurobiol, 26, 110-116. https://doi.org/10.1016/j.conb.2014.01.006
Carceller, H., Guirado, R., Ripolles-Campos, E., Teruel-Marti, V., & Nacher, J. (2020). Perineuronal nets regulate the inhibitory perisomatic input onto parvalbumin interneurons and gamma activity in the prefrontal cortex. J Neurosci, 40(26), 5008-5018. https://doi.org/10.1523/JNEUROSCI.0291-20.2020
Cardin, J. A., Carlen, M., Meletis, K., Knoblich, U., Zhang, F., Deisseroth, K., Tsai, L. H., & Moore, C. I. (2009). Driving fast-spiking cells induces gamma rhythm and controls sensory responses. Nature, 459(7247), 663-667. https://doi.org/10.1038/nature08002
Carlén, M. (2017). What constitutes the prefrontal cortex? Science, 358(6362), 478-482. https://doi.org/doi:10.1126/science.aan8868
Carrive, P. (1993). The periaqueductal gray and defensive behavior: Functional representation and neuronal organization. Behav Brain Res, 58(1-2), 27-47. https://doi.org/10.1016/0166-4328(93)90088-8
Carulli, D., Pizzorusso, T., Kwok, J. C., Putignano, E., Poli, A., Forostyak, S., Andrews, M. R., Deepa, S. S., Glant, T. T., & Fawcett, J. W. (2010). Animals lacking link protein have attenuated perineuronal nets and persistent plasticity. Brain, 133(Pt 8), 2331-2347. https://doi.org/10.1093/brain/awq145
Cea-del Rio, C. A., Lawrence, J. J., Tricoire, L., Erdelyi, F., Szabo, G., & McBain, C. J. (2010). M3 muscarinic acetylcholine receptor expression confers differential cholinergic modulation to neurochemically distinct hippocampal basket cell subtypes. J Neurosci, 30(17), 6011-6024. https://doi.org/10.1523/JNEUROSCI.5040-09.2010
Chagnac-Amitai, Y., Luhmann, H. J., & Prince, D. A. (1990). Burst generating and regular spiking layer 5 pyramidal neurons of rat neocortex have different morphological features. J Comp Neurol, 296(4), 598-613. https://doi.org/10.1002/cne.902960407

Chamberland, S., & Topolnik, L. (2012). Inhibitory control of hippocampal inhibitory neurons. Front Neurosci, 6, 165. https://doi.org/10.3389/fnins.2012.00165
Chen, Y. H., Lan, Y. J., Zhang, S. R., Li, W. P., Luo, Z. Y., Lin, S., Zhuang, J. P., Li, X. W., Li, S. J., Yang, J. M., & Gao, T. M. (2017). Erbb4 signaling in the prelimbic cortex regulates fear expression. Transl Psychiatry, 7(7), e1168. https://doi.org/10.1038/tp.2017.139
Ciocchi, S., Herry, C., Grenier, F., Wolff, S. B., Letzkus, J. J., Vlachos, I., Ehrlich, I., Sprengel, R., Deisseroth, K., Stadler, M. B., Muller, C., & Luthi, A. (2010). Encoding of conditioned fear in central amygdala inhibitory circuits. Nature, 468(7321), 277-282. https://doi.org/10.1038/nature09559
Cobb, S. R., Buhl, E. H., Halasy, K., Paulsen, O., & Somogyi, P. (1995). Synchronization of neuronal activity in hippocampus by individual gabaergic interneurons. Nature, 378(6552), 75-78. https://doi.org/10.1038/378075a0
Collins, D. R., & Pare, D. (2000). Differential fear conditioning induces reciprocal changes in the sensory responses of lateral amygdala neurons to the cs(+) and cs(-). Learn Mem, 7(2), 97-103. https://doi.org/10.1101/lm.7.2.97
Cope, D. W., Maccaferri, G., Marton, L. F., Roberts, J. D., Cobden, P. M., & Somogyi, P. (2002). Cholecystokinin-immunopositive basket and schaffer collateral-associated interneurones target different domains of pyramidal cells in the ca1 area of the rat hippocampus. Neuroscience, 109(1), 63-80. https://doi.org/10.1016/s0306-4522(01)00440-7
Cope, E. C., Zych, A. D., Katchur, N. J., Waters, R. C., Laham, B. J., Diethorn, E. J., Park, C. Y., Meara, W. R., & Gould, E. (2022). Atypical perineuronal nets in the ca2 region interfere with social memory in a mouse model of social dysfunction. Mol Psychiatry, 27(8), 3520-3531. https://doi.org/10.1038/s41380-021-01174-2
Corder, G., Ahanonu, B., Grewe, B. F., Wang, D., Schnitzer, M. J., & Scherrer, G. (2019). An amygdalar neural ensemble that encodes the unpleasantness of pain. Science, 363(6424), 276-281. https://doi.org/10.1126/science.aap8586
Coulon, P., & Landisman, C. E. (2017). The potential role of gap junctional plasticity in the regulation of state. Neuron, 93(6), 1275-1295. https://doi.org/10.1016/j.neuron.2017.02.041
Cox, J., & Witten, I. B. (2019). Striatal circuits for reward learning and decision-making. Nat Rev Neurosci, 20(8), 482-494. https://doi.org/10.1038/s41583-019-0189-2
Crawley, J. N. (1985). Comparative distribution of cholecystokinin and other neuropeptides. Why is this peptide different from all other peptides? Ann N Y Acad Sci, 448, 1-8. https://doi.org/10.1111/j.1749-6632.1985.tb29900.x
Crawley, J. N., & Corwin, R. L. (1994). Biological actions of cholecystokinin. Peptides, 15(4), 731-755. https://doi.org/10.1016/0196-9781(94)90104-x
Crochet, S., Poulet, J. F., Kremer, Y., & Petersen, C. C. (2011). Synaptic mechanisms underlying sparse coding of active touch. Neuron, 69(6), 1160-1175. https://doi.org/10.1016/j.neuron.2011.02.022
Daw, M. I., Tricoire, L., Erdelyi, F., Szabo, G., & McBain, C. J. (2009). Asynchronous transmitter release from cholecystokinin-containing inhibitory interneurons is widespread and target-cell independent. J Neurosci, 29(36), 11112-11122. https://doi.org/10.1523/JNEUROSCI.5760-08.2009
De-May, C. L., & Ali, A. B. (2013). Cell type-specific regulation of inhibition via cannabinoid type 1 receptors in rat neocortex. J Neurophysiol, 109(1), 216-224. https://doi.org/10.1152/jn.00272.2012
de Oliveira, A. R., Reimer, A. E., de Macedo, C. E., de Carvalho, M. C., Silva, M. A., & Brandao, M. L. (2011). Conditioned fear is modulated by d2 receptor pathway

connecting the ventral tegmental area and basolateral amygdala. Neurobiol Learn Mem, 95(1), 37-45. https://doi.org/10.1016/j.nlm.2010.10.005
DeFelipe, J., Hendry, S. H., Jones, E. G., & Schmechel, D. (1985). Variability in the terminations of gabaergic chandelier cell axons on initial segments of pyramidal cell axons in the monkey sensory-motor cortex. J Comp Neurol, 231(3), 364-384. https://doi.org/10.1002/cne.902310307
DeFelipe, J., Hendry, S. H., & Jones, E. G. (1989). Visualization of chandelier cell axons by parvalbumin immunoreactivity in monkey cerebral cortex. Proc Natl Acad Sci U S A, 86(6), 2093-2097. https://doi.org/10.1073/pnas.86.6.2093
DeFelipe, J., & Farinas, I. (1992). The pyramidal neuron of the cerebral cortex: Morphological and chemical characteristics of the synaptic inputs. Prog Neurobiol, 39(6), 563-607. https://doi.org/10.1016/0301-0082(92)90015-7
Degenetais, E., Thierry, A. M., Glowinski, J., & Gioanni, Y. (2003). Synaptic influence of hippocampus on pyramidal cells of the rat prefrontal cortex: An in vivo intracellular recording study. Cereb Cortex, 13(7), 782-792. https://doi.org/10.1093/cercor/13.7.782
Deng, P. Y., Xiao, Z., Jha, A., Ramonet, D., Matsui, T., Leitges, M., Shin, H. S., Porter, J. E., Geiger, J. D., & Lei, S. (2010). Cholecystokinin facilitates glutamate release by increasing the number of readily releasable vesicles and releasing probability. J Neurosci, 30(15), 5136-5148. https://doi.org/10.1523/JNEUROSCI.5711-09.2010
Dienel, S. J., Schoonover, K. E., & Lewis, D. A. (2022). Cognitive dysfunction and prefrontal cortical circuit alterations in schizophrenia: Developmental trajectories. Biol Psychiatry, 92(6), 450-459. https://doi.org/10.1016/j.biopsych.2022.03.002
Drake, C. T., & Milner, T. A. (2002). Mu opioid receptors are in discrete hippocampal interneuron subpopulations. Hippocampus, 12(2), 119-136. https://doi.org/10.1002/hipo.1107
Dudok, B., Klein, P. M., Hwaun, E., Lee, B. R., Yao, Z., Fong, O., Bowler, J. C., Terada, S., Sparks, F. T., Szabo, G. G., Farrell, J. S., Berg, J., Daigle, T. L., Tasic, B., Dimidschstein, J., Fishell, G., Losonczy, A., Zeng, H., & Soltesz, I. (2021). Alternating sources of perisomatic inhibition during behavior. Neuron, 109(6), 997-1012 e1019. https://doi.org/10.1016/j.neuron.2021.01.003
Dudok, B., Szoboszlay, M., Paul, A., Klein, P. M., Liao, Z., Hwaun, E., Szabo, G. G., Geiller, T., Vancura, B., Wang, B. S., McKenzie, S., Homidan, J., Klaver, L. M. F., English, D. F., Huang, Z. J., Buzsaki, G., Losonczy, A., & Soltesz, I. (2021). Recruitment and inhibitory action of hippocampal axo-axonic cells during behavior. Neuron, 109(23), 3838-3850 e3838. https://doi.org/10.1016/j.neuron.2021.09.033
Dudok, B., Fan, L. Z., Farrell, J. S., Malhotra, S., Homidan, J., Kim, D. K., Wenardy, C., Ramakrishnan, C., Li, Y., Deisseroth, K., & Soltesz, I. (2024). Retrograde endocannabinoid signaling at inhibitory synapses in vivo. Science, 383(6686), 967-970. https://doi.org/10.1126/science.adk3863
Eggermann, E., & Jonas, P. (2011). How the 'slow' ca(2+) buffer parvalbumin affects transmitter release in nanodomain-coupling regimes. Nat Neurosci, 15(1), 20-22. https://doi.org/10.1038/nn.3002
Ehrlich, I., Humeau, Y., Grenier, F., Ciocchi, S., Herry, C., & Luthi, A. (2009). Amygdala inhibitory circuits and the control of fear memory. Neuron, 62(6), 757-771. https://doi.org/10.1016/j.neuron.2009.05.026
Enwright, J. F., Sanapala, S., Foglio, A., Berry, R., Fish, K. N., & Lewis, D. A. (2016). Reduced labeling of parvalbumin neurons and perineuronal nets in the

dorsolateral prefrontal cortex of subjects with schizophrenia. Neuropsychopharmacology, 41(9), 2206-2214. https://doi.org/10.1038/npp.2016.24

Fadok, J. P., Dickerson, T. M., & Palmiter, R. D. (2009). Dopamine is necessary for cue-dependent fear conditioning. J Neurosci, 29(36), 11089-11097. https://doi.org/10.1523/JNEUROSCI.1616-09.2009

Fairen, A., & Valverde, F. (1980). A specialized type of neuron in the visual cortex of cat: A golgi and electron microscope study of chandelier cells. J Comp Neurol, 194(4), 761-779. https://doi.org/10.1002/cne.901940405

Fekete, Z., Weisz, F., Karlocai, M. R., Veres, J. M., Andrasi, T., & Hajos, N. (2024). Synaptic communication within the microcircuits of pyramidal neurons and basket cells in the mouse prefrontal cortex. J Physiol. https://doi.org/10.1113/JP286284

Feng, T., Alicea, C., Pham, V., Kirk, A., & Pieraut, S. (2021). Experience-dependent inhibitory plasticity is mediated by cck+ basket cells in the developing dentate gyrus. J Neurosci, 41(21), 4607-4619. https://doi.org/10.1523/JNEUROSCI.1207-20.2021

Fisahn, A., Pike, F. G., Buhl, E. H., & Paulsen, O. (1998). Cholinergic induction of network oscillations at 40 hz in the hippocampus in vitro. Nature, 394(6689), 186-189. https://doi.org/10.1038/28179

Foldy, C., Lee, S. Y., Szabadics, J., Neu, A., & Soltesz, I. (2007). Cell type-specific gating of perisomatic inhibition by cholecystokinin. Nat Neurosci, 10(9), 1128-1130. https://doi.org/10.1038/nn1952

Freund, T. F., & Buzsaki, G. (1996). Interneurons of the hippocampus. Hippocampus, 6(4), 347-470. https://doi.org/10.1002/(SICI)1098-1063(1996)6:4<347::AID-HIPO1>3.0.CO;2-I

Freund, T. F. (2003). Interneuron diversity series: Rhythm and mood in perisomatic inhibition. Trends Neurosci, 26(9), 489-495. https://doi.org/10.1016/S0166-2236(03)00227-3

Freund, T. F., & Katona, I. (2007). Perisomatic inhibition. Neuron, 56(1), 33-42. https://doi.org/10.1016/j.neuron.2007.09.012

Fuchs, E. C., Zivkovic, A. R., Cunningham, M. O., Middleton, S., Lebeau, F. E., Bannerman, D. M., Rozov, A., Whittington, M. A., Traub, R. D., Rawlins, J. N., & Monyer, H. (2007). Recruitment of parvalbumin-positive interneurons determines hippocampal function and associated behavior. Neuron, 53(4), 591-604. https://doi.org/10.1016/j.neuron.2007.01.031

Fuchs, P. N., Peng, Y. B., Boyette-Davis, J. A., & Uhelski, M. L. (2014). The anterior cingulate cortex and pain processing. Front Integr Neurosci, 8, 35. https://doi.org/10.3389/fnint.2014.00035

Fukuda, T., & Kosaka, T. (2000). Gap junctions linking the dendritic network of gabaergic interneurons in the hippocampus. J Neurosci, 20(4), 1519-1528. https://doi.org/10.1523/JNEUROSCI.20-04-01519.2000

Fukuda, T., Kosaka, T., Singer, W., & Galuske, R. A. (2006). Gap junctions among dendrites of cortical gabaergic neurons establish a dense and widespread intercolumnar network. J Neurosci, 26(13), 3434-3443. https://doi.org/10.1523/JNEUROSCI.4076-05.2006

Fuster, J. M. (2006). The cognit: A network model of cortical representation. Int J Psychophysiol, 60(2), 125-132. https://doi.org/10.1016/j.ijpsycho.2005.12.015

Galarreta, M., & Hestrin, S. (1998). Frequency-dependent synaptic depression and the balance of excitation and inhibition in the neocortex. Nat Neurosci, 1(7), 587-594. https://doi.org/10.1038/2822

Galarreta, M., & Hestrin, S. (1999). A network of fast-spiking cells in the neocortex connected by electrical synapses. Nature, 402(6757), 72-75. https://doi.org/10.1038/47029

Galarreta, M., & Hestrin, S. (2002). Electrical and chemical synapses among parvalbumin fast-spiking gabaergic interneurons in adult mouse neocortex. Proc Natl Acad Sci U S A, 99(19), 12438-12443. https://doi.org/10.1073/pnas.192159599

Galarreta, M., Erdelyi, F., Szabo, G., & Hestrin, S. (2008). Cannabinoid sensitivity and synaptic properties of 2 gabaergic networks in the neocortex. Cereb Cortex, 18(10), 2296-2305. https://doi.org/10.1093/cercor/bhm253

Gallo, N. B., Paul, A., & Van Aelst, L. (2020). Shedding light on chandelier cell development, connectivity, and contribution to neural disorders. Trends Neurosci, 43(8), 565-580. https://doi.org/10.1016/j.tins.2020.05.003

Gan, J., Weng, S. M., Pernia-Andrade, A. J., Csicsvari, J., & Jonas, P. (2017). Phase-locked inhibition, but not excitation, underlies hippocampal ripple oscillations in awake mice in vivo. Neuron, 93(2), 308-314. https://doi.org/10.1016/j.neuron.2016.12.018

Gangopadhyay, P., Chawla, M., Dal Monte, O., & Chang, S. W. C. (2021). Prefrontal-amygdala circuits in social decision-making. Nat Neurosci, 24(1), 5-18. https://doi.org/10.1038/s41593-020-00738-9

Geiger, J. R., Lubke, J., Roth, A., Frotscher, M., & Jonas, P. (1997). Submillisecond ampa receptor-mediated signaling at a principal neuron-interneuron synapse. Neuron, 18(6), 1009-1023. https://doi.org/10.1016/s0896-6273(00)80339-6

Gibson, J. R., Beierlein, M., & Connors, B. W. (1999). Two networks of electrically coupled inhibitory neurons in neocortex. Nature, 402(6757), 75-79. https://doi.org/10.1038/47035

Giustino, T. F., & Maren, S. (2018). Noradrenergic modulation of fear conditioning and extinction. Front Behav Neurosci, 12, 43. https://doi.org/10.3389/fnbeh.2018.00043

Glickfeld, L. L., & Scanziani, M. (2006). Distinct timing in the activity of cannabinoid-sensitive and cannabinoid-insensitive basket cells. Nat Neurosci, 9(6), 807-815. https://doi.org/10.1038/nn1688

Glickfeld, L. L., Roberts, J. D., Somogyi, P., & Scanziani, M. (2009). Interneurons hyperpolarize pyramidal cells along their entire somatodendritic axis. Nat Neurosci, 12(1), 21-23. https://doi.org/10.1038/nn.2230

Gogolla, N., Caroni, P., Luthi, A., & Herry, C. (2009). Perineuronal nets protect fear memories from erasure. Science, 325(5945), 1258-1261. https://doi.org/10.1126/science.1174146

Goldman-Rakic, P. S. (1988). Topography of cognition: Parallel distributed networks in primate association cortex. Annu Rev Neurosci, 11, 137-156. https://doi.org/10.1146/annurev.ne.11.030188.001033

Goldstein, R. Z., & Volkow, N. D. (2011). Dysfunction of the prefrontal cortex in addiction: Neuroimaging findings and clinical implications. Nat Rev Neurosci, 12(11), 652-669. https://doi.org/10.1038/nrn3119

Gonzalez-Burgos, G., Krimer, L. S., Povysheva, N. V., Barrionuevo, G., & Lewis, D. A. (2005). Functional properties of fast spiking interneurons and their synaptic connections with pyramidal cells in primate dorsolateral prefrontal cortex. J Neurophysiol, 93(2), 942-953. https://doi.org/10.1152/jn.00787.2004

Goosens, K. A., & Maren, S. (2001). Contextual and auditory fear conditioning are mediated by the lateral, basal, and central amygdaloid nuclei in rats. Learn Mem, 8(3), 148-155. https://doi.org/10.1101/lm.37601

Gore, F., Schwartz, E. C., Brangers, B. C., Aladi, S., Stujenske, J. M., Likhtik, E., Russo, M. J., Gordon, J. A., Salzman, C. D., & Axel, R. (2015). Neural representations of unconditioned stimuli in basolateral amygdala mediate innate and learned responses. Cell, 162(1), 134-145. https://doi.org/10.1016/j.cell.2015.06.027

Gray, E. G. (1959). Electron microscopy of synaptic contacts on dendrite spines of the cerebral cortex. Nature, 183(4675), 1592-1593. https://doi.org/10.1038/1831592a0

Grewe, B. F., Grundemann, J., Kitch, L. J., Lecoq, J. A., Parker, J. G., Marshall, J. D., Larkin, M. C., Jercog, P. E., Grenier, F., Li, J. Z., Luthi, A., & Schnitzer, M. J. (2017). Neural ensemble dynamics underlying a long-term associative memory. Nature, 543(7647), 670-675. https://doi.org/10.1038/nature21682

Gulyas, A. I., Megias, M., Emri, Z., & Freund, T. F. (1999). Total number and ratio of excitatory and inhibitory synapses converging onto single interneurons of different types in the ca1 area of the rat hippocampus. J Neurosci, 19(22), 10082-10097. https://doi.org/10.1523/JNEUROSCI.19-22-10082.1999

Gulyas, A. I., Buzsaki, G., Freund, T. F., & Hirase, H. (2006). Populations of hippocampal inhibitory neurons express different levels of cytochrome c. Eur J Neurosci, 23(10), 2581-2594. https://doi.org/10.1111/j.1460-9568.2006.04814.x

Gulyas, A. I., Szabo, G. G., Ulbert, I., Holderith, N., Monyer, H., Erdelyi, F., Szabo, G., Freund, T. F., & Hajos, N. (2010). Parvalbumin-containing fast-spiking basket cells generate the field potential oscillations induced by cholinergic receptor activation in the hippocampus. J Neurosci, 30(45), 15134-15145. https://doi.org/10.1523/JNEUROSCI.4104-10.2010

Hafner, G., Witte, M., Guy, J., Subhashini, N., Fenno, L. E., Ramakrishnan, C., Kim, Y. S., Deisseroth, K., Callaway, E. M., Oberhuber, M., Conzelmann, K. K., & Staiger, J. F. (2019). Mapping brain-wide afferent inputs of parvalbumin-expressing gabaergic neurons in barrel cortex reveals local and long-range circuit motifs. Cell Rep, 28(13), 3450-3461 e3458. https://doi.org/10.1016/j.celrep.2019.08.064

Hagihara, K. M., Bukalo, O., Zeller, M., Aksoy-Aksel, A., Karalis, N., Limoges, A., Rigg, T., Campbell, T., Mendez, A., Weinholtz, C., Mahn, M., Zweifel, L. S., Palmiter, R. D., Ehrlich, I., Luthi, A., & Holmes, A. (2021). Intercalated amygdala clusters orchestrate a switch in fear state. Nature, 594(7863), 403-407. https://doi.org/10.1038/s41586-021-03593-1

Hajos, N., Acsady, L., & Freund, T. F. (1996). Target selectivity and neurochemical characteristics of vip-immunoreactive interneurons in the rat dentate gyrus. Eur J Neurosci, 8(7), 1415-1431. https://doi.org/10.1111/j.1460-9568.1996.tb01604.x

Hajos, N., Papp, E. C., Acsady, L., Levey, A. I., & Freund, T. F. (1998). Distinct interneuron types express m2 muscarinic receptor immunoreactivity on their dendrites or axon terminals in the hippocampus. Neuroscience, 82(2), 355-376. https://doi.org/10.1016/s0306-4522(97)00300-x

Hajos, N., Palhalmi, J., Mann, E. O., Nemeth, B., Paulsen, O., & Freund, T. F. (2004). Spike timing of distinct types of gabaergic interneuron during hippocampal gamma oscillations in vitro. J Neurosci, 24(41), 9127-9137. https://doi.org/10.1523/JNEUROSCI.2113-04.2004

Hajos, N., Karlocai, M. R., Nemeth, B., Ulbert, I., Monyer, H., Szabo, G., Erdelyi, F., Freund, T. F., & Gulyas, A. I. (2013). Input-output features of anatomically

identified ca3 neurons during hippocampal sharp wave/ripple oscillation in vitro. J Neurosci, 33(28), 11677-11691. https://doi.org/10.1523/JNEUROSCI.5729-12.2013
Hajos, N. (2021). Interneuron types and their circuits in the basolateral amygdala. Front Neural Circuits, 15, 687257. https://doi.org/10.3389/fncir.2021.687257
Han, J. H., Kushner, S. A., Yiu, A. P., Cole, C. J., Matynia, A., Brown, R. A., Neve, R. L., Guzowski, J. F., Silva, A. J., & Josselyn, S. A. (2007). Neuronal competition and selection during memory formation. Science, 316(5823), 457-460. https://doi.org/10.1126/science.1139438
Han, J. H., Kushner, S. A., Yiu, A. P., Hsiang, H. L., Buch, T., Waisman, A., Bontempi, B., Neve, R. L., Frankland, P. W., & Josselyn, S. A. (2009). Selective erasure of a fear memory. Science, 323(5920), 1492-1496. https://doi.org/10.1126/science.1164139
Hart, S. A., Snyder, M. A., Smejkalova, T., & Woolley, C. S. (2007). Estrogen mobilizes a subset of estrogen receptor-alpha-immunoreactive vesicles in inhibitory presynaptic boutons in hippocampal ca1. J Neurosci, 27(8), 2102-2111. https://doi.org/10.1523/JNEUROSCI.5436-06.2007
Hartwich, K., Pollak, T., & Klausberger, T. (2009). Distinct firing patterns of identified basket and dendrite-targeting interneurons in the prefrontal cortex during hippocampal theta and local spindle oscillations. J Neurosci, 29(30), 9563-9574. https://doi.org/10.1523/JNEUROSCI.1397-09.2009
Hartzell, A. L., Martyniuk, K. M., Brigidi, G. S., Heinz, D. A., Djaja, N. A., Payne, A., & Bloodgood, B. L. (2018). Npas4 recruits cck basket cell synapses and enhances cannabinoid-sensitive inhibition in the mouse hippocampus. Elife, 7. https://doi.org/10.7554/eLife.35927
Hashimoto, T., Volk, D. W., Eggan, S. M., Mirnics, K., Pierri, J. N., Sun, Z., Sampson, A. R., & Lewis, D. A. (2003). Gene expression deficits in a subclass of gaba neurons in the prefrontal cortex of subjects with schizophrenia. J Neurosci, 23(15), 6315-6326. https://doi.org/10.1523/JNEUROSCI.23-15-06315.2003
Hattox, A. M., & Nelson, S. B. (2007). Layer v neurons in mouse cortex projecting to different targets have distinct physiological properties. J Neurophysiol, 98(6), 3330-3340. https://doi.org/10.1152/jn.00397.2007
Hefft, S., & Jonas, P. (2005). Asynchronous gaba release generates long-lasting inhibition at a hippocampal interneuron-principal neuron synapse. Nat Neurosci, 8(10), 1319-1328. https://doi.org/10.1038/nn1542
Heistek, T. S., Jaap Timmerman, A., Spijker, S., Brussaard, A. B., & Mansvelder, H. D. (2010). Gabaergic synapse properties may explain genetic variation in hippocampal network oscillations in mice. Front Cell Neurosci, 4, 18. https://doi.org/10.3389/fncel.2010.00018
Herry, C., Ciocchi, S., Senn, V., Demmou, L., Muller, C., & Luthi, A. (2008). Switching on and off fear by distinct neuronal circuits. Nature, 454(7204), 600-606. https://doi.org/10.1038/nature07166
Herry, C., Ferraguti, F., Singewald, N., Letzkus, J. J., Ehrlich, I., & Luthi, A. (2010). Neuronal circuits of fear extinction. Eur J Neurosci, 31(4), 599-612. https://doi.org/10.1111/j.1460-9568.2010.07101.x
Hijazi, S., Smit, A. B., & van Kesteren, R. E. (2023). Fast-spiking parvalbumin-positive interneurons in brain physiology and alzheimer's disease. Mol Psychiatry. https://doi.org/10.1038/s41380-023-02168-y
Hioki, H., Okamoto, S., Konno, M., Kameda, H., Sohn, J., Kuramoto, E., Fujiyama, F., & Kaneko, T. (2013). Cell type-specific inhibitory inputs to dendritic and somatic

compartments of parvalbumin-expressing neocortical interneuron. J Neurosci, 33(2), 544-555. https://doi.org/10.1523/JNEUROSCI.2255-12.2013

Hioki, H., Sohn, J., Nakamura, H., Okamoto, S., Hwang, J., Ishida, Y., Takahashi, M., & Kameda, H. (2018). Preferential inputs from cholecystokinin-positive neurons to the somatic compartment of parvalbumin-expressing neurons in the mouse primary somatosensory cortex. Brain Res, 1695, 18-30. https://doi.org/10.1016/j.brainres.2018.05.029

Hong, T., Falcone, C., Dufour, B., Amina, S., Castro, R. P., Regalado, J., Pearson, W., Noctor, S. C., & Martinez-Cerdeno, V. (2020). Gaba(a)ralpha2 is decreased in the axon initial segment of pyramidal cells in specific areas of the prefrontal cortex in autism. Neuroscience, 437, 76-86. https://doi.org/10.1016/j.neuroscience.2020.04.025

Howes, O. D., Bukala, B. R., & Beck, K. (2024). Schizophrenia: From neurochemistry to circuits, symptoms and treatments. Nat Rev Neurol, 20(1), 22-35. https://doi.org/10.1038/s41582-023-00904-0

Hu, H., Roth, F. C., Vandael, D., & Jonas, P. (2018). Complementary tuning of na(+) and k(+) channel gating underlies fast and energy-efficient action potentials in gabaergic interneuron axons. Neuron, 98(1), 156-165 e156. https://doi.org/10.1016/j.neuron.2018.02.024

Huang, S., Wu, S. J., Sansone, G., Ibrahim, L. A., & Fishell, G. (2024). Layer 1 neocortex: Gating and integrating multidimensional signals. Neuron, 112(2), 184-200. https://doi.org/10.1016/j.neuron.2023.09.041

Iascone, D. M., Li, Y., Sumbul, U., Doron, M., Chen, H., Andreu, V., Goudy, F., Blockus, H., Abbott, L. F., Segev, I., Peng, H., & Polleux, F. (2020). Whole-neuron synaptic mapping reveals spatially precise excitatory/inhibitory balance limiting dendritic and somatic spiking. Neuron, 106(4), 566-578 e568. https://doi.org/10.1016/j.neuron.2020.02.015

Iball, J., & Ali, A. B. (2011). Endocannabinoid release modulates electrical coupling between cck cells connected via chemical and electrical synapses in ca1. Front Neural Circuits, 5, 17. https://doi.org/10.3389/fncir.2011.00017

Ito, W., Fusco, B., & Morozov, A. (2020). Disinhibition-assisted long-term potentiation in the prefrontal-amygdala pathway via suppression of somatostatin-expressing interneurons. Neurophotonics, 7(1), 015007. https://doi.org/10.1117/1.NPh.7.1.015007

Janak, P. H., & Tye, K. M. (2015). From circuits to behaviour in the amygdala. Nature, 517(7534), 284-292. https://doi.org/10.1038/nature14188

Jiang, X., Shen, S., Cadwell, C. R., Berens, P., Sinz, F., Ecker, A. S., Patel, S., & Tolias, A. S. (2015). Principles of connectivity among morphologically defined cell types in adult neocortex. Science, 350(6264), aac9462. https://doi.org/10.1126/science.aac9462

Jones, R. T., Faas, G. C., & Mody, I. (2014). Intracellular bicarbonate regulates action potential generation via kcnq channel modulation. J Neurosci, 34(12), 4409-4417. https://doi.org/10.1523/JNEUROSCI.3836-13.2014

Jung, K., Chang, M., Steinecke, A., Burke, B., Choi, Y., Oisi, Y., Fitzpatrick, D., Taniguchi, H., & Kwon, H. B. (2023). An adaptive behavioral control motif mediated by cortical axo-axonic inhibition. Nat Neurosci, 26(8), 1379-1393. https://doi.org/10.1038/s41593-023-01380-x

Karlocai, M. R., Heredi, J., Benedek, T., Holderith, N., Lorincz, A., & Nusser, Z. (2021). Variability in the munc13-1 content of excitatory release sites. Elife, 10. https://doi.org/10.7554/eLife.67468

Karson, M. A., Tang, A. H., Milner, T. A., & Alger, B. E. (2009). Synaptic cross talk between perisomatic-targeting interneuron classes expressing cholecystokinin and parvalbumin in hippocampus. J Neurosci, 29(13), 4140-4154. https://doi.org/10.1523/JNEUROSCI.5264-08.2009

Katona, I., Sperlagh, B., Sik, A., Kafalvi, A., Vizi, E. S., Mackie, K., & Freund, T. F. (1999). Presynaptically located cb1 cannabinoid receptors regulate gaba release from axon terminals of specific hippocampal interneurons. J Neurosci, 19(11), 4544-4558. https://doi.org/10.1523/JNEUROSCI.19-11-04544.1999

Kawaguchi, Y., & Kubota, Y. (1996). Physiological and morphological identification of somatostatin- or vasoactive intestinal polypeptide-containing cells among gabaergic cell subtypes in rat frontal cortex. J Neurosci, 16(8), 2701-2715. https://doi.org/10.1523/JNEUROSCI.16-08-02701.1996

Kawaguchi, Y. (2017). Pyramidal cell subtypes and their synaptic connections in layer 5 of rat frontal cortex. Cereb Cortex, 27(12), 5755-5771. https://doi.org/10.1093/cercor/bhx252

Keimpema, E., Straiker, A., Mackie, K., Harkany, T., & Hjerling-Leffler, J. (2012). Sticking out of the crowd: The molecular identity and development of cholecystokinin-containing basket cells. J Physiol, 590(4), 703-714. https://doi.org/10.1113/jphysiol.2011.224386

Kerti-Szigeti, K., & Nusser, Z. (2016). Similar gabaa receptor subunit composition in somatic and axon initial segment synapses of hippocampal pyramidal cells. Elife, 5. https://doi.org/10.7554/eLife.18426

Kim, D., Jeong, H., Lee, J., Ghim, J. W., Her, E. S., Lee, S. H., & Jung, M. W. (2016). Distinct roles of parvalbumin- and somatostatin-expressing interneurons in working memory. Neuron, 92(4), 902-915. https://doi.org/10.1016/j.neuron.2016.09.023

Kisvarday, Z. F., Ferecsko, A. S., Kovacs, K., Buzas, P., Budd, J. M., & Eysel, U. T. (2002). One axon-multiple functions: Specificity of lateral inhibitory connections by large basket cells. J Neurocytol, 31(3-5), 255-264. https://doi.org/10.1023/a:1024122009448

Klausberger, T., Roberts, J. D., & Somogyi, P. (2002). Cell type- and input-specific differences in the number and subtypes of synaptic gaba(a) receptors in the hippocampus. J Neurosci, 22(7), 2513-2521. https://doi.org/10.1523/JNEUROSCI.22-07-02513.2002

Klausberger, T., Magill, P. J., Marton, L. F., Roberts, J. D., Cobden, P. M., Buzsaki, G., & Somogyi, P. (2003). Brain-state- and cell-type-specific firing of hippocampal interneurons in vivo. Nature, 421(6925), 844-848. https://doi.org/10.1038/nature01374

Klausberger, T., & Somogyi, P. (2008). Neuronal diversity and temporal dynamics: The unity of hippocampal circuit operations. Science, 321(5885), 53-57. https://doi.org/10.1126/science.1149381

Kohus, Z., Kali, S., Rovira-Esteban, L., Schlingloff, D., Papp, O., Freund, T. F., Hajos, N., & Gulyas, A. I. (2016). Properties and dynamics of inhibitory synaptic communication within the ca3 microcircuits of pyramidal cells and interneurons expressing parvalbumin or cholecystokinin. J Physiol, 594(13), 3745-3774. https://doi.org/10.1113/JP272231

Kole, M. H., & Stuart, G. J. (2012). Signal processing in the axon initial segment. Neuron, 73(2), 235-247. https://doi.org/10.1016/j.neuron.2012.01.007

Koukouli, F., Montmerle, M., Aguirre, A., De Brito Van Velze, M., Peixoto, J., Choudhary, V., Varilh, M., Julio-Kalajzic, F., Allene, C., Mendez, P., Zerlaut, Y.,

Marsicano, G., Schluter, O. M., Rebola, N., Bacci, A., & Lourenco, J. (2022). Visual-area-specific tonic modulation of gaba release by endocannabinoids sets the activity and coordination of neocortical principal neurons. Cell Rep, 40(8), 111202. https://doi.org/10.1016/j.celrep.2022.111202

Kow, L. M., & Pfaff, D. W. (1988). Neuromodulatory actions of peptides. Annu Rev Pharmacol Toxicol, 28, 163-188. https://doi.org/10.1146/annurev.pa.28.040188.001115

Krabbe, S., Grundemann, J., & Luthi, A. (2018). Amygdala inhibitory circuits regulate associative fear conditioning. Biol Psychiatry, 83(10), 800-809. https://doi.org/10.1016/j.biopsych.2017.10.006

Krabbe, S., Paradiso, E., d'Aquin, S., Bitterman, Y., Courtin, J., Xu, C., Yonehara, K., Markovic, M., Muller, C., Eichlisberger, T., Grundemann, J., Ferraguti, F., & Luthi, A. (2019). Adaptive disinhibitory gating by vip interneurons permits associative learning. Nat Neurosci, 22(11), 1834-1843. https://doi.org/10.1038/s41593-019-0508-y

Kubota, Y., Hatada, S., Kondo, S., Karube, F., & Kawaguchi, Y. (2007). Neocortical inhibitory terminals innervate dendritic spines targeted by thalamocortical afferents. J Neurosci, 27(5), 1139-1150. https://doi.org/10.1523/JNEUROSCI.3846-06.2007

Kubota, Y., Kondo, S., Nomura, M., Hatada, S., Yamaguchi, N., Mohamed, A. A., Karube, F., Lubke, J., & Kawaguchi, Y. (2015). Functional effects of distinct innervation styles of pyramidal cells by fast spiking cortical interneurons. Elife, 4. https://doi.org/10.7554/eLife.07919

Lagler, M., Ozdemir, A. T., Lagoun, S., Malagon-Vina, H., Borhegyi, Z., Hauer, R., Jelem, A., & Klausberger, T. (2016). Divisions of identified parvalbumin-expressing basket cells during working memory-guided decision making. Neuron, 91(6), 1390-1401. https://doi.org/10.1016/j.neuron.2016.08.010

Lanuza, E., Belekhova, M., Martinez-Marcos, A., Font, C., & Martinez-Garcia, F. (1998). Identification of the reptilian basolateral amygdala: An anatomical investigation of the afferents to the posterior dorsal ventricular ridge of the lizard podarcis hispanica. Eur J Neurosci, 10(11), 3517-3534. https://doi.org/10.1046/j.1460-9568.1998.00363.x

Lanuza, E., Moncho-Bogani, J., & Ledoux, J. E. (2008). Unconditioned stimulus pathways to the amygdala: Effects of lesions of the posterior intralaminar thalamus on foot-shock-induced c-fos expression in the subdivisions of the lateral amygdala. Neuroscience, 155(3), 959-968. https://doi.org/10.1016/j.neuroscience.2008.06.028

Le Merre, P., Ahrlund-Richter, S., & Carlen, M. (2021). The mouse prefrontal cortex: Unity in diversity. Neuron, 109(12), 1925-1944. https://doi.org/10.1016/j.neuron.2021.03.035

LeDoux, J. (2003). The emotional brain, fear, and the amygdala. Cell Mol Neurobiol, 23(4-5), 727-738. https://doi.org/10.1023/a:1025048802629

LeDoux, J. E. (2000). Emotion circuits in the brain. Annu Rev Neurosci, 23, 155-184. https://doi.org/10.1146/annurev.neuro.23.1.155

Lee, S., Kim, S. J., Kwon, O. B., Lee, J. H., & Kim, J. H. (2013). Inhibitory networks of the amygdala for emotional memory. Front Neural Circuits, 7, 129. https://doi.org/10.3389/fncir.2013.00129

Lee, S. H., & Soltesz, I. (2011). Requirement for cb1 but not gabab receptors in the cholecystokinin mediated inhibition of gaba release from cholecystokinin

expressing basket cells. J Physiol, 589(Pt 4), 891-902. https://doi.org/10.1113/jphysiol.2010.198499
Lee, S. Y., Foldy, C., Szabadics, J., & Soltesz, I. (2011). Cell-type-specific cck2 receptor signaling underlies the cholecystokinin-mediated selective excitation of hippocampal parvalbumin-positive fast-spiking basket cells. J Neurosci, 31(30), 10993-11002. https://doi.org/10.1523/JNEUROSCI.1970-11.2011
Lee, S. Y., & Soltesz, I. (2011). Cholecystokinin: A multi-functional molecular switch of neuronal circuits. Dev Neurobiol, 71(1), 83-91. https://doi.org/10.1002/dneu.20815
Lien, C. C., & Jonas, P. (2003). Kv3 potassium conductance is necessary and kinetically optimized for high-frequency action potential generation in hippocampal interneurons. J Neurosci, 23(6), 2058-2068. https://doi.org/10.1523/JNEUROSCI.23-06-02058.2003
Losonczy, A., Zemelman, B. V., Vaziri, A., & Magee, J. C. (2010). Network mechanisms of theta related neuronal activity in hippocampal ca1 pyramidal neurons. Nat Neurosci, 13(8), 967-972. https://doi.org/10.1038/nn.2597
Lu, J., Tucciarone, J., Padilla-Coreano, N., He, M., Gordon, J. A., & Huang, Z. J. (2017). Selective inhibitory control of pyramidal neuron ensembles and cortical subnetworks by chandelier cells. Nat Neurosci, 20(10), 1377-1383. https://doi.org/10.1038/nn.4624
Lucas, E. K., Jegarl, A. M., Morishita, H., & Clem, R. L. (2016). Multimodal and site-specific plasticity of amygdala parvalbumin interneurons after fear learning. Neuron, 91(3), 629-643. https://doi.org/10.1016/j.neuron.2016.06.032
Maccaferri, G., Roberts, J. D., Szucs, P., Cottingham, C. A., & Somogyi, P. (2000). Cell surface domain specific postsynaptic currents evoked by identified gabaergic neurones in rat hippocampus in vitro. J Physiol, 524 Pt 1(Pt 1), 91-116. https://doi.org/10.1111/j.1469-7793.2000.t01-3-00091.x
Marin, O. (2012). Interneuron dysfunction in psychiatric disorders. Nat Rev Neurosci, 13(2), 107-120. https://doi.org/10.1038/nrn3155
Martina, M., Schultz, J. H., Ehmke, H., Monyer, H., & Jonas, P. (1998). Functional and molecular differences between voltage-gated k+ channels of fast-spiking interneurons and pyramidal neurons of rat hippocampus. J Neurosci, 18(20), 8111-8125. https://doi.org/10.1523/JNEUROSCI.18-20-08111.1998
Martinez-Garcia, F., Novejarque, A., & Lanuza, E. (2008). Two interconnected functional systems in the amygdala of amniote vertebrates. Brain Res Bull, 75(2-4), 206-213. https://doi.org/10.1016/j.brainresbull.2007.10.019
Massi, L., Lagler, M., Hartwich, K., Borhegyi, Z., Somogyi, P., & Klausberger, T. (2012). Temporal dynamics of parvalbumin-expressing axo-axonic and basket cells in the rat medial prefrontal cortex in vivo. J Neurosci, 32(46), 16496-16502. https://doi.org/10.1523/JNEUROSCI.3475-12.2012
Mate, Z., Poles, M. Z., Szabo, G., Bagyanszki, M., Talapka, P., Fekete, E., & Bodi, N. (2013). Spatiotemporal expression pattern of dsredt3/cck gene construct during postnatal development of myenteric plexus in transgenic mice. Cell Tissue Res, 352(2), 199-206. https://doi.org/10.1007/s00441-013-1552-7
Matuszewich, L., Karney, J. J., Carter, S. R., Janasik, S. P., O'Brien, J. L., & Friedman, R. D. (2007). The delayed effects of chronic unpredictable stress on anxiety measures. Physiol Behav, 90(4), 674-681. https://doi.org/10.1016/j.physbeh.2006.12.006
Mátyás, F., Freund, T. F., & Gulyás, A. I. (2004). Convergence of excitatory and inhibitory inputs onto cck-containing basket cells in the ca1 area of the rat

hippocampus. European Journal of Neuroscience, 19(5), 1243-1256. https://doi.org/https://doi.org/10.1111/j.1460-9568.2004.03225.x
McCormick, D. A., Connors, B. W., Lighthall, J. W., & Prince, D. A. (1985). Comparative electrophysiology of pyramidal and sparsely spiny stellate neurons of the neocortex. J Neurophysiol, 54(4), 782-806. https://doi.org/10.1152/jn.1985.54.4.782
McDonald, A. J. (1992). Projection neurons of the basolateral amygdala: A correlative golgi and retrograde tract tracing study. Brain Res Bull, 28(2), 179-185. https://doi.org/10.1016/0361-9230(92)90177-y
McKernan, M. G., & Shinnick-Gallagher, P. (1997). Fear conditioning induces a lasting potentiation of synaptic currents in vitro. Nature, 390(6660), 607-611. https://doi.org/10.1038/37605
Megias, M., Emri, Z., Freund, T. F., & Gulyas, A. I. (2001). Total number and distribution of inhibitory and excitatory synapses on hippocampal ca1 pyramidal cells. Neuroscience, 102(3), 527-540. https://doi.org/10.1016/s0306-4522(00)00496-6
Mesulam, M. M. (1998). From sensation to cognition. Brain, 121 (Pt 6), 1013-1052. https://doi.org/10.1093/brain/121.6.1013
Meyer, A. H., Katona, I., Blatow, M., Rozov, A., & Monyer, H. (2002). In vivo labeling of parvalbumin-positive interneurons and analysis of electrical coupling in identified neurons. J Neurosci, 22(16), 7055-7064. https://doi.org/10.1523/JNEUROSCI.22-16-07055.2002
Miles, R., Toth, K., Gulyas, A. I., Hajos, N., & Freund, T. F. (1996). Differences between somatic and dendritic inhibition in the hippocampus. Neuron, 16(4), 815-823. https://doi.org/10.1016/s0896-6273(00)80101-4
Miyamae, T., Chen, K., Lewis, D. A., & Gonzalez-Burgos, G. (2017). Distinct physiological maturation of parvalbumin-positive neuron subtypes in mouse prefrontal cortex. J Neurosci, 37(19), 4883-4902. https://doi.org/10.1523/JNEUROSCI.3325-16.2017
Miyata, S., Komatsu, Y., Yoshimura, Y., Taya, C., & Kitagawa, H. (2012). Persistent cortical plasticity by upregulation of chondroitin 6-sulfation. Nat Neurosci, 15(3), 414-422, S411-412. https://doi.org/10.1038/nn.3023
Morales, M., Hein, K., & Vogel, Z. (2008). Hippocampal interneurons co-express transcripts encoding the alpha7 nicotinic receptor subunit and the cannabinoid receptor 1. Neuroscience, 152(1), 70-81. https://doi.org/10.1016/j.neuroscience.2007.12.019
Moser, E. I., Kropff, E., & Moser, M. B. (2008). Place cells, grid cells, and the brain's spatial representation system. Annu Rev Neurosci, 31, 69-89. https://doi.org/10.1146/annurev.neuro.31.061307.090723
Murray, E. A. (2007). The amygdala, reward and emotion. Trends Cogn Sci, 11(11), 489-497. https://doi.org/10.1016/j.tics.2007.08.013
Myers, K. M., & Davis, M. (2007). Mechanisms of fear extinction. Mol Psychiatry, 12(2), 120-150. https://doi.org/10.1038/sj.mp.4001939
Nagy-Pal, P., Veres, J. M., Fekete, Z., Karlocai, M. R., Weisz, F., Barabas, B., Reeb, Z., & Hajos, N. (2023). Structural organisation of perisomatic inhibition in the mouse medial prefrontal cortex. J Neurosci. https://doi.org/10.1523/JNEUROSCI.0432-23.2023
Nakashima, M., Ikegaya, Y., & Morikawa, S. (2022). Genetic labeling of axo-axonic cells in the basolateral amygdala. Neurosci Res, 178, 33-40. https://doi.org/10.1016/j.neures.2022.02.002

Nelson, R. J., & Trainor, B. C. (2007). Neural mechanisms of aggression. Nat Rev Neurosci, 8(7), 536-546. https://doi.org/10.1038/nrn2174

Nimchinsky, E. A., Sabatini, B. L., & Svoboda, K. (2002). Structure and function of dendritic spines. Annu Rev Physiol, 64, 313-353. https://doi.org/10.1146/annurev.physiol.64.081501.160008

Nunez, A., Amzica, F., & Steriade, M. (1993). Electrophysiology of cat association cortical cells in vivo: Intrinsic properties and synaptic responses. J Neurophysiol, 70(1), 418-430. https://doi.org/10.1152/jn.1993.70.1.418

O'Keefe, J., & Speakman, A. (1987). Single unit activity in the rat hippocampus during a spatial memory task. Exp Brain Res, 68(1), 1-27. https://doi.org/10.1007/BF00255230

Olah, S., Fule, M., Komlosi, G., Varga, C., Baldi, R., Barzo, P., & Tamas, G. (2009). Regulation of cortical microcircuits by unitary gaba-mediated volume transmission. Nature, 461(7268), 1278-1281. https://doi.org/10.1038/nature08503

Olah, V. J., Goettemoeller, A. M., Rayaprolu, S., Dammer, E. B., Seyfried, N. T., Rangaraju, S., Dimidschstein, J., & Rowan, M. J. M. (2022). Biophysical k(v)3 channel alterations dampen excitability of cortical pv interneurons and contribute to network hyperexcitability in early alzheimer's. Elife, 11. https://doi.org/10.7554/eLife.75316

Ozdemir, A. T., Lagler, M., Lagoun, S., Malagon-Vina, H., Lasztoczi, B., & Klausberger, T. (2020). Unexpected rule-changes in a working memory task shape the firing of histologically identified delay-tuned neurons in the prefrontal cortex. Cell Rep, 30(5), 1613-1626 e1614. https://doi.org/10.1016/j.celrep.2019.12.102

Passecker, J., Mikus, N., Malagon-Vina, H., Anner, P., Dimidschstein, J., Fishell, G., Dorffner, G., & Klausberger, T. (2019). Activity of prefrontal neurons predict future choices during gambling. Neuron, 101(1), 152-164 e157. https://doi.org/10.1016/j.neuron.2018.10.050

Paul, A., Crow, M., Raudales, R., He, M., Gillis, J., & Huang, Z. J. (2017). Transcriptional architecture of synaptic communication delineates gabaergic neuron identity. Cell, 171(3), 522-539 e520. https://doi.org/10.1016/j.cell.2017.08.032

Pawelzik, H., Hughes, D. I., & Thomson, A. M. (2002). Physiological and morphological diversity of immunocytochemically defined parvalbumin- and cholecystokinin-positive interneurones in ca1 of the adult rat hippocampus. J Comp Neurol, 443(4), 346-367. https://doi.org/10.1002/cne.10118

Pelkey, K. A., Calvigioni, D., Fang, C., Vargish, G., Ekins, T., Auville, K., Wester, J. C., Lai, M., Mackenzie-Gray Scott, C., Yuan, X., Hunt, S., Abebe, D., Xu, Q., Dimidschstein, J., Fishell, G., Chittajallu, R., & McBain, C. J. (2020). Paradoxical network excitation by glutamate release from vglut3+ gabaergic interneurons. eLife, 9, e51996. https://doi.org/10.7554/eLife.51996

Perumal, M. B., Latimer, B., Xu, L., Stratton, P., Nair, S., & Sah, P. (2021). Microcircuit mechanisms for the generation of sharp-wave ripples in the basolateral amygdala: A role for chandelier interneurons. Cell Rep, 35(6), 109106. https://doi.org/10.1016/j.celrep.2021.109106

Peterfi, Z., Urban, G. M., Papp, O. I., Nemeth, B., Monyer, H., Szabo, G., Erdelyi, F., Mackie, K., Freund, T. F., Hajos, N., & Katona, I. (2012). Endocannabinoid-mediated long-term depression of afferent excitatory synapses in hippocampal pyramidal cells and gabaergic interneurons. J Neurosci, 32(41), 14448-14463. https://doi.org/10.1523/JNEUROSCI.1676-12.2012

Pfeffer, C. K., Xue, M., He, M., Huang, Z. J., & Scanziani, M. (2013). Inhibition of inhibition in visual cortex: The logic of connections between molecularly distinct interneurons. Nat Neurosci, 16(8), 1068-1076. https://doi.org/10.1038/nn.3446

Pi, H. J., Hangya, B., Kvitsiani, D., Sanders, J. I., Huang, Z. J., & Kepecs, A. (2013). Cortical interneurons that specialize in disinhibitory control. Nature, 503(7477), 521-524. https://doi.org/10.1038/nature12676

Pietersen, A. N., Ward, P. D., Hagger-Vaughan, N., Wiggins, J., Jefferys, J. G., & Vreugdenhil, M. (2014). Transition between fast and slow gamma modes in rat hippocampus area ca1 in vitro is modulated by slow ca3 gamma oscillations. J Physiol, 592(4), 605-620. https://doi.org/10.1113/jphysiol.2013.263889

Pitler, T. A., & Alger, B. E. (1992). Postsynaptic spike firing reduces synaptic gabaa responses in hippocampal pyramidal cells. J Neurosci, 12(10), 4122-4132. https://doi.org/10.1523/JNEUROSCI.12-10-04122.1992

Pouille, F., & Scanziani, M. (2004). Routing of spike series by dynamic circuits in the hippocampus. Nature, 429(6993), 717-723. https://doi.org/10.1038/nature02615

Poulet, J. F., & Petersen, C. C. (2008). Internal brain state regulates membrane potential synchrony in barrel cortex of behaving mice. Nature, 454(7206), 881-885. https://doi.org/10.1038/nature07150

Povysheva, N. V., Zaitsev, A. V., Gonzalez-Burgos, G., & Lewis, D. A. (2013). Electrophysiological heterogeneity of fast-spiking interneurons: Chandelier versus basket cells. PLoS One, 8(8), e70553. https://doi.org/10.1371/journal.pone.0070553

Price, J. L., & Drevets, W. C. (2010). Neurocircuitry of mood disorders. Neuropsychopharmacology, 35(1), 192-216. https://doi.org/10.1038/npp.2009.104

Quirk, G. J., Armony, J. L., & LeDoux, J. E. (1997). Fear conditioning enhances different temporal components of tone-evoked spike trains in auditory cortex and lateral amygdala. Neuron, 19(3), 613-624. https://doi.org/10.1016/s0896-6273(00)80375-x

Quirk, G. J., Russo, G. K., Barron, J. L., & Lebron, K. (2000). The role of ventromedial prefrontal cortex in the recovery of extinguished fear. J Neurosci, 20(16), 6225-6231. https://doi.org/10.1523/JNEUROSCI.20-16-06225.2000

Raudales, R., Kim, G., Kelly, S. M., Hatfield, J., Guan, W., Zhao, S., Paul, A., Qian, Y., Li, B., & Huang, Z. J. (2024). Specific and comprehensive genetic targeting reveals brain-wide distribution and synaptic input patterns of gabaergic axo-axonic interneurons. Elife, 13. https://doi.org/10.7554/eLife.93481

Reyes, A., Lujan, R., Rozov, A., Burnashev, N., Somogyi, P., & Sakmann, B. (1998). Target-cell-specific facilitation and depression in neocortical circuits. Nat Neurosci, 1(4), 279-285. https://doi.org/10.1038/1092

Rogan, M. T., Staubli, U. V., & LeDoux, J. E. (1997). Fear conditioning induces associative long-term potentiation in the amygdala. Nature, 390(6660), 604-607. https://doi.org/10.1038/37601

Rolls, E. T. (2023). Emotion, motivation, decision-making, the orbitofrontal cortex, anterior cingulate cortex, and the amygdala. Brain Struct Funct, 228(5), 1201-1257. https://doi.org/10.1007/s00429-023-02644-9

Romanski, L. M., Clugnet, M. C., Bordi, F., & LeDoux, J. E. (1993). Somatosensory and auditory convergence in the lateral nucleus of the amygdala. Behav Neurosci, 107(3), 444-450. https://doi.org/10.1037//0735-7044.107.3.444

Rose, J. E., & Woolsey, C. N. (1948). The orbitofrontal cortex and its connections with the mediodorsal nucleus in rabbit, sheep and cat. Res Publ Assoc Res Nerv Ment Dis, 27 (1 vol.), 210-232. https://www.ncbi.nlm.nih.gov/pubmed/18106857

Rovira-Esteban, L., Peterfi, Z., Vikor, A., Mate, Z., Szabo, G., & Hajos, N. (2017). Morphological and physiological properties of cck/cb1r-expressing interneurons in the basal amygdala. Brain Struct Funct, 222(8), 3543-3565. https://doi.org/10.1007/s00429-017-1417-z

Rovira-Esteban, L., Hajos, N., Nagy, G. A., Crespo, C., Nacher, J., Varea, E., & Blasco-Ibanez, J. M. (2020). Semilunar granule cells are the primary source of the perisomatic excitatory innervation onto parvalbumin-expressing interneurons in the dentate gyrus. eNeuro, 7(4). https://doi.org/10.1523/ENEURO.0323-19.2020

Rudy, B., & McBain, C. J. (2001). Kv3 channels: Voltage-gated k+ channels designed for high-frequency repetitive firing. Trends Neurosci, 24(9), 517-526. https://doi.org/10.1016/s0166-2236(00)01892-0

Rumpel, S., LeDoux, J., Zador, A., & Malinow, R. (2005). Postsynaptic receptor trafficking underlying a form of associative learning. Science, 308(5718), 83-88. https://doi.org/10.1126/science.1103944

Runyan, J. D., Moore, A. N., & Dash, P. K. (2004). A role for prefrontal cortex in memory storage for trace fear conditioning. J Neurosci, 24(6), 1288-1295. https://doi.org/10.1523/JNEUROSCI.4880-03.2004

Ryan, T. J., Roy, D. S., Pignatelli, M., Arons, A., & Tonegawa, S. (2015). Memory. Engram cells retain memory under retrograde amnesia. Science, 348(6238), 1007-1013. https://doi.org/10.1126/science.aaa5542

Sah, P., Faber, E. S., Lopez De Armentia, M., & Power, J. (2003). The amygdaloid complex: Anatomy and physiology. Physiol Rev, 83(3), 803-834. https://doi.org/10.1152/physrev.00002.2003

Salzman, C. D., & Fusi, S. (2010). Emotion, cognition, and mental state representation in amygdala and prefrontal cortex. Annu Rev Neurosci, 33, 173-202. https://doi.org/10.1146/annurev.neuro.051508.135256

Sanders, S. K., & Shekhar, A. (1995). Regulation of anxiety by gabaa receptors in the rat amygdala. Pharmacol Biochem Behav, 52(4), 701-706. https://doi.org/10.1016/0091-3057(95)00153-n

Sassoe-Pognetto, M., & Fritschy, J. M. (2000). Mini-review: Gephyrin, a major postsynaptic protein of gabaergic synapses. Eur J Neurosci, 12(7), 2205-2210. https://doi.org/10.1046/j.1460-9568.2000.00106.x

Schlingloff, D., Kali, S., Freund, T. F., Hajos, N., & Gulyas, A. I. (2014). Mechanisms of sharp wave initiation and ripple generation. J Neurosci, 34(34), 11385-11398. https://doi.org/10.1523/JNEUROSCI.0867-14.2014

Schneider-Mizell, C. M., Bodor, A. L., Collman, F., Brittain, D., Bleckert, A., Dorkenwald, S., Turner, N. L., Macrina, T., Lee, K., Lu, R., Wu, J., Zhuang, J., Nandi, A., Hu, B., Buchanan, J., Takeno, M. M., Torres, R., Mahalingam, G., Bumbarger, D. J., . . . Costa, N. M. D. (2021). Structure and function of axo-axonic inhibition. Elife, 10. https://doi.org/10.7554/eLife.73783

Schubert, D., Kotter, R., Zilles, K., Luhmann, H. J., & Staiger, J. F. (2003). Cell type-specific circuits of cortical layer iv spiny neurons. J Neurosci, 23(7), 2961-2970. https://doi.org/10.1523/JNEUROSCI.23-07-02961.2003

Schuman, B., Dellal, S., Pronneke, A., Machold, R., & Rudy, B. (2021). Neocortical layer 1: An elegant solution to top-down and bottom-up integration. Annu Rev Neurosci, 44, 221-252. https://doi.org/10.1146/annurev-neuro-100520-012117

Seamans, J. K., Lapish, C. C., & Durstewitz, D. (2008). Comparing the prefrontal cortex of rats and primates: Insights from electrophysiology. Neurotox Res, 14(2-3), 249-262. https://doi.org/10.1007/BF03033814

Seignette, K., Jamann, N., Papale, P., Terra, H., Porneso, R. O., de Kraker, L., van der Togt, C., van der Aa, M., Neering, P., Ruimschotel, E., Roelfsema, P. R., Montijn, J. S., Self, M. W., Kole, M. H. P., & Levelt, C. N. (2024). Experience shapes chandelier cell function and structure in the visual cortex. Elife, 12. https://doi.org/10.7554/eLife.91153

Senn, V., Wolff, S. B., Herry, C., Grenier, F., Ehrlich, I., Grundemann, J., Fadok, J. P., Muller, C., Letzkus, J. J., & Luthi, A. (2014). Long-range connectivity defines behavioral specificity of amygdala neurons. Neuron, 81(2), 428-437. https://doi.org/10.1016/j.neuron.2013.11.006

Shaban, H., Humeau, Y., Herry, C., Cassasus, G., Shigemoto, R., Ciocchi, S., Barbieri, S., van der Putten, H., Kaupmann, K., Bettler, B., & Luthi, A. (2006). Generalization of amygdala ltp and conditioned fear in the absence of presynaptic inhibition. Nat Neurosci, 9(8), 1028-1035. https://doi.org/10.1038/nn1732

Shepherd, G. M. (1996). The dendritic spine: A multifunctional integrative unit. J Neurophysiol, 75(6), 2197-2210. https://doi.org/10.1152/jn.1996.75.6.2197

Shu, S., Xu, S. Y., Ye, L., Liu, Y., Cao, X., Jia, J. Q., Bian, H. J., Liu, Y., Zhu, X. L., & Xu, Y. (2023). Prefrontal parvalbumin interneurons deficits mediate early emotional dysfunction in alzheimer's disease. Neuropsychopharmacology, 48(2), 391-401. https://doi.org/10.1038/s41386-022-01435-w

Shultz, B., Farkash, A., Collins, B., Mohammadmirzaei, N., & Knox, D. (2022). Fear learning-induced changes in ampar and nmdar expression in the fear circuit. Learn Mem, 29(3), 83-92. https://doi.org/10.1101/lm.053525.121

Sierra-Mercado, D., Padilla-Coreano, N., & Quirk, G. J. (2011). Dissociable roles of prelimbic and infralimbic cortices, ventral hippocampus, and basolateral amygdala in the expression and extinction of conditioned fear. Neuropsychopharmacology, 36(2), 529-538. https://doi.org/10.1038/npp.2010.184

Sigurdsson, T., Doyere, V., Cain, C. K., & LeDoux, J. E. (2007). Long-term potentiation in the amygdala: A cellular mechanism of fear learning and memory. Neuropharmacology, 52(1), 215-227. https://doi.org/10.1016/j.neuropharm.2006.06.022

Sik, A., Penttonen, M., Ylinen, A., & Buzsaki, G. (1995). Hippocampal ca1 interneurons: An in vivo intracellular labeling study. J Neurosci, 15(10), 6651-6665. https://doi.org/10.1523/JNEUROSCI.15-10-06651.1995

Singewald, N., Salchner, P., & Sharp, T. (2003). Induction of c-fos expression in specific areas of the fear circuitry in rat forebrain by anxiogenic drugs. Biol Psychiatry, 53(4), 275-283. https://doi.org/10.1016/s0006-3223(02)01574-3

Singh, S., & Topolnik, L. (2023). Inhibitory circuits in fear memory and fear-related disorders. Front Neural Circuits, 17, 1122314. https://doi.org/10.3389/fncir.2023.1122314

Sohal, V. S., Zhang, F., Yizhar, O., & Deisseroth, K. (2009). Parvalbumin neurons and gamma rhythms enhance cortical circuit performance. Nature, 459(7247), 698-702. https://doi.org/10.1038/nature07991

Somogyi, J., Baude, A., Omori, Y., Shimizu, H., El Mestikawy, S., Fukaya, M., Shigemoto, R., Watanabe, M., & Somogyi, P. (2004). Gabaergic basket cells expressing cholecystokinin contain vesicular glutamate transporter type 3 (vglut3)

in their synaptic terminals in hippocampus and isocortex of the rat. Eur J Neurosci, 19(3), 552-569. https://doi.org/10.1111/j.0953-816x.2003.03091.x

Somogyi, P. (1977). A specific 'axo-axonal' interneuron in the visual cortex of the rat. Brain Res, 136(2), 345-350. https://doi.org/10.1016/0006-8993(77)90808-3

Somogyi, P., Freund, T. F., Hodgson, A. J., Somogyi, J., Beroukas, D., & Chubb, I. W. (1985). Identified axo-axonic cells are immunoreactive for gaba in the hippocampus and visual cortex of the cat. Brain Res, 332(1), 143-149. https://doi.org/10.1016/0006-8993(85)90397-x

Spampanato, J., Polepalli, J., & Sah, P. (2011). Interneurons in the basolateral amygdala. Neuropharmacology, 60(5), 765-773. https://doi.org/10.1016/j.neuropharm.2010.11.006

Stark, E., Roux, L., Eichler, R., Senzai, Y., Royer, S., & Buzsaki, G. (2014). Pyramidal cell-interneuron interactions underlie hippocampal ripple oscillations. Neuron, 83(2), 467-480. https://doi.org/10.1016/j.neuron.2014.06.023

Stratford, K. J., Tarczy-Hornoch, K., Martin, K. A., Bannister, N. J., & Jack, J. J. (1996). Excitatory synaptic inputs to spiny stellate cells in cat visual cortex. Nature, 382(6588), 258-261. https://doi.org/10.1038/382258a0

Struber, M., Sauer, J. F., & Bartos, M. (2022). Parvalbumin expressing interneurons control spike-phase coupling of hippocampal cells to theta oscillations. Sci Rep, 12(1), 1362. https://doi.org/10.1038/s41598-022-05004-5

Stujenske, J. M., O'Neill, P. K., Fernandes-Henriques, C., Nahmoud, I., Goldburg, S. R., Singh, A., Diaz, L., Labkovich, M., Hardin, W., Bolkan, S. S., Reardon, T. R., Spellman, T. J., Salzman, C. D., Gordon, J. A., Liston, C., & Likhtik, E. (2022). Prelimbic cortex drives discrimination of non-aversion via amygdala somatostatin interneurons. Neuron, 110(14), 2258-2267 e2211. https://doi.org/10.1016/j.neuron.2022.03.020

Szabadics, J., Lorincz, A., & Tamas, G. (2001). Beta and gamma frequency synchronization by dendritic gabaergic synapses and gap junctions in a network of cortical interneurons. J Neurosci, 21(15), 5824-5831. https://doi.org/10.1523/JNEUROSCI.21-15-05824.2001

Szabadics, J., Varga, C., Molnar, G., Olah, S., Barzo, P., & Tamas, G. (2006). Excitatory effect of gabaergic axo-axonic cells in cortical microcircuits. Science, 311(5758), 233-235. https://doi.org/10.1126/science.1121325

Szabo, G. G., Holderith, N., Gulyas, A. I., Freund, T. F., & Hajos, N. (2010). Distinct synaptic properties of perisomatic inhibitory cell types and their different modulation by cholinergic receptor activation in the ca3 region of the mouse hippocampus. Eur J Neurosci, 31(12), 2234-2246. https://doi.org/10.1111/j.1460-9568.2010.07292.x

Szabo, G. G., Papp, O. I., Mate, Z., Szabo, G., & Hajos, N. (2014). Anatomically heterogeneous populations of cb1 cannabinoid receptor-expressing interneurons in the ca3 region of the hippocampus show homogeneous input-output characteristics. Hippocampus, 24(12), 1506-1523. https://doi.org/10.1002/hipo.22330

Takacs, V. T., Szonyi, A., Freund, T. F., Nyiri, G., & Gulyas, A. I. (2015). Quantitative ultrastructural analysis of basket and axo-axonic cell terminals in the mouse hippocampus. Brain Struct Funct, 220(2), 919-940. https://doi.org/10.1007/s00429-013-0692-6

Tamamaki, N., & Nojyo, Y. (1993). Projection of the entorhinal layer ii neurons in the rat as revealed by intracellular pressure-injection of neurobiotin. Hippocampus, 3(4), 471-480. https://doi.org/10.1002/hipo.450030408

Tamas, G., Buhl, E. H., & Somogyi, P. (1997). Fast ipsps elicited via multiple synaptic release sites by different types of gabaergic neurone in the cat visual cortex. J Physiol, 500 (Pt 3)(Pt 3), 715-738. https://doi.org/10.1113/jphysiol.1997.sp022054

Tamas, G., Buhl, E. H., Lorincz, A., & Somogyi, P. (2000). Proximally targeted gabaergic synapses and gap junctions synchronize cortical interneurons. Nat Neurosci, 3(4), 366-371. https://doi.org/10.1038/73936

Tamas, G., Lorincz, A., Simon, A., & Szabadics, J. (2003). Identified sources and targets of slow inhibition in the neocortex. Science, 299(5614), 1902-1905. https://doi.org/10.1126/science.1082053

Tan, T., Wang, W., Liu, T., Zhong, P., Conrow-Graham, M., Tian, X., & Yan, Z. (2021). Neural circuits and activity dynamics underlying sex-specific effects of chronic social isolation stress. Cell Rep, 34(12), 108874. https://doi.org/10.1016/j.celrep.2021.108874

Taniguchi, H., Lu, J., & Huang, Z. J. (2013). The spatial and temporal origin of chandelier cells in mouse neocortex. Science, 339(6115), 70-74. https://doi.org/10.1126/science.1227622

Topolnik, L., & Tamboli, S. (2022). The role of inhibitory circuits in hippocampal memory processing. Nat Rev Neurosci, 23(8), 476-492. https://doi.org/10.1038/s41583-022-00599-0

Tovote, P., Fadok, J. P., & Luthi, A. (2015). Neuronal circuits for fear and anxiety. Nat Rev Neurosci, 16(6), 317-331. https://doi.org/10.1038/nrn3945

Tremblay, R., Lee, S., & Rudy, B. (2016). Gabaergic interneurons in the neocortex: From cellular properties to circuits. Neuron, 91(2), 260-292. https://doi.org/10.1016/j.neuron.2016.06.033

Trouche, S., Sasaki, J. M., Tu, T., & Reijmers, L. G. (2013). Fear extinction causes target-specific remodeling of perisomatic inhibitory synapses. Neuron, 80(4), 1054-1065. https://doi.org/10.1016/j.neuron.2013.07.047

Tukker, J. J., Fuentealba, P., Hartwich, K., Somogyi, P., & Klausberger, T. (2007). Cell type-specific tuning of hippocampal interneuron firing during gamma oscillations in vivo. J Neurosci, 27(31), 8184-8189. https://doi.org/10.1523/JNEUROSCI.1685-07.2007

Tully, K., Li, Y., Tsvetkov, E., & Bolshakov, V. Y. (2007). Norepinephrine enables the induction of associative long-term potentiation at thalamo-amygdala synapses. Proc Natl Acad Sci U S A, 104(35), 14146-14150. https://doi.org/10.1073/pnas.0704621104

Tye, K. M., Stuber, G. D., de Ridder, B., Bonci, A., & Janak, P. H. (2008). Rapid strengthening of thalamo-amygdala synapses mediates cue-reward learning. Nature, 453(7199), 1253-1257. https://doi.org/10.1038/nature06963

Tye, K. M., Prakash, R., Kim, S. Y., Fenno, L. E., Grosenick, L., Zarabi, H., Thompson, K. R., Gradinaru, V., Ramakrishnan, C., & Deisseroth, K. (2011). Amygdala circuitry mediating reversible and bidirectional control of anxiety. Nature, 471(7338), 358-362. https://doi.org/10.1038/nature09820

Uylings, H. B., Groenewegen, H. J., & Kolb, B. (2003). Do rats have a prefrontal cortex? Behav Brain Res, 146(1-2), 3-17. https://doi.org/10.1016/j.bbr.2003.09.028

Vereczki, V. K., Veres, J. M., Muller, K., Nagy, G. A., Racz, B., Barsy, B., & Hajos, N. (2016). Synaptic organization of perisomatic gabaergic inputs onto the principal cells of the mouse basolateral amygdala. Front Neuroanat, 10, 20. https://doi.org/10.3389/fnana.2016.00020

Vereczki, V. K., Muller, K., Krizsan, E., Mate, Z., Fekete, Z., Rovira-Esteban, L., Veres, J. M., Erdelyi, F., & Hajos, N. (2021). Total number and ratio of gabaergic neuron types in the mouse lateral and basal amygdala. J Neurosci, 41(21), 4575-4595. https://doi.org/10.1523/JNEUROSCI.2700-20.2021

Veres, J. M., Nagy, G. A., Vereczki, V. K., Andrasi, T., & Hajos, N. (2014). Strategically positioned inhibitory synapses of axo-axonic cells potently control principal neuron spiking in the basolateral amygdala. J Neurosci, 34(49), 16194-16206. https://doi.org/10.1523/JNEUROSCI.2232-14.2014

Veres, J. M., Nagy, G. A., & Hajos, N. (2017). Perisomatic gabaergic synapses of basket cells effectively control principal neuron activity in amygdala networks. Elife, 6. https://doi.org/10.7554/eLife.20721

Veres, J. M., Fekete, Z., Muller, K., Andrasi, T., Rovira-Esteban, L., Barabas, B., Papp, O. I., & Hajos, N. (2023). Fear learning and aversive stimuli differentially change excitatory synaptic transmission in perisomatic inhibitory cells of the basal amygdala. Front Cell Neurosci, 17, 1120338. https://doi.org/10.3389/fncel.2023.1120338

Viney, T. J., Lasztoczi, B., Katona, L., Crump, M. G., Tukker, J. J., Klausberger, T., & Somogyi, P. (2013). Network state-dependent inhibition of identified hippocampal ca3 axo-axonic cells in vivo. Nat Neurosci, 16(12), 1802-1811. https://doi.org/10.1038/nn.3550

Volk, D. W., Pierri, J. N., Fritschy, J. M., Auh, S., Sampson, A. R., & Lewis, D. A. (2002). Reciprocal alterations in pre- and postsynaptic inhibitory markers at chandelier cell inputs to pyramidal neurons in schizophrenia. Cereb Cortex, 12(10), 1063-1070. https://doi.org/10.1093/cercor/12.10.1063

Wang, Y., Toledo-Rodriguez, M., Gupta, A., Wu, C., Silberberg, G., Luo, J., & Markram, H. (2004). Anatomical, physiological and molecular properties of martinotti cells in the somatosensory cortex of the juvenile rat. J Physiol, 561(Pt 1), 65-90. https://doi.org/10.1113/jphysiol.2004.073353

Wang, Z. J., Shwani, T., Liu, J., Zhong, P., Yang, F., Schatz, K., Zhang, F., Pralle, A., & Yan, Z. (2022). Molecular and cellular mechanisms for differential effects of chronic social isolation stress in males and females. Mol Psychiatry, 27(7), 3056-3068. https://doi.org/10.1038/s41380-022-01574-y

Whittle, N., Fadok, J., MacPherson, K. P., Nguyen, R., Botta, P., Wolff, S. B. E., Muller, C., Herry, C., Tovote, P., Holmes, A., Singewald, N., Luthi, A., & Ciocchi, S. (2021). Central amygdala micro-circuits mediate fear extinction. Nat Commun, 12(1), 4156. https://doi.org/10.1038/s41467-021-24068-x

Wilson, R. I., Kunos, G., & Nicoll, R. A. (2001). Presynaptic specificity of endocannabinoid signaling in the hippocampus. Neuron, 31(3), 453-462. https://doi.org/10.1016/s0896-6273(01)00372-5

Wilson, R. I., & Nicoll, R. A. (2001). Endogenous cannabinoids mediate retrograde signalling at hippocampal synapses. Nature, 410(6828), 588-592. https://doi.org/10.1038/35069076

Witter, M. P., Doan, T. P., Jacobsen, B., Nilssen, E. S., & Ohara, S. (2017). Architecture of the entorhinal cortex a review of entorhinal anatomy in rodents with some comparative notes. Front Syst Neurosci, 11, 46. https://doi.org/10.3389/fnsys.2017.00046

Wolff, S. B., Grundemann, J., Tovote, P., Krabbe, S., Jacobson, G. A., Muller, C., Herry, C., Ehrlich, I., Friedrich, R. W., Letzkus, J. J., & Luthi, A. (2014). Amygdala interneuron subtypes control fear learning through disinhibition. Nature, 509(7501), 453-458. https://doi.org/10.1038/nature13258

Woodruff, A., Xu, Q., Anderson, S. A., & Yuste, R. (2009). Depolarizing effect of neocortical chandelier neurons. Front Neural Circuits, 3, 15. https://doi.org/10.3389/neuro.04.015.2009

Woodruff, A. R., Monyer, H., & Sah, P. (2006). Gabaergic excitation in the basolateral amygdala. J Neurosci, 26(46), 11881-11887. https://doi.org/10.1523/JNEUROSCI.3389-06.2006

Woodruff, A. R., & Sah, P. (2007). Inhibition and synchronization of basal amygdala principal neuron spiking by parvalbumin-positive interneurons. J Neurophysiol, 98(5), 2956-2961. https://doi.org/10.1152/jn.00739.2007

Woodruff, A. R., McGarry, L. M., Vogels, T. P., Inan, M., Anderson, S. A., & Yuste, R. (2011). State-dependent function of neocortical chandelier cells. J Neurosci, 31(49), 17872-17886. https://doi.org/10.1523/JNEUROSCI.3894-11.2011

Yap, E. L., Pettit, N. L., Davis, C. P., Nagy, M. A., Harmin, D. A., Golden, E., Dagliyan, O., Lin, C., Rudolph, S., Sharma, N., Griffith, E. C., Harvey, C. D., & Greenberg, M. E. (2021). Bidirectional perisomatic inhibitory plasticity of a fos neuronal network. Nature, 590(7844), 115-121. https://doi.org/10.1038/s41586-020-3031-0

Yi, F., Ball, J., Stoll, K. E., Satpute, V. C., Mitchell, S. M., Pauli, J. L., Holloway, B. B., Johnston, A. D., Nathanson, N. M., Deisseroth, K., Gerber, D. J., Tonegawa, S., & Lawrence, J. J. (2014). Direct excitation of parvalbumin-positive interneurons by m1 muscarinic acetylcholine receptors: Roles in cellular excitability, inhibitory transmission and cognition. J Physiol, 592(16), 3463-3494. https://doi.org/10.1113/jphysiol.2014.275453

Yiu, A. P., Mercaldo, V., Yan, C., Richards, B., Rashid, A. J., Hsiang, H. L., Pressey, J., Mahadevan, V., Tran, M. M., Kushner, S. A., Woodin, M. A., Frankland, P. W., & Josselyn, S. A. (2014). Neurons are recruited to a memory trace based on relative neuronal excitability immediately before training. Neuron, 83(3), 722-735. https://doi.org/10.1016/j.neuron.2014.07.017

Yu, K., Garcia da Silva, P., Albeanu, D. F., & Li, B. (2016). Central amygdala somatostatin neurons gate passive and active defensive behaviors. J Neurosci, 36(24), 6488-6496. https://doi.org/10.1523/JNEUROSCI.4419-15.2016

Zaitsev, A. V., Povysheva, N. V., Lewis, D. A., & Krimer, L. S. (2007). P/q-type, but not n-type, calcium channels mediate gaba release from fast-spiking interneurons to pyramidal cells in rat prefrontal cortex. J Neurophysiol, 97(5), 3567-3573. https://doi.org/10.1152/jn.01293.2006

Zhu, P. J., & Lovinger, D. M. (2005). Retrograde endocannabinoid signaling in a postsynaptic neuron/synaptic bouton preparation from basolateral amygdala. J Neurosci, 25(26), 6199-6207. https://doi.org/10.1523/JNEUROSCI.1148-05.2005

Zucker, R. S., & Regehr, W. G. (2002). Short-term synaptic plasticity. Annu Rev Physiol, 64, 355-405. https://doi.org/10.1146/annurev.physiol.64.092501.114547

9. BIBLIOGRAPHY OF PUBLICATIONS

Publications related to the thesis:

Fekete, Z., Weisz, Veres, J. M., F., Karlócai, M. K., Andrási, T., Hájos, N. (2024). Synaptic communication within the microcircuits of pyramidal neurons and basket cells in the mouse prefrontal cortex. The Journal of Physiology. https://doi.org/10.1113/JP286284
IF: 4.7

Veres, J. M., Fekete, Z., Müller, K., Andrási, T., Rovira-Esteban, L., Barabás, B., Papp, O. I., Hájos, N. (2023). Fear learning and aversive stimuli differentially change excitatory synaptic transmission in perisomatic inhibitory cells of the basal amygdala. Front. Cell. Neurosci 17:1102338. https://doi.org/10.3389/fncel.2023.1120338
IF: 4.2

Publications not related to the thesis:

Nagy-Pál, P., Veres, J. M., Fekete, Z., Karlócai, M. K., Weisz, F., Barabás, B., Reéb, Z., Hájos, N. (2023). Structural organization of perisomatic inhibition in the mouse medial prefrontal cortex. The Journal of Neuroscience 43(42) 6972-6987. https://doi.org/10.1523/JNEUROSCI.0432-23.2023
IF: 4.4

Vereczki, V. K., Müller, K., Krizsán, É., Máté, Z., Fekete, Z., Rovira-Esteban, L., Veres, J. M., Erdélyi, F., Hájos, N. (2021). Total number and ratio of GABAergic neuron types in the mouse lateral and basal amygdala. The Journal of Neuroscience 41(21) 4575-4595. https://doi.org/10.1523/JNEUROSCI.2700-20.2021
IF: 6.709

10. ACKNOWLEDGEMENTS

I would like to express my gratitude to present and past members of the lab for making this helpful and friendly environment created by you feel natural, although it is a privilege. Thank you for caring deeply not only about the work we do, but also about how the victories and occasional struggles make us feel along our journey. I am also grateful for Norbert for his encouragement, positive thinking and contagious enthusiasm about scientific questions and discoveries that have been an antidote to my doubts. I have enjoyed being intrigued about the mysteries of the brain with you.

I also deeply appreciate the endless support of my family and friends, who continue to believe in me and my decisions, thank you for holding my hand while I'm taking my cautious steps. I consider myself lucky for being surrounded by all of you.